SAPIENZA
UNIVERSITÀ DI ROMA

Optimization Models and Algorithms for Electricity Markets, Redispatch, and Market Interactions

Department of Computer, Control and Management Engineering Antonio Ruberti (DIAG)
Automatic Control, Bioengineering and Operations Research (ABRO) (XXXVIII cycle)

Giulio Scarponi
ID number 1802941

Advisor
Prof. Marco Sciandrone

Academic Year 2025/2026

This research work has been funded by the European Union - NextGenerationEU, Mission 4, Component I.4.1, CUP B83C22003220006.

Optimization Models and Algorithms for Electricity Markets, Redispatch, and Market Interactions
PhD Thesis. Sapienza University of Rome

This thesis has been typeset by LaTeX and the Sapthesis class.

Author's email: giulio.scarponi at uniroma1 dot it

Abstract

This thesis studies electricity and redispatch markets from an operations research perspective, with a focus on market-clearing models, equilibrium analysis, and algorithmic solutions under network constraints. In particular, the thesis examines how market outcomes are affected by nonconvexities, decomposition strategies, and the level of detail adopted in network modeling.

Chapter 2 provides a critical examination and technical reconstruction of an existing equilibrium framework for competitive electricity markets with price-taking participants in both convex and nonconvex settings. It revisits the approaches introduced in the literature, reorganizes its main theoretical components, and presents in full several proofs that were omitted or only briefly outlined in the original source. The chapter's main original contribution lies in extending the framework to an Alternating Current Optimal Power Flow setting, where the same theoretical logic is examined in a different modeling environment and complemented by a computational test case.

Chapter 3 addresses the computational solution of a day-ahead market-clearing problem with demand response and Direct Current Optimal Power Flow (DCOPF) constraints. It proposes a nonmonotone restart and acceptance framework for accelerated Alternating Direction Method of Multipliers (ADMM), based on a sliding-window residual criterion, and uses it to compare several acceleration schemes under a unified computational setting. The computational study shows that the effectiveness of acceleration depends significantly on the interaction between the chosen method, the problem instance, and the safeguard configuration.

Chapter 4 adopts a modeling perspective on centralized redispatch. It compares a zonal formulation and a DC power-flow-based formulation, both including reserve-related mechanisms, and evaluates their outcomes through dedicated recovery models designed to restore nodal feasibility while limiting deviations from prior market results. The computational analysis shows that incorporating nodal network constraints directly into the redispatch model can improve overall economic performance without materially increasing computational burden. It also highlights relevant trade-offs among alternative recovery formulations in terms of cost, tractability, and robustness under changing operating conditions.

Overall, the thesis contributes to the study of electricity markets by combining critical analysis of existing equilibrium theory with original work on algorithmic design and redispatch modeling, with particular emphasis on the role of network constraints in determining feasible and economically efficient outcomes.

Contents

Chapter 1

Introduction

Electricity and redispatch markets, as well as power systems in general, involve complex decision-making processes carried out by multiple interacting actors, each with a distinct role and subject to technical and legal constraints. This complexity creates the need for consistent and rigorous tools that can provide reliable and practically useful solutions while accounting for the economic and physical requirements under which the system operates. Typical examples include the maximization of social welfare as an economic objective and the minimization of generation costs as an operational requirement for secure system functioning. In an interconnected power grid, total injections into and withdrawals from the network must be balanced at every moment, within a small tolerance, and while accounting for physical phenomena such as network losses. Without going into the details of transmission and distribution system operations, it is worth emphasizing that both detailed and simplified network models lie at the core of many energy-related optimization problems. Operations research provides the methodological framework needed to address such problems. This thesis investigates several aspects of electricity and redispatch markets, with a focus on algorithmic and modeling perspectives, as well as on the interactions among market participants in market-clearing problems.

This introduction first provides a concise overview of the electric power system, with particular emphasis on the Italian electricity markets and on the operational mechanisms used to ensure system security, including redispatch and balancing actions. Then it briefly introduces the two main network models, reviews the main applications of operations research to power systems, and concludes with an outline of the thesis.

1.1 Electric power system

Since market design and institutional arrangements vary across jurisdictions, the discussion focuses on components and roles that are common to most liberalized power systems.

The electric power system can be described in terms of four tightly coupled layers:

- Generation
- Transmission
- Distribution

- Supply and consumption.

Generation. Generation is the physical production of electricity from primary energy sources. In liberalized contexts, generation is closely linked to wholesale trading (e.g., forward, day-ahead, and intraday markets) and to cross-border exchanges enabled by interconnectors. Market outcomes determine commercial schedules, while real-time operation must still comply with network and security constraints.

Transmission. Transmission refers to the transport of electricity over the extra-high and high-voltage interconnected network. Beyond the transport function, transmission-level system operations include security analysis, congestion management, and the procurement and activation of reserves and ancillary services needed to keep frequency and other operational variables within secure limits. System operations must continuously reconcile physical feasibility with market-based schedules.

Distribution. Distribution is the transport of electricity over distribution networks (high-, medium- and low-voltage) for delivery to customers, excluding supply. Distribution system operation covers network planning, maintenance and operation at the local level and increasingly involves active network management and flexibility procurement (often discussed under the umbrella of "smart grids"), especially with high penetration of distributed energy resources.

Supply and consumption. In the retail segment, suppliers sell (and may resell) electricity to customers. Customers can be household or non-household; a final customer purchases electricity for their own use. Although retail is often treated separately from system operation, consumption patterns, demand response, and distributed generation directly affect both distribution- and transmission-level operations.

Participants and roles. Each layer involves specific actors with defined responsibilities. Producers (generators) inject electricity into the grid. From an operational standpoint, it is often useful to distinguish between *dispatchable* resources (whose output can be controlled within technical limits, e.g., gas-fired units or reservoir hydro) and *variable renewable energy (VRE)* resources (e.g., wind and solar PV), whose availability depends on weather conditions and therefore introduces forecast uncertainty. Another relevant classification concerns *flexibility*, i.e., the ability to change output over time (ramping capability), including start-up/shut-down constraints and minimum stable generation levels.

Transmission system operation is typically carried out by a Transmission System Operator (TSO), i.e., the entity responsible for operating, maintaining and, where necessary, developing the transmission system and its interconnections so that the system can meet reasonable transmission demand in the long term. Distribution networks are managed by Distribution System Operators (DSOs), with analogous responsibilities at the distribution level.

Closely connected to system operation, the economic layer is generally organized through market mechanisms. These markets determine the commercial schedules, which in turn provide the basis for subsequent technical processes. A prominent example is the spot market, particularly the Day-

Ahead Market. In the Italian system, this market-based scheduling layer is articulated across the day-ahead, intraday, and balancing stages described in the next section.

1.2 Italian electricity market and dispatching framework

The Italian wholesale electricity market (*Mercato Elettrico*, ME) is organized and managed by the *Gestore dei Mercati Energetici* (GME) and is divided into the spot market (*Mercato Elettrico a Pronti*, MPE) and the forward market with physical delivery (*Mercato Elettrico a Termine*, MTE) [33]. The MPE includes the Day-Ahead Market (*Mercato del Giorno Prima*, MGP) and the Intraday Market (*Mercato Infragiornaliero*, MI); other organized segments (e.g., the *Mercato dei Prodotti Giornalieri*) are omitted here for brevity [33].

In the MGP, energy for delivery on the following day is traded through a single auction. Participants submit sell offers (minimum acceptable price and quantity) and buy bids (maximum acceptable price and quantity). Market clearing determines zonal schedules and a zonal marginal price for each bidding zone. Since 1 January 2025, withdrawals (purchase bids) are also settled at zonal prices; GME publishes the *PUN Index GME* as an ex-post reference index, and ARERA has introduced equalization mechanisms during the transition from the historical PUN-based settlement [4, 3].

The MI allows market participants to adjust the schedules defined on the MGP as updated information becomes available (e.g., demand and renewable generation forecasts). In practice, the MI is implemented through a set of intraday auctions (MI-A) and a continuous trading session coupled with Europe (MI-XBID) within the Single Intraday Coupling (SIDC), in line with the Capacity Allocation and Congestion Management (CACM) Regulation [32, 33, 24]. Cross-zonal capacity is allocated implicitly, subject to the available transfer capacity between zones [24, 33].

System operation, congestion management, and real-time balancing are managed by Terna, the Italian transmission system operator (TSO), through the balancing and redispatching market/process (*Mercato per il bilanciamento e il ridispacciamento*, hereafter MBR). In accordance with the Electricity Balancing Guideline [25], the MBR comprises an Integrated Scheduling Process (ISP), which includes several ex-ante redispatching phases (commonly referred to as MSD), and the Balancing Market (MB), whose scope is increasingly coordinated with the European balancing platforms [3]. Within the MSD, the TSO selects upward and downward bids/offers under a pay-as-bid mechanism to resolve network constraints, procure reserves, and support system balancing [3].

Within the MBR, accepted upward offers represent a cost for the TSO, whereas accepted downward offers correspond to payments from market participants to the TSO. Offer submission is subject to validation rules defined in Terna's framework, including constraints on price consistency across offer components. When these constraints are not satisfied, offers can be automatically modified according to predefined correction rules [69, 70]. For each ISP period, Terna makes available at least the accepted bids, the total accepted upward and downward quantities and their average activation prices, and the feasibility ranges (*intervalli di fattibilità*) used to define admissible operating ranges for balancing [3].

1.3 Network models

When electricity market models explicitly account for the transmission grid, the literature relies on a few standard representations. In many day-ahead market designs, the network is described through a *zonal* model: individual buses are aggregated into bidding zones and network constraints are represented only through limits on exchanges between zones (e.g., via available transfer capacities or flow-based parameters) [67, 21, 66]. This aggregation reduces data and computational requirements and is often sufficient when internal constraints within each zone are not binding or are managed by subsequent operational procedures.

When a *nodal* representation is required, for example, to capture congestion patterns at the level of individual buses, two main modeling approaches are commonly considered. The most detailed one is the Alternating Current Optimal Power Flow (ACOPF), which determines an economically efficient operating point while enforcing the full AC power flow physics and operational constraints. ACOPF models active and reactive power, voltage magnitudes and phase angles, and may include losses, transformers, and other network devices. This physical fidelity comes at a significant computational cost; in particular, even feasibility testing for AC power flow has been shown to be strongly NP-hard [9]. For a detailed overview of the mathematical formulations of ACOPF, see [11].

To improve tractability, a widely used alternative is the Direct Current Optimal Power Flow (DCOPF), obtained by linearizing the AC model under standard assumptions. In essence, DCOPF neglects resistive losses (lossless network), assumes voltage magnitudes close to 1 p.u., and relies on small angle differences so that active power flows can be approximated linearly. The resulting model is computationally efficient and therefore attractive for large-scale market-clearing and planning applications, at the price of ignoring reactive power and voltage-related phenomena.

1.4 Operations research applications to power systems

Electricity markets tightly couple economic interactions between multiple agents with the physical constraints of power networks. This coupling generates large-scale decision problems in which feasibility is dictated by network laws and operational limits, while optimality reflects economic objectives and market rules. Operations research provides a unified methodological framework to model these problems and design algorithms that can handle heterogeneous constraints, nonlinearity, discreteness, uncertainty, and strategic behavior.

Building on the DCOPF and ACOPF formulations introduced earlier, optimal power flow represents a central building block for many market and system-operation tasks, including dispatch, market clearing formulations with network constraints, and security-constrained decision models. Research in continuous optimization spans linear and nonlinear programming, convexification techniques, and conic relaxations aimed at improving tractability and solution quality for AC network models [54, 55, 11, 10]. These developments are complemented by complexity results that clarify the intrinsic difficulty of AC feasibility and related decision problems [51, 9]. Conic programming also appears in distribution-network modeling, for instance in radial load-flow formulations [48]. A complementary direction focuses on decomposition and distributed optimization to address scale, decentralization, and privacy requirements that arise in market architectures and multi-area system operation [60, 79, 77].

Discrete decisions are pervasive in power-system planning and market operation, motivating mixed-integer models for unit commitment, expansion planning, and topology control, and for market-clearing formulations that include start-up decisions or non-convex bid features [63, 73, 52, 46]. Uncertainty introduced by demand variability, renewable generation, and outages leads to stochastic, robust, and chance-constrained formulations, and often to multi-stage or bilevel structures when investment decisions or strategic interactions are explicitly represented [65, 7, 49, 36]. Equilibrium and pricing models further connect optimization with game-theoretic viewpoints on market outcomes and incentives [39, 42].

For a systematic and operations research-oriented overview of emerging methodologies and applications around optimal power flow, including links to power-system operation and market problems, see [68].

1.5 Thesis Outline

This thesis investigates electricity and redispatch markets from algorithmic and modeling perspectives, with particular attention to market-clearing problems and the interactions among market participants.

Chapter 2 provides an analysis of the framework introduced in [39] for the study of equilibrium prices in electricity markets, considering different types of market participants in both convex and non-convex settings. The chapter ends with an application of the framework to an Alternating Current Optimal Power Flow (ACOPF) setting, illustrated through a small test case.

Chapter 3 studies the Accelerated Alternating Direction Method of Multipliers (ADMM) applied to a day-ahead market clearing problem with demand response and DCOPF constraints. In particular, it proposes a non-monotone restart framework and evaluates it on this problem through a comparison of several ADMM acceleration techniques and an additional variant. Each method is tested both within and outside the proposed framework, and under different parameter settings, in order to assess the performance of both the restart framework and the acceleration schemes.

Chapter 4 adopts a modeling perspective to study a centralized redispatch market. It presents two main models: a zonal-constraint model that builds on a baseline formulation introduced in a technical report and is extended with additional mechanisms, and a DCOPF-based model. Their performance is compared using two recovery models, with the aim of showing that incorporating network constraints from the outset leads to better overall performance. To this end, the chapter presents computational comparisons on multiple instances under different operating conditions.

Chapter 2

A Global Framework for the Electricity Market

2.1 Introduction

This chapter examines the study by Grübel et al. [39], which investigates equilibrium existence and computation in competitive energy-market models in the presence of nonconvexities. The paper considers a general equilibrium formulation with price-taking players and market-clearing conditions, and develops algorithmic criteria to decide whether an equilibrium exists and to compute one when it does. The central methodological idea is to exploit the structure of the welfare maximization problem and the associated dual price information in order to infer equilibrium properties. The objective of this chapter is to assess the proposed methodology, its modeling assumptions, and the main theoretical results, highlighting both strengths and limitations. Where appropriate, omitted proofs and extended arguments with respect to the original presentation are provided. Moreover, beyond the numerical experiments originally reported, the framework is tested on an additional model of practical relevance. Specifically, this model is based on an alternating current optimal power flow (ACOPF) formulation, not addressed in the original paper, in which the AC network constraints are encoded through the transmission system operator's problem and the market-clearing conditions.

The framework considered by Grübel et al. is centered on a welfare maximization problem. The welfare model seeks a feasible allocation satisfying the technical and economic constraints of market participants as well as market-clearing conditions, while maximizing social welfare. The authors then study how welfare optima relate to market equilibria, with the aim of deriving verifiable conditions under which a welfare-optimal allocation can be supported by an equilibrium price vector. Their analysis covers nonconvex settings arising from continuous nonlinear network physics and from discrete operational decisions. At the same time, the nonconvex results rely on assumptions that may be restrictive in practice, most notably the requirement of global optimality and additional technical conditions needed to handle price components that are not uniquely determined by first-order conditions. A formal description of the framework and of the associated problems is provided in Section 2.3.

The main contributions of the paper examined in this analysis can be summarized as follows:

- the proposal of an algorithm that determines whether a market equilibrium exists and computes an equilibrium if one exists, covering both convex and nonconvex player problems;
- the application of the algorithm to two energy-market models of practical relevance: a gas network model with nonlinear stationary flow equations and a power network model with DC line switching.

Relying on the equilibrium characterization developed in Harks (2020), the paper specializes the framework to competitive energy-market models and derives an implementable procedure to test for equilibrium existence and compute an equilibrium when it exists.

This chapter is organized as follows. Section 2.2 briefly introduces the theoretical fundamentals required in the remainder of the chapter. Section 2.3 formally defines the problems and presents the structure of the framework. Section 2.4 reports the theoretical results, including expanded proofs where appropriate. Section 2.5 presents and briefly discusses the proposed algorithm. Section 2.6 presents a new application of the framework to an Alternating Current Optimal Power Flow problem, complemented by a small case study.

2.2 Context and theory

This chapter relies on standard concepts from mathematical optimization, including Lagrangian duality, Karush–Kuhn–Tucker conditions, and related results. This section briefly recalls the definitions and key statements used throughout.

The following results, up to (2.2), are taken from [38].

KKT conditions
Consider an optimization problem of the form:

$$\begin{aligned} \min_{\mathbf{x}} \quad & f(\mathbf{x}) \\ \text{s.t.} \quad & g_i(\mathbf{x}) \leq 0, \quad i = 1, \dots, m, \\ & h_j(\mathbf{x}) = 0, \quad j = 1, \dots, p, \end{aligned} \tag{P}$$

where $f : \mathbb{R}^n \to \mathbb{R}$, $\mathbf{g} = (g_1, \dots, g_m) : \mathbb{R}^n \to \mathbb{R}^m$, and $\mathbf{h} = (h_1, \dots, h_l) : \mathbb{R}^n \to \mathbb{R}^l$ are assumed to be continuously differentiable on an open neighborhood of the region of interest.
The feasible set of problem (P) is denoted by $S = \{x \in \mathbb{R}^n : \mathbf{h}(x) = 0, \mathbf{g}(x) \leq 0\}$ and is assumed to be non-empty. The set denoted as $I_0(x^*) = \{i : g_i(x^*) = 0\}$ is the index set of the inequality constraints active at $x^* \in S$.

Proposition 2.1 (Karush-Kuhn-Tucker Necessary Optimality Conditions)**.** *Let $x^* \in S$ be a local minimum point and suppose that the functions f, g, h are continuously differentiable in an open neighborhood of x^*.*
Suppose further that at x^* one of the following constraints qualification holds.

(C1) Linear independence of the gradients of active constraints at x^*.

(C2) Concavity at x^* of the constraints active at x^*.

(C3) Mangasarian-Fromovitz conditions.

(C4) Slater's condition.

Then there exist $\lambda^* \in \mathbb{R}^m$ *and* $\mu^* \in \mathbb{R}^p$ *such that the following KKT conditions hold.*

$$
\begin{aligned}
&\nabla f(x^*) + \nabla g(x^*)\lambda + \nabla h(x^*) = 0 \\
&g(x^*) \leq 0, \qquad h(x^*) = 0 \\
&\lambda^{*\top} g(x^*) = 0 \\
&\lambda^* \geq 0
\end{aligned}
\tag{2.1}
$$

Proposition 2.2 (Sufficiency of KKT Conditions in the Convex Case)**.** *Assume that the functions* f, g_i *for* $i = 1, \dots, m$ *are convex and that the equality constraints* h_i *are defined by affine functions, that is* $h(x) \equiv Ax - b$*, for some* $A \in \mathbb{R}^{p \times n}$ *and* $b \in \mathbb{R}^p$*. Assume also that all the problem functions are continuously differentiable on an open set containing the feasible set.*
Then, if there exist multipliers λ^* *and* μ^* *such that the KKT conditions are satisfied at a point* $x^* \in \mathbb{R}^n$*, that is*

$$
\begin{aligned}
&\nabla f(x^*) + \nabla g(x^*)\lambda + \nabla h(x^*) = 0 \\
&g(x^*) \leq 0, \qquad h(x^*) = 0 \\
&\lambda^{*\top} g(x^*) = 0 \\
&\lambda^* \geq 0
\end{aligned}
\tag{2.2}
$$

the point x^**is a global minimum point of the constrained problem; moreover if* f *is strictly convex, the point* x^**is the unique global solution.*

The remaining results in this section follow [6].

Lagrangian duality

Consider a generic optimization problem, hereafter referred to as the Primal Problem (P), of the form:

$$
\begin{aligned}
\min_{\mathbf{x}} \quad & f(\mathbf{x}) \\
\text{s.t.} \quad & g_i(\mathbf{x}) \leq 0, \quad i = 1, \dots, m, \\
& h_j(\mathbf{x}) = 0, \quad j = 1, \dots, p, \\
& \mathbf{x} \in X
\end{aligned}
\tag{P}
$$

where $f: \mathbb{R}^n \to \mathbb{R}$, $g_i: \mathbb{R}^n \to \mathbb{R}$ $i = 1, \dots, m$, $h_j: \mathbb{R}^n \to \mathbb{R}$, $j = 1, \dots, p.$

A problem of the form defined below is referred to as the Dual Problem (D).

$$
\begin{aligned}
\max_{\mathbf{u}, \mathbf{v}} \quad & \theta(\mathbf{u}, \mathbf{v}) \\
\text{s.t.} \quad & \mathbf{u} \geq \mathbf{0}
\end{aligned}
\tag{D}
$$

where

$$\theta(\mathbf{u},\mathbf{v}) := \inf_{\mathbf{x}\in X} \left\{ f(\mathbf{x}) + \mathbf{u}^\top \mathbf{g}(\mathbf{x}) + \mathbf{v}^\top \mathbf{h}(\mathbf{x}) \right\}. \tag{2.3}$$

Note that, given a nonlinear programming problem, different Lagrangian dual problems can be defined depending on which constraints are included in $\mathbf{g}(\mathbf{x}) \leq \mathbf{0}$ and $\mathbf{h}(\mathbf{x}) = \mathbf{0}$, and which constraints are incorporated into the set X.

Theorem 2.3 (Weak Duality)**.** *Let* $\mathbf{x}$ *be a feasible solution to Problem P. Also, let* $(\mathbf{u},\mathbf{v})$ *be a feasible solution to Problem D. Then:*

$$f(\mathbf{x}) \geq \theta(\mathbf{u},\mathbf{v}) \tag{2.4}$$

Theorem 2.4 (Strong Duality)**.** *Let* X *be a non-empty convex set in* R^n*, let* $f : R^n \to R$ *and* $\boldsymbol{g} : R^n \to R^m$ *be convex, and let* $\boldsymbol{h} : R^n \to R^l$ *be affine; that is,* $\boldsymbol{h}$ *is of the form* $\boldsymbol{h(x)} = \boldsymbol{Ax} - b$*. Suppose that the following constraint qualification holds true. There exists an* $\hat{\mathbf{x}} \in X$ *such that* $\mathbf{g}(\hat{\mathbf{x}}) < 0$ *and* $\mathbf{h}(\hat{\mathbf{x}}) = \mathbf{0}$*, and* $\mathbf{0} \in int\, \mathbf{h}(\mathbf{X})$*, where* $\mathbf{h}(\mathbf{X}) = \{\mathbf{h}(\mathbf{x}) : \mathbf{x} \in \mathbf{X}\}$*. Then*

$$inf\{f(\boldsymbol{x}) : \boldsymbol{x} \in X, \boldsymbol{g(x)} \leq \boldsymbol{0}, \boldsymbol{h(x)} = \boldsymbol{0}\} = sup\{\theta(\boldsymbol{u,v}) : \boldsymbol{u} \geq \boldsymbol{0}\}$$

Furthermore, if the inf *is finite, the* $\sup\{\theta(\mathbf{u},\mathbf{v}) : \mathbf{u} \geq \boldsymbol{0}\}$ *is achieved at* $(\bar{\mathbf{u}},\bar{\mathbf{v}})$ *with* $\bar{\mathbf{u}} \geq 0$*. If the* inf *is achieved at* $\mathbf{x}$*, then* $\bar{\mathbf{u}}^T \mathbf{g}(\bar{\mathbf{x}}) = 0$*.*

Given a primal Problem P, the Lagrangian function is defined:

$$\phi(\mathbf{x},\mathbf{u},\mathbf{v}) = f(\mathbf{x}) + \mathbf{u}^t \mathbf{g}(\mathbf{x}) + \mathbf{v}^t \mathbf{h}(\mathbf{x}) \tag{2.5}$$

Definition 2.5 (Lagrangian Saddle Point)**.** A solution $(\bar{\mathbf{x}},\bar{\mathbf{u}},\bar{\mathbf{v}})$ is called a *saddle point* of the Lagrangian function if $\bar{\mathbf{x}} \in X, \bar{\mathbf{u}}$, and

$$\phi(\bar{\mathbf{x}},\mathbf{u},\mathbf{v}) \leq \phi(\bar{\mathbf{x}},\bar{\mathbf{u}},\bar{\mathbf{v}}) \leq \phi(\mathbf{x},\bar{\mathbf{u}},\bar{\mathbf{v}}) \quad \forall \mathbf{x} \in X, \text{and all } (\mathbf{u},\mathbf{v}) with \mathbf{u} \geq 0 \tag{2.6}$$

Theorem 2.6 (Saddle Point Optimality and Absence of a Duality Gap)**.** *A solution* $(\bar{x},\bar{u},\bar{v})$ *with* $\bar{x} \in X$ *and* $\bar{u} \geq 0$ *is a saddle point for the Lagrangian function* $\phi(\mathbf{x},\mathbf{u},\mathbf{v}) = f(\mathbf{x}) + \mathbf{u}^\mathbf{t} \mathbf{g}(\mathbf{x}) + \mathbf{v}^\mathbf{t} \mathbf{h}(\mathbf{x})$ *if and only if:*

a. $\phi(\bar{\mathbf{x}},\bar{\mathbf{u}},\bar{\mathbf{v}}) = min\{\phi(\mathbf{x},\bar{\mathbf{u}},\bar{\mathbf{v}}) : \mathbf{x} \in X\}$

b. $\mathbf{g}(\bar{\mathbf{x}}) \leq 0$, $\mathbf{h}(\bar{\mathbf{x}}) = \mathbf{0}$*, and*

c. $\bar{\mathbf{u}}^\mathbf{t} \mathbf{g}(\bar{\mathbf{x}}) = 0$

Moreover,$(\bar{\mathbf{x}},\bar{\mathbf{u}},\bar{\mathbf{v}})$ *is a saddle point if and only if* $\bar{\mathbf{x}}$ *and* $(\bar{\mathbf{u}},\bar{\mathbf{v}})$ *are, respectively, optimal solutions to the primal and dual problems P and D with no duality gap, that is, with* $f(\bar{\mathbf{x}}) = \theta(\bar{\mathbf{u}},\bar{\mathbf{v}})$*.*

2.3 Framework

In what follows, formal definitions of the problems that constitute the framework are given.

Player Optimization Problem. Each player $i \in I$ that participates in the market solves, given exogenously a price vector $\pi \in \mathbb{R}^{n_\pi}$, an optimization problem of the form

$$\min_{y_i} \; f_i(y_i, \pi) := c_i(y_i) + \pi^\top h_i(y_i) \quad \text{s.t.} \quad y_i \in Y_i. \tag{2.7}$$

Here, $y_i \in \mathbb{R}^{n_i}$ denotes the decision variables of player i and $Y_i \subseteq \mathbb{R}^{n_i}$ is a non-empty feasible set. The objective function $f_i : \mathbb{R}^{n_i} \times \mathbb{R}^{n_\pi} \to \mathbb{R}$ is composed of two terms: the cost function $c_i : \mathbb{R}^{n_i} \to \mathbb{R}$ and the term $\pi^\top h_i(y_i)$, where $h_i : \mathbb{R}^{n_i} \to \mathbb{R}^{n_\pi}$ represents the net quantity of goods traded by player i at prices π.

Welfare Optimization Problem (WFP). The *Welfare Optimization Problem* consists in minimizing the sum of all players' objective functions, subject to the individual feasibility constraints of each player and to the market-clearing condition. The problem is defined as:

$$\begin{aligned} \min_{y \in Y} \quad & \sum_{i \in I} c_i(y_i) \\ \text{s.t.} \quad & \sum_{i \in I} h_i(y_i) = 0. \end{aligned} \tag{WFP}$$

Here, $y := (y_i)_{i \in I} \in \mathbb{R}^{n_y}$, with $n_y = \sum_{i \in I} n_i$, and $Y := \prod_{i \in I} Y_i$ denotes the Cartesian product of the individual feasible sets.

Lagrangian and dual problem. Define the Lagrangian associated with (WFP) as

$$L(y, \pi) := \sum_{i \in I} \left(c_i(y_i) + \pi^\top h_i(y_i)\right), \qquad y \in Y, \; \pi \in \mathbb{R}^{n_\pi}. \tag{2.8}$$

The corresponding dual problem is:

$$\sup_{\pi \in \mathbb{R}^{n_\pi}} \; d(\pi), \tag{2.9}$$

where the dual function d is defined by

$$d(\pi) := \inf_{y \in Y} L(y, \pi). \tag{2.10}$$

Market Equilibrium Problem (MEP). Consider a competitive equilibrium model in which each player solves an individual optimization problem and market equilibrium is enforced through a market-clearing condition requiring aggregate demand to equal aggregate supply. The analysis is carried out under the assumption of perfect competition. This framework gives rise to the *Market Equilibrium Problem* (MEP). A solution to the MEP consists of a price vector π such that, for every player $i \in I$, an optimal solution to the corresponding optimization problem exists and the resulting decisions jointly satisfy the market-clearing condition.

Formally, the MEP is defined by the collection of players' optimization problems together with the market-clearing condition

$$\begin{aligned} \forall i \in I: \quad & \min_{y_i \in Y_i} \; c_i(y_i) + \pi^\top h_i(y_i), \\ & \sum_{i \in I} h_i(y_i) = 0. \end{aligned} \tag{MEP}$$

The Market Equilibrium Problem can be reformulated as a Nash Equilibrium Problem by introducing an artificial player. This player controls the price vector π and solves an unconstrained optimization problem whose objective function is unbounded whenever the market-clearing condition is violated, while it is constant otherwise. As a result, any Nash equilibrium of the reformulated game satisfies the market-clearing condition and corresponds to a market equilibrium. The resulting Nash Equilibrium Problem is defined by the collection of the players' optimization problems (2.7) together with the artificial player's problem:

$$\begin{aligned} \forall i \in I: \quad & \min_{y_i \in Y_i} \; c_i(y_i) + \pi^\top h_i(y_i), \\ & \min_{\pi \in \mathbb{R}^{n_\pi}} \; \pi^\top \sum_{i \in I} h_i(y_i). \end{aligned} \tag{2.11}$$

The Market Equilibrium Problem and the Welfare Optimization Problem are closely related. When the individual players' optimization problems are convex for any given price vector π, it is well known that, whenever the Welfare Optimization Problem (WFP) admits an optimal solution, the corresponding primal solution and the Lagrange multipliers associated with the market-clearing condition jointly induce a market equilibrium. However, when nonconvexities are present in the players' optimization problems, this property no longer holds, and the existence of a market equilibrium is not guaranteed.

Given the presented problem structure, the following auxiliary lemma is stated.

Lemma 2.7. *The following equivalence holds:*

$$y^* \in \arg\min_{y \in Y} L(y, \pi) \iff y_i^* \in \arg\min_{y_i \in Y_i} \{c_i(y_i) + \pi^\top h_i(y_i)\}, \quad \forall i \in I, \tag{2.12}$$

where $L(y, \pi) = \sum_{i \in I} (c_i(y_i) + \pi^\top h_i(y_i))$ *and* $Y = \prod_{i \in I} Y_i$.

Proof. First, it is shown that

$$y^* \in \arg\min_{y \in Y} L(y, \pi) \;\Rightarrow\; y_i^* \in \arg\min_{y_i \in Y_i} \{c_i(y_i) + \pi^\top h_i(y_i)\}, \quad \forall i \in I.$$

Assume by contradiction that $y^* \in \arg\min_{y \in Y} L(y, \pi)$, and suppose that there exists a non-empty subset $J \subseteq I$ and a vector $\hat{y} \in Y$ such that, for every $j \in J$,

$$c_j(\hat{y}_j) + \pi^\top h_j(\hat{y}_j) < c_j(y_j^*) + \pi^\top h_j(y_j^*).$$

Then,

$$\sum_{i \in I \setminus J} (c_i(y_i^*) + \pi^\top h_i(y_i^*)) + \sum_{j \in J} (c_j(\hat{y}_j) + \pi^\top h_j(\hat{y}_j)) < \sum_{i \in I} (c_i(y_i^*) + \pi^\top h_i(y_i^*)).$$

Define $\bar{y} \in Y$ by

$$\bar{y}_i = \begin{cases} y_i^*, & i \in I \setminus J, \\ \hat{y}_i, & i \in J. \end{cases}$$

Then $L(\bar{y}, \pi) < L(y^*, \pi)$, contradicting the assumption that y^* minimizes $L(\cdot, \pi)$ over Y.

Now, assume that

$$y_i^* \in \arg\min_{y_i \in Y_i} \{c_i(y_i) + \pi^\top h_i(y_i)\}, \quad \forall i \in I.$$

Equivalently, for every $i \in I$ and every $y_i \in Y_i$,

$$c_i(y_i) + \pi^\top h_i(y_i) \geq c_i(y_i^*) + \pi^\top h_i(y_i^*).$$

Let $y \in Y$ be arbitrary. Since $Y = \prod_{i \in I} Y_i$, it holds that $y_i \in Y_i$ for all $i \in I$. Summing the above inequalities over $i \in I$ yields

$$L(y, \pi) = \sum_{i \in I} (c_i(y_i) + \pi^\top h_i(y_i)) \geq \sum_{i \in I} (c_i(y_i^*) + \pi^\top h_i(y_i^*)) = L(y^*, \pi).$$

Hence $y^* \in \arg\min_{y \in Y} L(y, \pi)$. □

Set Π of Market Equilibrium Prices. Let $\Pi(y^*) \subseteq \mathbb{R}^{n_\pi}$ be the set that includes all the market equilibrium prices, i.e., it satisfies the property:

$$(y^*, \pi^*) \text{ is a market equilibrium of (MEP)} \Rightarrow \pi^* \in \Pi(y^*) \tag{2.13}$$

Assume $\Pi(y^*) \neq \emptyset$, since otherwise no market equilibrium exists. The set $\Pi(y^*)$ contains all the prices that constitute a market equilibrium in pair with the solution y^*.

Assumption 2.8. An enclosing box for $\Pi(y^*)$ can be computed in the form

$$\{\pi \in \mathbb{R}^{n_\pi} : \pi_k^- \leq \pi_k \leq \pi_k^+ \quad \forall k \in \{1, \ldots, n_\pi\}\}, \tag{2.14}$$

where $\pi_k^-, \pi_k^+ \in \mathbb{R} \cup \{-\infty, \infty\}$.

2.4 Theoretical results

The main purpose of this section is to propose the analysis of the relationship between the welfare optimization problem and the market equilibrium problem. In particular, as it is one of the main contributions of the analyzed paper, the study focuses on how to use global solutions of WFP to find a market equilibrium or to determine that no market equilibria exist. The algorithm proposed is discussed in depth in Section 2.5. To this end, in what follows, theoretical results are presented and explained, with additional proofs specific to this context.

The first result, Theorem 2.9, is an adaptation to the context of a result from [42], which states the equivalence between the market equilibria of MEP and primal-dual pairs of solutions of the WFP problem with zero duality gap.

Theorem 2.9. *The pair (y^*, π^*) is a market equilibrium of (MEP) if and only if y^* and π^* are global solutions of the welfare optimization problem* (WFP) *and the corresponding Lagrangian dual problem* (2.9)*, respectively, with zero duality gap.*

Proof. Assume that the duality gap is zero. It is shown that (y^*, π^*) is a market equilibrium.

By definition, (y^*, π^*) is a market equilibrium if no player can benefit from a unilateral deviation. This condition is satisfied if, for every $i \in I$,

$$y_i^* \in \arg\min_{y_i \in Y_i} \{c_i(y_i) + {\pi^*}^\top h_i(y_i)\},$$

under the feasibility conditions $y_i^* \in Y_i$ and $\sum_{i \in I} h_i(y_i^*) = 0$, which coincide with the constraints of the welfare optimization problem (WFP).

Since y^* is a global solution of the WFP, feasibility is guaranteed and the conditions

$$y^* \in Y \quad \text{and} \quad \sum_{i \in I} h_i(y_i^*) = 0$$

are satisfied.

It remains to verify that y_i^* solves the individual optimization problem for each $i \in I$. By the hypothesis of zero duality gap, it holds that

$$\min_{y \in Y} \sum_{i \in I} c_i(y_i) = \max_{\pi \in \mathbb{R}^{n_\pi}} \inf_{y \in Y} L(y, \pi),$$

and, in particular,

$$\sum_{i \in I} c_i(y_i^*) = \inf_{y \in Y} L(y, \pi^*) = \inf_{y \in Y} \sum_{i \in I} (c_i(y_i) + \pi^{*\top} h_i(y_i)).$$

By Theorem 2.6, the pair (y^*, π^*) is a saddle point of the Lagrangian if and only if y^* and π^* are optimal solutions of the primal and dual problems, respectively, with zero duality gap. Equivalently,

$$L(y^*, \pi^*) = \min_{y \in Y} L(y, \pi^*).$$

Finally, by Lemma 2.7, the separability of the Lagrangian implies

$$y^* \in \arg\min_{y \in Y} L(y, \pi^*) \iff y_i^* \in \arg\min_{y_i \in Y_i} \{c_i(y_i) + \pi^{*\top} h_i(y_i)\}, \quad \forall i \in I.$$

This proves the first implication.

Assume now that (y^*, π^*) is a market equilibrium. It is then shown that the duality gap is zero.

Since (y^*, π^*) is an equilibrium, the feasibility condition

$$\sum_{i \in I} h_i(y_i^*) = 0$$

holds, and for each $i \in I$,

$$y_i^* \in \arg\min_{y_i \in Y_i} \{c_i(y_i) + \pi^{*\top} h_i(y_i)\}.$$

Define the dual function as

$$\mu(\pi) = \inf_{y \in Y} \sum_{i \in I} (c_i(y_i) + \pi^\top h_i(y_i)).$$

Then,

$$\begin{aligned}
\mu(\pi^*) &= \inf_{y \in Y} \sum_{i \in I} (c_i(y_i) + \pi^{*\top} h_i(y_i)) \\
&= \sum_{i \in I} (c_i(y_i^*) + \pi^{*\top} h_i(y_i^*)) \\
&= \sum_{i \in I} c_i(y_i^*) + \pi^{*\top} \sum_{i \in I} h_i(y_i^*) \\
&= \sum_{i \in I} c_i(y_i^*).
\end{aligned}$$

Therefore, the optimal primal and dual values coincide, and the duality gap is zero. □

Authors derive new results from the Theorem 2.9, stated in the following Corollary.

Corollary 2.10. *(a) If (y^*, π^*) is a market equilibrium of (MEP), then y^* is a global solution of the welfare problem (WFP).*

(b) If (y^*, π^*) is a market equilibrium of (MEP), then (y, π^*) is a market equilibrium of (MEP) for all global solutions y of the welfare problem.

(c) If (y^*, π^*) and $(\hat{y}, \hat{\pi})$ are two market equilibria of (MEP), then so are $(y^*, \hat{\pi})$ and $(\hat{y}, \pi^*)$.

(d) If y^* is a global solution of the welfare problem (WFP) for which there exists no π such that (y^*, π) is a market equilibrium of (MEP), then the market equilibrium problem (MEP) has no solution.

Proof. (a) The statement follows directly from Theorem 2.9.

(b) Let $\hat{y}$ be a global solution of the welfare problem (WFP). Since (y^*, π^*) is a market equilibrium of (MEP), Theorem 2.9 implies that π^* is a global solution of the dual problem and that

$$\sum_{i \in I} c_i(y_i^*) = d(\pi^*).$$

Moreover, since $\hat{y}$ is also a global solution of (WFP), global optimality implies that

$$\sum_{i \in I} c_i(\hat{y}_i) = \sum_{i \in I} c_i(y_i^*).$$

Hence,

$$\sum_{i \in I} c_i(\hat{y}_i) = d(\pi^*),$$

and Theorem 2.9 applies to the pair $(\hat{y}, \pi^*)$, which is therefore a market equilibrium of (MEP).

(c) Assume that (y^*, π^*) and $(\hat{y}, \hat{\pi})$ are two market equilibria of (MEP). By Theorem 2.9, y^* and $\hat{y}$ are global solutions of the welfare problem and π^* and $\hat{\pi}$ are global solutions of the dual problem, with zero duality gap. Therefore,

$$\sum_{i \in I} c_i(y_i^*) = d(\pi^*), \qquad \sum_{i \in I} c_i(\hat{y}_i) = d(\hat{\pi}).$$

Since y^* and $\hat{y}$ are both global solutions of (WFP), it follows that

$$\sum_{i \in I} c_i(y_i^*) = \sum_{i \in I} c_i(\hat{y}_i).$$

Consequently,

$$\sum_{i \in I} c_i(y_i^*) = d(\hat{\pi}), \qquad \sum_{i \in I} c_i(\hat{y}_i) = d(\pi^*).$$

Applying again Theorem 2.9, both pairs $(y^*, \hat{\pi})$ and $(\hat{y}, \pi^*)$ are market equilibria of (MEP).

(d) A pair (y, π) is a market equilibrium of (MEP) if and only if y is a global solution of the welfare problem (WFP) and π is a global solution of the dual problem, with zero duality gap.

Assume by contradiction that the market equilibrium problem (MEP) admits at least one solution, but that there exists a global solution y^* of (WFP) for which no π makes (y^*, π) a market equilibrium. Then there exists another global solution $\hat{y}$ of (WFP) and some π such that $(\hat{y}, \pi)$ is a market equilibrium. By part (b), (y^*, π) must also be a market equilibrium, contradicting the hypothesis. Hence, the market equilibrium problem (MEP) has no solution.

□

Corollary 2.10 formalize specific properties of the framework. Part (a) shows that only the global solutions of the welfare problem are candidates for a market equilibrium. Part (b) states that if there exists a global solution of the (WFP) which participates in an equilibrium, then all other global solutions of the (WFP) (if there is any) constitute an equilibrium with the same dual solution. It follows directly that the same property holds for any dual global solution in pair with a fixed global solution of the primal. Part (c) states that different solutions pairs can be mixed. Under the stated assumptions, all market equilibria associated with zero duality gap are equivalent with respect to the welfare criterion and the individual optimality conditions. Nevertheless, such equilibria may differ in terms of the underlying allocations and in the decomposition between real costs and monetary transfers, which are not explicitly evaluated by the model. As a consequence, the mathematical equivalence of equilibria does not necessarily imply equivalence with respect to unmodeled economic or operational considerations. Part (d) states that if there exists no dual solution such that (y^*, π), with y^* a global solution of the (WFP), is an equilibrium, then the (MEP) has no solution.

As already discussed, in nonconvex settings the requirement of a zero duality gap may represent a significant obstacle. The following results provide the foundation for the proposed algorithm, which exploits the presence of players with a unique best response in order to recover global properties of the equilibrium structure. A player has a *unique best response* if its optimization problem (2.7) admits at most one global optimal solution for any given price vector. This property is satisfied, for instance, when the feasible set is convex and the objective function is strictly convex. In terms of equilibria, this implies that, for any given equilibrium price vector π^*, the equilibrium decision y_i^* is unique for every player i with a unique best response. Consequently, if the Welfare Optimization Problem admits multiple global optimal solutions, these solutions must coincide on the components y_i of all players with a unique best response; any multiplicity can only occur in the decisions of the remaining players. This observation is formalized by the original authors in the following corollary, which characterizes the implications of unique best responses on equilibrium allocations.

Corollary 2.11. *Let $S \subseteq I$ be the set of players with unique best responses for all price vectors $\pi \in \mathbb{R}^n_\pi$.*

(a) If (y^*, π^*) and $(\hat{y}, \hat{\pi})$ are two market equilibria of (MEP), then $y^*_S = \hat{y}_S$.

(b) If y^* and $\hat{y}$ are two global solutions of the welfare problem (WFP) with $y^*_S \neq \hat{y}_S$, then the market equilibrium problem (MEP) does not have a solution.

Proof. (a) By Corollary 2.10 part (c), $(\hat{y}, \pi^*)$ is also a market equilibrium. Consequently, both y_i^* and $\hat{y}_i$ are global solutions of the optimization problem (1) for player i with price π^*. For all players $i \in S$, this solution is unique, and therefore $y^*_S = \hat{y}_S$ holds.

(b) If the market equilibrium problem admits a solution for some price vector π, then both (y^*, π) and $(\hat{y}, \pi)$ are market equilibria. By Corollary 2.10 part (a), it follows that $y_S^* = \hat{y}_S$.

□

The following result characterizes the existence of a market equilibrium by relating it to a global solution of the welfare optimization problem together with a specific price vector. The price vector considered is determined as a function of the net quantities of goods exchanged by the players at the WFP solution.

Theorem 2.12. *Let y^* be a global solution of the welfare problem WFP, and let $\Pi(y^*) \neq \emptyset$ be a set satisfying Condition* (2.13)*. Assume that for all $k \in \{1, \dots, n_\pi\}$ at least one of the following properties is satisfied:*

(a) $\pi_k^- = \pi_k^+$,

(b) $\pi_k^+ < \infty$ *and* $(h_i(y_i^*))_k \leq (h_i(y_i))_k$ *for all* $y_i \in Y_i$ *and all players* $i \in I$,

(c) $\pi_k^- > -\infty$ *and* $(h_i(y_i^*))_k \geq (h_i(y_i))_k$ *for all* $y_i \in Y_i$ *and all players* $i \in I$,

(d) $\pi_k^- = -\infty$, $\pi_k^+ = \infty$, *and* $(h_i(y_i^*))_k = (h_i(y_i))_k$ *for all* $y_i \in Y_i$ *and all players* $i \in I$.

Then, there exists a market equilibrium of MEP if and only if $(y^*, \hat{\pi})$ is a market equilibrium, where the critical price $\hat{\pi}$ is defined as

$$\hat{\pi} = \begin{cases} \pi_k^- = \pi_k^+, & \text{if (a) applies,} \\ \pi_k^+, & \text{if (b) applies,} \\ \pi_k^-, & \text{if (c) applies,} \\ 0, & \text{if (d) applies.} \end{cases}$$

Proof. The "only if" direction is immediate: if $(y^*, \hat{\pi})$ is a market equilibrium, then a market equilibrium exists by definition.

It remains to verify that if there exists a market equilibrium, y^* is a global solution of the welfare problem (WFP), $\Pi(y^*)$ is non-empty and satisfies Condition 2.13, and one of properties (a)-(d) is satisfied, then $(y^*, \hat{\pi})$ is a market equilibrium, where $\hat{\pi}$ is the critical price.
The argument now proceeds by contraposition: it suffices to show that if $(y^*, \hat{\pi})$ is not a market equilibrium, then (y^*, π) is not a market equilibrium for any $\pi \in \Pi(y^*)$. By Corollary 2.10, part (d), if y^* is a global solution of (WFP) and there exists no price π such that (y^*, π) is a market equilibrium, then the market equilibrium problem (MEP) admits no solution. Therefore, establishing the above implication suffices to conclude the proof. Recalling the individual objective function (2.7) and the fact that y^* is feasible, (y^*, π) fails to be a market equilibrium if and only if there exist a player $i \in I$ and a feasible strategy $y_i \in Y_i$ such that

$$f_i(y_i, \pi) - f_i(y_i^*, \pi) < 0.$$

Assume now that $(y^*, \hat{\pi})$ is not a market equilibrium. For every player $i \in I$ and all $y_i \in Y_i$ as well as all $\pi \in \Pi(y^*)$, the difference in the player's objective function values is

$$\begin{aligned} f_i(y_i, \pi) - f_i(y_i^*, \pi) &= c_i(y_i) - c_i(y_i^*) + \pi^\top (h_i(y_i) - h_i(y_i^*)) \\ &= c_i(y_i) - c_i(y_i^*) + \sum_{k=1}^{n} \pi_k (h_i(y_i) - h_i(y_i^*))_k. \end{aligned}$$

For fixed $i \in I$ and $y_i \in Y_i$, the function

$$\pi \mapsto f_i(y_i, \pi) - f_i(y_i^*, \pi)$$

is affine in π. Under assumptions (a)–(d), each component of this function is monotone with respect to π_k over the interval $[\pi_k^-, \pi_k^+]$. Consequently, its maximum over $\Pi(y^*)$ is attained at the critical price $\hat{\pi}$. More precisely:

- in case (a), the price is uniquely determined;
- in case (b), $(h_i(y_i) - h_i(y_i^*))_k \geq 0$, hence the maximum is attained at π_k^+;
- in case (c), $(h_i(y_i) - h_i(y_i^*))_k \leq 0$, hence the maximum is attained at π_k^-;
- in case (d), $(h_i(y_i) - h_i(y_i^*))_k = 0$, so the price choice is irrelevant and is set to zero.

It follows that, for all $\pi \in \Pi(y^*)$,

$$f_i(y_i, \pi) - f_i(y_i^*, \pi) \leq f_i(y_i, \hat{\pi}) - f_i(y_i^*, \hat{\pi}).$$

Since $(y^*, \hat{\pi})$ is not a market equilibrium, the right-hand side is strictly negative for some $i \in I$ and $y_i \in Y_i$. Therefore,

$$f_i(y_i, \pi) - f_i(y_i^*, \pi) < 0 \quad \forall \pi \in \Pi(y^*),$$

which implies that no price $\pi \in \Pi(y^*)$ supports y^* as a market equilibrium. This concludes the proof. □

Theorem 2.12 relies heavily on set $\Pi(y^*)$ and the resulting enclosing box. Since it can be hard to compute the set or the associated enclosing box, it becomes essential to exploit the necessary optimality conditions of the players' optimization problems. These conditions, evaluated at a global solution of (WFP), restrict the pool of market equilibrium prices. Problem (2.7) does not depend on strict assumptions, aside from the objective function structure, thus it is flexile enough to allow for different players and different optimality conditions. For the player whose optimization problem is characterized by necessary and sufficient KKT conditions, the authors propose a modification of Theorem 2.12, weakening the assumptions by using the optimality condition to compute the set $\Pi(y^*)$. This result is formally stated in the following Corollary.

Corollary 2.13. *Let y^* be a global solution of the welfare problem (WFP). Moreover, let $C \subseteq I$ denote the subset of players for which the KKT conditions (2.2) are necessary and sufficient optimality conditions, and choose the candidate set $\Pi(y^*)$ such that Condition (2.13) as well as the KKT conditions of all players $i \in C$ are satisfied, i.e.,*

$$\Pi(y^*) \subseteq \{\pi \in \mathbb{R}^{n_\pi} : \forall\, i \in C \text{ there exists } \mu_i \text{ such that } (2.2) \text{ holds}\}.$$

Assume that for all $k \in \{1, \ldots, n_\pi\}$ at least one of the following properties is satisfied:

(a) $\pi_k^- = \pi_k^+$,

(b) $\pi_k^+ < \infty$ *and* $(h_i(y_i^*))_k \leq (h_i(y_i))_k$ *for all* $y_i \in Y_i$ *and all players* $i \in I \setminus C$,

(c) $\pi_k^- > -\infty$ *and* $(h_i(y_i^*))_k \geq (h_i(y_i))_k$ *for all* $y_i \in Y_i$ *and all players* $i \in I \setminus C$,

(d) $\pi_k^- = -\infty$, $\pi_k^+ = \infty$, *and* $(h_i(y_i^*))_k = (h_i(y_i))_k$ *for all* $y_i \in Y_i$ *and all players* $i \in I \setminus C$.

Now, let the critical price $\hat{\pi}$ *be defined as*

$$\hat{\pi}_k := \begin{cases} \pi_k^- = \pi_k^+, & \textit{if (a) applies,} \\ \pi_k^+, & \textit{if (b) applies,} \\ \pi_k^-, & \textit{if (c) applies,} \\ 0, & \textit{if (d) applies.} \end{cases}$$

If the critical price satisfies $\hat{\pi} \in \Pi(y^*)$, *then there exists a market equilibrium of (MEP) if and only if* $(y^*, \hat{\pi})$ *is a market equilibrium.*

Proof. The "if" direction follows directly from the definition: if $(y^*, \hat{\pi})$ is a market equilibrium, then a market equilibrium exists by definition.

The "only if" direction is proved by contradiction. Assume that $(y^*, \hat{\pi})$ is not a market equilibrium. By construction of the candidate set $\Pi(y^*)$ and since $\hat{\pi} \in \Pi(y^*)$, the KKT conditions are satisfied for all players $i \in C$, and y_i^* constitutes a best response to $\hat{\pi}$ for all $i \in C$. Consequently, if $(y^*, \hat{\pi})$ is not a market equilibrium, this must be due to the existence of at least one player $i \in I \setminus C$ for whom there exists a strategy $y_i \in Y_i$ such that

$$f_i(y_i, \hat{\pi}) < f_i(y_i^*, \hat{\pi}).$$

The remainder of the proof follows analogously to that of Theorem 2.12. □

Compared with Theorem 2.12, Corollary 2.13 requires conditions (a)–(d) to be verified only for players whose KKT optimality conditions are not inherently satisfied for pairs $(y^*, \pi) : \pi \in \Pi(y^*)$. However, it becomes necessary to verify whether the critical price belongs to the set $\Pi(y^*)$, which accounts for players with known optimality conditions.

The versions of Theorem 2.12 and Corollary 2.13 for the maximization case of problem (2.7), together with the corresponding market equilibrium and welfare optimization problems, are now stated without proof.

The maximization player optimization problem is:

$$\max_{y_i} \quad f_i(y_i, \pi) := c_i(y_i) + \pi^\top h_i(y_i) \quad \text{s.t.} \quad y_i \in Y_i. \tag{max-OFP}$$

The corresponding market equilibrium problem reads:

$$\begin{aligned} \forall i \in I: \quad & \max_{y_i \in Y_i} \; c_i(y_i) + \pi^\top h_i(y_i), \\ & \sum_{i \in I} h_i(y_i) = 0. \end{aligned} \tag{max-MEP}$$

The maximization welfare optimization problem becomes:

$$\max_{y} \quad \sum_{i\in I} c_i(y_i) \quad s.t. \quad y \in Y, \sum_{i\in I} h_i(y_i) = 0 \tag{max-WFP}$$

Corollary 2.14. *Let y^* be a global solution of the maximization welfare problem* (max-WFP), *and let $\Pi(y^*) \neq \emptyset$ be a set satisfying the condition*

$$(y^*, \pi^*) \text{ is a market equilibrium of (max-MEP)} \;\Rightarrow \pi^* \in \Pi(y^*).$$

Assume that for all $k \in \{1, \dots, n_\pi\}$ at least one of the following properties is satisfied:

(a) $\pi_k^- = \pi_k^+$,

(b) $\pi_k^+ < \infty$ *and* $(h_i(y_i^*))_k \geq (h_i(y_i))_k$ *for all* $y_i \in Y_i$ *and all players* $i \in I$,

(c) $\pi_k^- > -\infty$ *and* $(h_i(y_i^*))_k \leq (h_i(y_i))_k$ *for all* $y_i \in Y_i$ *and all players* $i \in I$,

(d) $\pi_k^- = -\infty$, $\pi_k^+ = \infty$, *and* $(h_i(y_i^*))_k = (h_i(y_i))_k$ *for all* $y_i \in Y_i$ *and all players* $i \in I$.

Then, there exists a market equilibrium of MEP if and only if $(y^*, \hat{\pi})$ is a market equilibrium, where the critical price $\hat{\pi}$ is defined as

$$\hat{\pi} = \begin{cases} \pi_k^- = \pi_k^+, & \text{if (a) applies,} \\ \pi_k^+, & \text{if (b) applies,} \\ \pi_k^-, & \text{if (c) applies,} \\ 0, & \text{if (d) applies.} \end{cases}$$

Corollary 2.15. *Let y^* be a global solution of the welfare problem (max-WFP). Moreover, let $C \subseteq I$ denote the subset of players for which the KKT conditions are necessary and sufficient optimality conditions, and choose the candidate set $\Pi(y^*)$ such that the condition condition*

$$(y^*, \pi^*) \text{ is a market equilibrium of max-MEP } \;\Rightarrow \pi^* \in \Pi(y^*)$$

as well as the KKT conditions of all players $i \in C$ are satisfied, i.e.,

$$\Pi(y^*) \subseteq \{\pi \in \mathbb{R}^{n_\pi} : \forall\, i \in C \text{ there exists } \mu_i \text{ such that KKT conditions holds}\}.$$

Assume that for all $k \in \{1, \dots, n_\pi\}$ at least one of the following properties is satisfied:

(a) $\pi_k^- = \pi_k^+$,

(b) $\pi_k^+ < \infty$ *and* $(h_i(y_i^*))_k \geq (h_i(y_i))_k$ *for all* $y_i \in Y_i$ *and all players* $i \in I \setminus C$,

(c) $\pi_k^- > -\infty$ *and* $(h_i(y_i^*))_k \leq (h_i(y_i))_k$ *for all* $y_i \in Y_i$ *and all players* $i \in I \setminus C$,

(d) $\pi_k^- = -\infty$, $\pi_k^+ = \infty$, *and* $(h_i(y_i^*))_k = (h_i(y_i))_k$ *for all* $y_i \in Y_i$ *and all players* $i \in I \setminus C$.

Now, let the critical price $\hat{\pi}$ be defined as

$$\hat{\pi}_k := \begin{cases} \pi_k^- = \pi_k^+, & \textit{if (a) applies,} \\ \pi_k^+, & \textit{if (b) applies,} \\ \pi_k^-, & \textit{if (c) applies,} \\ 0, & \textit{if (d) applies.} \end{cases}$$

If the critical price satisfies $\hat{\pi} \in \Pi(y^*)$, then there exists a market equilibrium of (MEP) if and only if $(y^*, \hat{\pi})$ is a market equilibrium.

2.5 Algorithm

One of the main contributions of [39] is an algorithm for determining whether an equilibrium of the Market Equilibrium Problem exists for both convex and nonconvex player problems, provided that the Welfare Problem can be solved to global optimality. In addition, the algorithm requires bounds on equilibrium prices, or, when prices are not uniquely determined by these bounds, a technical assumption.
The theoretical results presented in Section 2.4 provide the basis for the algorithm. The main idea is to combine the global solution of problem WFP with a given price vector to obtain a candidate equilibrium pair, and then to verify whether the global solution is optimal for each player's optimization problem under that price vector. The price vector to be tested is defined as in Theorem 2.12, or as in Corollary 2.13 if its assumptions are satisfied.
The authors underline a critical aspect of the proposed algorithm: the need to solve the Welfare Optimization Problem (WFP), which may be nonconvex, to global optimality in order to start the algorithm. Many problems in the energy field are NP-hard, as all the ones including the Alternate-Current Optimal Power Flow (ACOPF) equations. However, the wide variety of applications, while not reducing the inherent complexity of the problem, increases the number of techniques studied to help solving these problems to global optimality.
Another aspect to be considered is that the algorithm computes only a single equilibrium, even when multiple equilibria exist. Note that, in the case considered in Corollary 2.13, the algorithm has to be modified at Line 8, where it suffices to check whether y_i^* is a best response to the price vector $\hat{\pi}$ for all players in $I \setminus C$.

Theorem 2.16. *If the assumptions of Theorem 2.12 are satisfied and if the welfare optimization problem* (WFP) *can be solved to global optimality or it can be decided that it has no solution, then Algorithm 1 terminates correctly with either a market equilibrium of* (MEP) *or with the information that such an equilibrium does not exist.*

Proof. The result follows directly from Theorem 2.12 and Corollary 2.13. □

The algorithm proposed by Grübel et al. does not explicitly address the case in which the assumptions of Theorem 2.12 or Corollary 2.13 are not satisfied. Theorem 2.16 states that the assumptions of Theorem 2.12 or Corollary 2.13 have to be verified, thus avoiding the need for the algorithm to handle the opposite case. To generalize Algorithm 1, the pseudocode of Algorithm 2 is shown hereafter. It accounts for the possibility that the solution found does not satisfy the conditions of either Theorem 2.12 or Corollary 2.13, while also unifying the two cases covered by the theoretical results.

Algorithm 1 Deciding the existence of an equilibrium of (MEP) and computing an equilibrium in case of existence

Input: Market equilibrium problem (MEP)

Compute a global solution y^* of the welfare optimization problem (WFP).
if (WFP) cannot be solved **then**
    "No claim regarding the existence of equilibria can be made"
else if (WFP) does not have a solution **then**
    "No market equilibrium exists"
else
    Define the critical price vector $\hat{\pi}$ as in Theorem 2.12
    if y_i^* is a best response to the price vector $\hat{\pi}$ for all players $i \in I$ **then**
        $(y^*, \hat{\pi})$ is a market equilibrium
    else
        "No market equilibrium exists"
    end if
end if

Algorithm 2 Deciding the existence of an equilibrium of (MEP) and computing an equilibrium in case of existence

Compute a global solution y^* of the welfare optimization problem (WFP).
if (WFP) cannot be solved **then**
    "No claim regarding the existence of equilibria can be made"
    stop
else if (WFP) does not have a solution **then**
    "No market equilibrium exists"
    stop
end if
if Assumptions of Corollary 2.13 are satisfied **then**
    Define the critical price vector $\hat{\pi}$ as in Corollary 2.13
    Set $J \leftarrow I \setminus C$
else if Assumptions of Theorem 2.12 are satisfied **then**
    Define the critical price vector $\hat{\pi}$ as in Theorem 2.12
    Set $J \leftarrow I$
else
    "No claim regarding the existence of equilibria can be made"
    stop
end if
for each player $i \in J$ **do**
    if y_i^* is not a best response to the price vector $\hat{\pi}$ **then**
        "No market equilibrium exists"
        stop
    end if
end for
$(y^*, \hat{\pi})$ is a market equilibrium

2.6 ACOPF Application

The authors propose, in the original article, a scheme tailored to applications in energy market modeling. However, the ACOPF setting does not align naturally with the specific TSO problem structure and market-clearing conditions adopted in the paper. In that framework, the TSO verifies feasibility primarily through network flow variables, which are linked to demand and generation via the market-clearing conditions. As discussed by Bienstock et al. [11], the current and the injected power associated with a physical line generally differ at its two ends, due, for instance, to the presence of a transformer near one end or to line charging susceptance. Accordingly, the formulation is based on a directed graph, modeling each physical line by a pair of antiparallel arcs. The same representation is adopted here for the ACOPF case study. In what follows, buses are partitioned into three disjoint sets, depending on whether they host a producer, a consumer, or no market participant. Assume that each bus hosts at most one market participant. In particular, N is partitioned into N^+ (producer buses), N^- (consumer buses), and N^0 (empty buses). Let $g : N^+ \to G$ map each producer bus to its unique generator, and let $b : G \to N^+$ denote its inverse, i.e., $b(g(b)) = b$ for all $b \in N^+$ and $g(b(g)) = g$ for all $g \in G$. The following simplifications are imposed with respect to the formulations in [11]: (i) at most one pair of antiparallel arcs is allowed between any two buses (no parallel lines); (ii) transformers are not modeled on lines; (iii) shunt admittance is neglected. Moreover, no reactive power market is considered, and reactive power is treated solely as a technical requirement of the network. Now Table 2.1 introduces the variables used in the following section, Table 2.2 the sets and the parameters. Furthermore, using the notation introduced, Figure 2.1 provides a schematic illustration of the graph representation adopted in the ACOPF case study. The figure is intended only to clarify the notation: it shows the partition of buses into N^+, N^-, and N^0, together with the construction of the directed arc set L from the representative set L_0.

Table 2.1. Decision variables of the Producer, Consumer, and TSO problems.

Name	**Domain**	**Description**
p_b^r	$\mathbb{R}$	Active power produced at bus b by generators (producer decision variable).
d_b	$\mathbb{R}$	Electricity demand at bus b (consumer decision variable).
V_b^r	$\mathbb{R}$	Real part of the complex voltage at bus b.
V_b^c	$\mathbb{R}$	Imaginary part of the complex voltage at bus b.
I_{ba}^r	$\mathbb{R}$	Real part of the complex current flowing on arc (b, a).
I_{ba}^c	$\mathbb{R}$	Imaginary part of the complex current flowing on arc (b, a).
S_{ba}^r	$\mathbb{R}$	Active power injected on transmission arc (b, a).
S_{ba}^c	$\mathbb{R}$	Reactive power injected on transmission arc (b, a).
p_g^c	$\mathbb{R}$	Reactive power produced by generator g.

Table 2.2. Sets and parameters of the Producer, Consumer, and TSO problems.

Name	Domain	Description
N	set	Set of buses (nodes) in the transmission network.
N^+	set	Set of buses (nodes) in the transmission network which host a producer.
N^-	set	Set of buses (nodes) in the transmission network which host a consumer.
N^0	set	Set of buses (nodes) in the transmission network which do not host a player.
L	set	Set of directed transmission arcs (b, a).
L_0	set	Subset of arcs for which the oriented π-model parameters are defined.
G	set	Set of generators.
π_b	$\mathbb{R}$	Locational marginal price (nodal price) at bus b.
c^t	$\mathbb{R}$	Transportation or network operating cost borne by the TSO.
$c_g(\cdot)$	function	Generation cost function of generator g.
$PQ(\cdot)$	function	Inverse demand function representing consumer willingness to pay.
$\overline{p}_b^r$	$\mathbb{R}$	Upper bound on active power production at bus b.
$\underline{p}_b^c$, $\overline{p}_b^c$	$\mathbb{R}$	Lower and upper bounds on reactive power production at bus b.
$\underline{V}_b$, $\overline{V}_b$	$\mathbb{R}_+$	Lower and upper bounds on voltage magnitude at bus b.
$\underline{\eta}_{ba}$, $\overline{\eta}_{ba}$	$\mathbb{R}$	Lower and upper bounds on voltage phase angle differences across arc (b, a).
$\overline{S}_{ba}$	$\mathbb{R}_+$	Maximum apparent power capacity of transmission arc (b, a).
$\widetilde{S}_b^c$	$\mathbb{R}$	Reactive power demand at bus b.
Y_{ba}^{ff}, Y_{ba}^{ft}	$\mathbb{C}$	From–from and from–to admittance parameters of arc (b, a).
Y_{ba}^{tf}, Y_{ba}^{tt}	$\mathbb{C}$	To–from and to–to admittance parameters of arc (b, a).
r	element of N	Reference (slack) bus with fixed voltage phase.

The formulation is now specified by presenting the producer, consumer, and TSO problems.

Producer problem. Each producer $g \in G$ located at bus $b \in N^+$ chooses its active power production level in order to maximize profit. Production is remunerated at the nodal price π_b and incurs a generation cost. The producer is subject to lower and upper capacity limits. The optimization problem is given by

$$\begin{aligned} \max_{p_{g(b)}^r} \quad & \pi_b p_{g(b)}^r - c_g(p_{g(b)}^r) \\ \text{s.t.} \quad & 0 \leq p_{g(b)}^r \leq \overline{p}_{g(b)}^r \end{aligned} \tag{2.15}$$

where $p_{g(b)}^r$ denotes the active power produced by generator g at bus b and $c_g(\cdot)$ is the production cost function. This problem can easily be reformulated as the generic player optimization problem (2.7), in the maximization form, by defining:

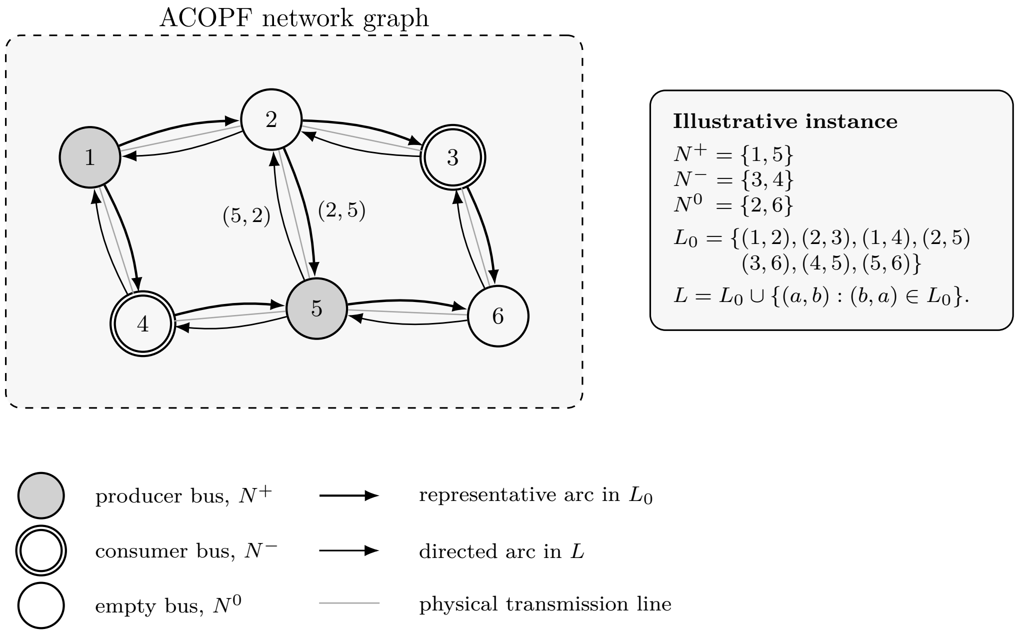

Figure 2.1. Illustrative graph representation used in the ACOPF case study. The sets N^+, N^-, and N^0 identify producer, consumer, and empty buses, respectively. Each physical transmission line is modeled by a pair of antiparallel directed arcs in L, while L_0 contains one representative orientation for each physical line.

$$
\begin{aligned}
y_{g(b)} &:= p^r_{g(b)} \\
Y_{g(b)} &:= \{p^r_{g(b)} : 0 \leq p^r_{g(b)} \leq \overline{p}^r_{g(b)}\} \\
c_{g(b)}(y_{g(b)}) &:= -c_g(p^r_{g(b)}) \\
h_{g(b)}(y_{g(b)}) &:= p^r_{g(b)} e_b,
\end{aligned}
\tag{2.16}
$$

where $e_b \in \mathbb{R}^{|N|}$ is the canonical unit vector associated with bus b. Thus, for any price vector $\pi \in \mathbb{R}^{|N|}$, one has $\pi^\top e_b = \pi_b$. The subscript $g(b)$ indicates a variable of a producer located at bus b.

Consumer problem. The consumer located at bus $b \in N^-$ chooses its demand level in order to maximize consumer surplus. Preferences are represented by an inverse demand function $PQ_b(\cdot)$, while consumption is priced at the nodal price π_b. The consumer problem is formulated as

$$
\begin{aligned}
\max_{d_b} \quad & \int_0^{d_b} PQ_b(t)\, dt - \pi_b\, d_b \\
\text{s.t.} \quad & 0 \leq d_b,
\end{aligned}
\tag{2.17}
$$

where d_b denotes the demand at bus b. To express the consumer problem in the form (2.7), again as a maximization problem, it is possible to define its components as follows:

$$\begin{aligned}
y_b &:= d_b \\
Y_b &:= \{d_b : 0 \ \leq \ d_b\} \\
c_b(y_b) &:= \int_0^{d_b} PQ_b(t)\, dt \\
h_b(y_b) &:= -d_b e_b.
\end{aligned} \tag{2.18}$$

where $e_b \in \mathbb{R}^{|N|}$ is the canonical unit vector associated with bus b. Thus, for any price vector $\pi \in \mathbb{R}^{|N|}$, one has $\pi^\top e_b = \pi_b$.

Transmission System Operator problem. The Transmission System Operator verifies the feasibility of the market outcome with respect to the physical constraints of the transmission network. Power flow equations are interpreted as market-clearing conditions that ensure consistency between injections, withdrawals, and network flows. The TSO problem is therefore formulated as follows:

$$
\begin{aligned}
\max_{y_{TSO}} \quad & \sum_{b\in N} \pi_b \left(- \sum_{(b,a)\in L} S^r_{ba} \right) \; - \; c^t(y_{TSO}) & & \text{(2.19a)}\\
\text{s.t.} \quad & \underline{p}^c_g \le p^c_g \le \overline{p}^c_g & \forall g \in G & \quad \text{(2.19b)}\\
& (S^r_{ba})^2 + (S^c_{ba})^2 \le \overline{S}^2_{ba} & \forall (b,a) \in L & \quad \text{(2.19c)}\\
& \tan(\underline{\eta}_{ba})\,(V^r_b V^r_a + V^c_b V^c_a) \;\le\; V^c_b V^r_a - V^r_b V^c_a & \forall (b,a) \in L_0 & \quad \text{(2.19d)}\\
& V^c_b V^r_a - V^r_b V^c_a \;\le\; \tan(\overline{\eta}_{ba})\,(V^r_b V^r_a + V^c_b V^c_a) & \forall (b,a) \in L_0 & \quad \text{(2.19e)}\\
& V^r_b V^r_a + V^c_b V^c_a \ge 0 & \forall (b,a) \in L_0 & \quad \text{(2.19f)}\\
& \underline{V}^2_b \le (V^r_b)^2 + (V^c_b)^2 \le \overline{V}^2_b & \forall b \in N & \quad \text{(2.19g)}\\
& V^c_r = 0, \qquad V^r_r \ge 0 & & \quad \text{(2.19h)}\\
& \sum_{(b,a)\in L} S^c_{ba} = p^c_{g(b)} & \forall b \in N^+ & \quad \text{(2.19i)}\\
& \sum_{(b,a)\in L} S^c_{ba} + \widetilde{S}^c_b = 0 & \forall b \in N^- & \quad \text{(2.19j)}\\
& \sum_{(b,a)\in L} S^c_{ba} = 0 & \forall b \in N^0 & \quad \text{(2.19k)}\\
& 0 \le \sum_{(b,a)\in L} S^r_{ba} \le \overline{p}^r_{g(b)} & \forall b \in N^+ & \quad \text{(2.19l)}\\
& \sum_{(b,a)\in L} S^r_{ba} \le 0 & \forall b \in N^- & \quad \text{(2.19m)}\\
& \sum_{(b,a)\in L} S^r_{ba} = 0 & \forall b \in N^0 & \quad \text{(2.19n)}\\
& S^r_{ba} = V^r_b I^r_{ba} + V^c_b I^c_{ba} & \forall (b,a) \in L & \quad \text{(2.19o)}\\
& S^c_{ba} = V^c_b I^r_{ba} - V^r_b I^c_{ba} & \forall (b,a) \in L & \quad \text{(2.19p)}\\
& I^r_{ba} = (Y^{ff}_{ba})^r V^r_b - (Y^{ff}_{ba})^c V^c_b + (Y^{ft}_{ba})^r V^r_a - (Y^{ft}_{ba})^c V^c_a & \forall (b,a) \in L_0 & \quad \text{(2.19q)}\\
& I^c_{ba} = (Y^{ff}_{ba})^r V^c_b + (Y^{ff}_{ba})^c V^r_b + (Y^{ft}_{ba})^r V^c_a + (Y^{ft}_{ba})^c V^r_a & \forall (b,a) \in L_0 & \quad \text{(2.19r)}\\
& I^r_{ab} = (Y^{tf}_{ba})^r V^r_b - (Y^{tf}_{ba})^c V^c_b + (Y^{tt}_{ba})^r V^r_a - (Y^{tt}_{ba})^c V^c_a & \forall (b,a) \in L_0 & \quad \text{(2.19s)}\\
& I^c_{ab} = (Y^{tf}_{ba})^r V^c_b + (Y^{tf}_{ba})^c V^r_b + (Y^{tt}_{ba})^r V^c_a + (Y^{tt}_{ba})^c V^r_a & \forall (b,a) \in L_0 & \quad \text{(2.19t)}\\
& V^r_b,\, V^c_b \in \mathbb{R} & \forall b \in N & \quad \text{(2.19u)}\\
& I^r_{ba},\, I^c_{ba} \in \mathbb{R}, \quad S^r_{ba},\, S^c_{ba} \in \mathbb{R} & \forall (b,a) \in L & \quad \text{(2.19v)}\\
& p^c_g \in \mathbb{R} & \forall g \in G. & \quad \text{(2.19w)}
\end{aligned}
$$

where $r \in N$ is the reference bus and y_{TSO} is the vector collecting the decision variables of the problem. In particular $y_{TSO} = (V^r, V^c, I^r, I^c, S^r, S^c, p^c)$.
The active power losses on each physical line $\{b, a\}$ are:

$$P^{loss}_{ba} := S^r_{ba} + S^r_{ab}. \tag{2.20}$$

Since L_0 contains exactly one directed arc per physical line, total losses are computed as

$$P^{loss} := \sum_{(b,a)\in L_0} (S^r_{ba} + S^r_{ab}). \tag{2.21}$$

Then, the transportation cost is set accordingly to

$$c^t(y_{TSO}) := \alpha P^{loss}. \tag{2.22}$$

The objective function is designed to follow the structure of the framework, while the TSOs often rely on different incomes other than congestion rent.

The TSO problem can also be mapped to the maximization form of (2.7) by expressing its components as:

$$\begin{aligned} &y_i := y_{TSO} \\ &Y_i := \{y_{TSO} : (2.19\text{b}) - (2.19\text{w}) \text{ hold}\} \\ &c_i(y_i) := -c^t(y_{TSO}) \\ &h_i(y_i) := h_{TSO}(y_{TSO}) \end{aligned} \tag{2.23}$$

where $h_{TSO} : Y_{TSO} \to \mathbb{R}^{|N|}$ and it is defined componentwise as:

$$(h_{TSO}(y_{TSO}))_b = -\sum_{(b,a)\in L} S^r_{ba} \qquad \forall b \in N.$$

Market-clearing conditions. The TSO model contains part of the active power balance for the ACOPF, therefore, to complete the model, it is necessary to complete the active power balance equations governing the interaction between producers and consumers. These conditions in general ensure that, at each bus, the net active power injected into the network equals the total power generated locally minus the demand at that bus. For the case presented, two different market conditions are defined: one for nodes hosting a producer and one for nodes hosting a consumer.

$$\sum_{(b,a)\in L} S^r_{ba} = p^r_{g(b)} \qquad \forall b \in N^+ \tag{2.24}$$

$$\sum_{(b,a)\in L} S^r_{ba} = -d_b \qquad \forall b \in N^- \tag{2.25}$$

Market Equilibrium Problem The complete market equilibrium problem is defined by the previously introduced players' optimization problems and market-clearing conditions. It consists of the producers' problems (2.15), the consumers' problems (2.17), the TSO problem (2.19), and the market-clearing conditions (2.24) and (2.25).

– Consumer' problem (2.17),
– Producers' problems (2.15),
– The TSO problem (2.19),
– The market clearing conditions (2.24), (2.25)

$\left(\substack{\text{MEP}\\\text{ACOPF}}\right)$

Welfare Optimization Problem The welfare optimization problem is defined with an objective function equal to the sum of the objective functions of the individual optimization problems. Given that $N^+ \cup N^- \cup N^0 = N$ and $N^+ \cap N^- \cap N^0 = \emptyset$, the resulting objective function is:

$$\sum_{b \in N^-} \left(\int_0^{d_b} PQ(t)\, dt - \pi_b d_b \right) + \sum_{g \in G} \left(\pi_{b(g)} p_g^r - c_g(p_g^r) \right) - \sum_{b \in N} \pi_b \sum_{(b,a) \in L} S_{ba}^r - c^t(y_{TSO}).$$

where $\pi_{b(g)}$ denotes the price at the bus b to which generator g is connected.

The terms depending on nodal prices are separated from those that do not. Define

$$R := \sum_{b \in N^-} \int_0^{d_b} PQ(t)\, dt - \sum_{g \in G} c_g(p_{g(b)}^r) - c^t(y_{TSO}).$$

The price-dependent component of the objective function can be rewritten as

$$\begin{aligned}
&- \sum_{b \in N^-} \pi_b d_b + \sum_{b \in N^+} \pi_b p_{g(b)}^r - \sum_{b \in N} \pi_b \sum_{(b,a) \in L} S_{ba}^r \\
&= \sum_{b \in N^-} \pi_b \left(-d_b - \sum_{(b,a) \in L} S_{ba}^r \right) + \sum_{b \in N^+} \pi_b \left(p_{g(b)}^r - \sum_{(b,a) \in L} S_{ba}^r \right) + \sum_{b \in N^0} \pi_b \left(- \sum_{(b,a) \in L} S_{ba}^r \right).
\end{aligned}$$

By the nodal balance constraints and the market clearing conditions

$$\begin{aligned}
&\sum_{(b,a) \in L} S_{ba}^r = -d_b && \forall b \in N^- \\
&\sum_{(b,a) \in L} S_{ba}^r = p_{g(b)}^r && \forall b \in N^+ \\
&\sum_{(b,a) \in L} S_{ba}^r = 0 && \forall b \in N^0,
\end{aligned}$$

the entire price-dependent component vanishes. Hence, the objective function reduces to R, which is independent of nodal prices. The Welfare Optimization Problem for the presented ACOPF is then:

$$
\begin{aligned}
\max_{y_{TSO}, p^r, d} \quad & \sum_{b \in N} \int_0^{d_b} PQ(t)\, dt - \sum_{g \in G} c_g(p^r_{g(b)}) - c^t(y_{TSO}) && \\
\text{s.t.} \quad & \underline{p}^c_g \le p^c_g \le \overline{p}^c_g && \forall g \in G \\
& (S^r_{ba})^2 + (S^c_{ba})^2 \le \overline{S}^2_{ba} && \forall (b,a) \in L \\
& \tan(\underline{\eta}_{ba})\,(V^r_b V^r_a + V^c_b V^c_a) \;\le\; V^c_b V^r_a - V^r_b V^c_a && \forall (b,a) \in L_0 \\
& V^c_b V^r_a - V^r_b V^c_a \;\le\; \tan(\overline{\eta}_{ba})\,(V^r_b V^r_a + V^c_b V^c_a) && \forall (b,a) \in L_0 \\
& V^r_b V^r_a + V^c_b V^c_a \ge 0 && \forall (b,a) \in L_0 \\
& \underline{V}^2_b \le (V^r_b)^2 + (V^c_b)^2 \le \overline{V}^2_b && \forall b \in N \\
& V^c_r = 0, \qquad V^r_r \ge 0 && \\
& \sum_{(b,a) \in L} S^c_{ba} = p^c_{g(b)} && \forall b \in N^+ \\
& \sum_{(b,a) \in L} S^c_{ba} + \widetilde{S}^c_b = 0 && \forall b \in N^- \\
& \sum_{(b,a) \in L} S^c_{ba} = 0 && \forall b \in N^0 \\
& \sum_{(b,a) \in L} S^r_{ba} = p^r_{g(b)} && \forall b \in N^+ \\
& \sum_{(b,a) \in L} S^r_{ba} = -d_b && \forall b \in N^- \\
& \sum_{(b,a) \in L} S^r_{ba} = 0 && \forall b \in N^0 \\
& S^r_{ba} = V^r_b I^r_{ba} + V^c_b I^c_{ba} && \forall (b,a) \in L \\
& S^c_{ba} = V^c_b I^r_{ba} - V^r_b I^c_{ba} && \forall (b,a) \in L \\
& I^r_{ba} = (Y^{ff}_{ba})^r V^r_b - (Y^{ff}_{ba})^c V^c_b + (Y^{ft}_{ba})^r V^r_a - (Y^{ft}_{ba})^c V^c_a && \forall (b,a) \in L_0 \\
& I^c_{ba} = (Y^{ff}_{ba})^r V^c_b + (Y^{ff}_{ba})^c V^r_b + (Y^{ft}_{ba})^r V^c_a + (Y^{ft}_{ba})^c V^r_a && \forall (b,a) \in L_0 \\
& I^r_{ab} = (Y^{tf}_{ba})^r V^r_b - (Y^{tf}_{ba})^c V^c_b + (Y^{tt}_{ba})^r V^r_a - (Y^{tt}_{ba})^c V^c_a && \forall (b,a) \in L_0 \\
& I^c_{ab} = (Y^{tf}_{ba})^r V^c_b + (Y^{tf}_{ba})^c V^r_b + (Y^{tt}_{ba})^r V^c_a + (Y^{tt}_{ba})^c V^r_a && \forall (b,a) \in L_0 \\
& 0 \;\le\; d_b && \forall b \in N \\
& 0 \le p^r_{g(b)} \le \overline{p}^r_{g(b)} && \forall g \in G \\
& V^r_b,\, V^c_b \in \mathbb{R} && \forall b \in N \\
& I^r_{ba},\, I^c_{ba} \in \mathbb{R}, \quad S^r_{ba},\, S^c_{ba} \in \mathbb{R} && \forall (b,a) \in L \\
& p^c_g \in \mathbb{R}\, p^r_{g(b)} \in \mathbb{R} && \forall g \in G \\
& d_b \in \mathbb{R}_{\ge 0} && \forall b \in N.
\end{aligned}
\tag{WFP AC}
$$

where $p^r = (p_1, \dots, p_{|G|})$ and $d = (d_1, \dots, d_{|N|})$, and r is the reference bus. Constraints (2.19l) and (2.19m) have been joined directly with the market clearing conditions (2.25) and (2.24) respectively.

As in the original material, some assumptions are made:

Assumption 2.17. 1. The inverse demand functions $PQ_b(\cdot)$ are continuous and strictly decreasing for all $b \in N^-$.

2. The cost function $c_b(\cdot)$ are monotonically increasing with $c_b(0) = 0$, convex and continuously differentiable for all $b \in N^+$.

Assumption 2.17 ensures that both producers and consumers have concave maximization problems, subject to linear constraints. By Proposition 2.2, KKT conditions of problems (2.17) and (2.15) characterize their solutions.

The consumer and producer problems considered in this study coincide with those presented by Grübel et al. in Section 4 of [39]. The main differences arise in the TSO problem, particularly through the ACOPF power-flow equations and the associated network physics. Since the structure of the proposed case study is analogous to that considered by Grübel et al., the same conclusions as in Theorem 4.1 of [39] carry over to the present setting. The argument presented below follows the same overall structure as the proof of Theorem 4.1, with the adaptations required by the present model. To this end, the KKT conditions for the two problems are stated as a first step.
For a consumer located at a bus $b \in N^-$, through basic transformations:

$$\begin{aligned} & d_b \geq 0 \\ & \pi_b - PQ_b(d_b) \geq 0 \\ & (\pi_b - PQ_b(d_b))d_b = 0. \end{aligned} \tag{2.26}$$

For a producer located at a bus $b \in N^+$:

$$\begin{aligned} & p_b^r \geq 0 \\ & \overline{p}_b^r - p_b^r \geq 0 \\ & \pi_b - c_b'(p_b^r) + \beta_b^- - \beta_b^+ = 0 \\ & \beta_b^+(p_b^r - \overline{p}_b^r) = 0 \\ & \beta_b^- p_b^r = 0 \\ & \beta^+, \beta^- \geq 0, \end{aligned} \tag{2.27}$$

where β_b^+ and β_b^- denote the dual variables.

Given a solution $(d^*, (p^r)^*, y_{TSO}^*)$ of $\binom{\text{WFP}}{\text{AC}}$, the KKT conditions (2.26), (2.27) can be used to define the set $\Pi(d^*, (p^r)^*, y_{TSO}^*)$:

$$\Pi(d^*, (p^r)^*, y_{TSO}^*) = \left\{ \pi \in \mathbb{R}^{|N^+ \cup N^-|} : \ \pi_b \in \left\{ \begin{array}{ll} \{PQ_b(d_b^*)\}, & \text{if } b \in N^-, \ d_b^* > 0, \\ [PQ_b(d_b^*), \infty), & \text{if } b \in N^-, \ d_b^* = 0, \\ \{c_b'((p_b^r)^*)\}, & \text{if } b \in N^+, \ \overline{p}_b^r > (p_b^r)^* > 0, \\ (-\infty, c_b'((p_b^r)^*)], & \text{if } b \in N^+, \ (p_b^r)^* = 0, \\ [c_u'((p_b^r)^*), +\infty), & \text{if } b \in N^+, \ (p_b^r)^* = \overline{p}_b^r, \end{array} \right\} \right\}.$$

By the definition of $\Pi(d^*, (p^r)^*, y^*_{TSO})$, and since $\hat{\pi} \in \Pi(d^*, (p^r)^*, y^*_{TSO})$, the KKT conditions of the consumers and producers are satisfied at $\hat{\pi}$. Hence, d^* and $(p^r)^*$ are best responses to the critical price vector $\hat{\pi}$. To verify all the remaining hypotheses of Corollary 2.15, it remains to show that for the TSO, the only player in $I \setminus C$, at least one of properties (a)-(d) of Corollary 2.15 holds for every relevant index k.

To begin, consider the cases $d^*_b > 0$ and $0 < (p^r_b)^* < \overline{p}_b$ are discussed. For $b \in N^-$, $d^*_b > 0$ implies $\pi_b = PQ_b(d^*_b)$, while for $b \in N^+$, $0 < (p^r_b)^* < \overline{p}_b$ implies $\pi_b = c'_b((p^r_b)^*)$. Therefore, both cases fall under Case (a) of Corollary 2.15.

Consider now nodes $b \in N^-$ for which $d^*_b = 0$. Recall that

$$h_{TSO}(y_{TSO})_b = -\sum_{(b,a)\in L} S^r_{ba}\,,$$

and that the market-clearing conditions give

$$\sum_{(b,a)\in L} S^r_{ba} = x^-_b = -d_b\,.$$

Combining these relations yields

$$\begin{aligned} h_{TSO}(y_{TSO})_b &= -\sum_{(b,a)\in L} S^r_{ba} = d_b \geq 0,\\ h_{TSO}(y^*_{TSO})_b &= -\sum_{(b,a)\in L} (S^r_{ba})^* = d^*_b = 0. \end{aligned}$$

Therefore,

$$h_{TSO}(y^*_{TSO})_b \leq h_{TSO}(y_{TSO})_b \qquad \forall\,(y_{TSO})_b \in (Y_{TSO})_b.$$

For $d^*_b = 0$, the minimum nodal price in the set $\Pi(d^*, (p^r)^*, y^*_{TSO})$ is finite and equal to $PQ(d^*_b)$, hence $\pi^-_b > -\infty$. It follows that all conditions of Case (c) of Corollary 2.15 are satisfied.

For nodes $b \in N^+$ with $(p^r_b)^* = 0$, it follows that

$$\begin{aligned} h_{TSO}(y_{TSO})_b &= -\sum_{(b,a)\in L} S^r_{ba} = -p^r_b \leq 0,\\ h_{TSO}(y^*_{TSO})_b &= -\sum_{(b,a)\in L} (S^r_{ba})^* = -(p^r_b)^* = 0. \end{aligned}$$

This gives

$$h_{TSO}(y^*_{TSO})_b \geq h_{TSO}(y_{TSO})_b \qquad \forall\,(y_{TSO})_b \in (Y_{TSO})_b.$$

Since the maximum nodal price in the set $\Pi(d^*, (p^r)^*, y^*_{TSO})$ is finite and equal to $c'_b(0)$, it also holds that $\pi^+_b < \infty$. Therefore, all conditions of Case (b) of Corollary 2.15 are satisfied.

It remains to consider the case $(p^r_b)^* = \overline{p}^r_b$. In this setting,

$$\begin{aligned} h_{TSO}(y_{TSO})_b &= -\sum_{(b,a)\in L} S^r_{ba} = -p^r_b\\ h_{TSO}(y^*_{TSO})_b &= -\sum_{(b,a)\in L} (S^r_{ba})^* = -(p^r_b)^* = -\overline{p}^r_b. \end{aligned}$$

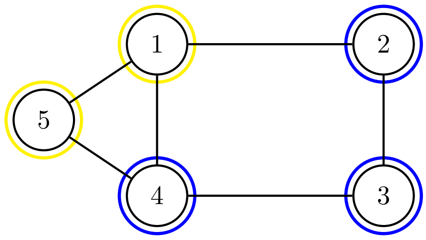

Figure 2.2. Graphical scheme of the 5-bus network. Yellow-marked nodes host a generator, blue-market nodes host a consumer.

Hence,

$$h_{TSO}(y^*_{TSO})_b \leq h_{TSO}(y_{TSO})_b \qquad \forall\, (y_{TSO})_b \in (Y_{TSO})_b.$$

The minimum nodal price in the set $\Pi(d^*, (p^r)^*, y^*_{TSO})$ is finite and equal to $c'_b((p^r_b)^*)$. Therefore, $\pi^-_b > -\infty$, and all conditions of Case (c) of Corollary 2.15 are satisfied.

All conditions of Corollary 2.15 are satisfied, with the critical price vector $\hat{\pi}$ defined componentwise as

$$\hat{\pi}_b = \begin{cases} PQ_b(d^*_b) & b \in N^-, \\ c'_b((p^r_b)^*) & b \in N^+. \end{cases} \tag{2.28}$$

Therefore, either $(d^*, (p^r)^*, y^*_{TSO})$ is a market equilibrium of $\left(^{\text{MEP}}_{\text{ACOPF}}\right)$, or no market equilibrium exists.

To verify whether $(d^*, (p^r)^*, y^*_{TSO})$ is a market equilibrium, it remains only to check that y^*_{TSO} is a best response of the TSO to the price vector $\hat{\pi}$.

Computational test. To validate the proposed ACOPF market formulation and illustrate the equilibrium-selection argument discussed above, a small test instance adapted from MATPOWER [82], namely the 5-bus PJM-derived case study in [53], is considered. The resulting transmission network is shown in Figure 2.2. In this experiment, the welfare optimization problem $\left(^{\text{WFP}}_{\text{AC}}\right)$ is solved first, and the KKT-based price characterization is then used to construct a candidate equilibrium price vector $\hat{\pi}$, as specified in (2.28), which specializes Corollary 2.15 to the present setting.

The buses are partitioned as follows: $N^+ = \{1, 5\}$ denotes the producer buses, $N^- = \{2, 3, 4\}$ denotes the consumer buses, and $N^0 = \emptyset$. The reference bus is bus 4, and the MATPOWER system base power is $\texttt{baseMVA} = 100$.

For each consumer bus $b \in N^-$, the inverse demand function is assumed to be affine:

$$PQ_b(x) = \alpha^0_b\, x + \beta^0_b \qquad \forall b \in N^-, \tag{2.29}$$

with $\alpha^0_b < 0$, sot that the inverse demand is downward sloping (Assumption 2.17). Therefore, the consumer-surplus CS_b term admits the following closed form

$$CS_b = \int_0^{d_b} PQ_b(x)\, dx = \frac{\alpha^0_b}{2} d_b^2 + \beta^0_b\, d_b. \tag{2.30}$$

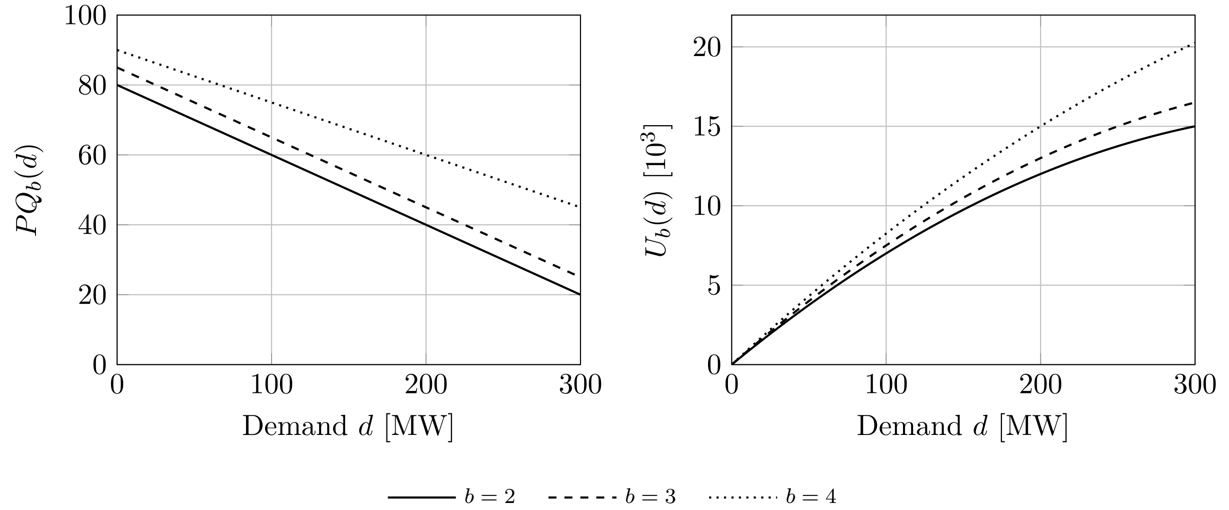

Figure 2.3. Demand and consumer surplus functions for the load buses ($N^- = \{2, 3, 4\}$) using $PQ_b(d) = a_b d + b_b$.

The generation cost functions $c_g(p^r_{b(g)})$ are modeled as linear functions, as in Assumption 2.17. Reactive power is not priced and is constrained only by network feasibility, as in (2.19).

$$c_g(p^r_{b(g)}) = a_g p^r_{b(g)} \qquad \forall g \in G \tag{2.31}$$

Specifically, the demand and generation parameters used in the test are as follows:

Bus 1 : $a_0 = 30$
Bus 2 : $\alpha_2^0 = -0.2$, $\beta_2^0 = 80$
Bus 3 : $\alpha_3^0 = -0.2$, $\beta_3^0 = 85$
Bus 4 : $\alpha_3^0 = -0.15$, $\beta_3^0 = 90$
Bus 5 : $a_1 = 10$

Figure 2.3 represents the demand and the consumer surplus for consumers located in buses 2,3,4.

Solving $\binom{\text{WFP}}{\text{AC}}$ yields an optimal welfare value of

$$\text{Welfare} = 34979.338$$

The optimal consumption and generation levels (in MW) are:

$$d^* = \{2 : 197.623,\ 3 : 203.175,\ 4 : 242.087\}, \qquad (p^r)^* = \{1 : 48.640,\ 5 : 600.0\}.$$

The optimal reactive power generation levels (in MVAr) are:

$$(p^c)^* = \{1 : 390.0,\ 5 : -78.486\}.$$

In particular, generator 5 is dispatched at its upper bound ($p_5^r = \overline{p}_5^r$), while generator 1 is strictly within its capacity range.

Given $(d^*, (p^r)^*, y_{TSO}^*)$, the critical price is defined using (2.28) as

$$\pi_b = PQ_b(d_b^*) \qquad \forall\, b \in N^-.$$

Consequently, the candidate price vector on consumer buses is

$$PQ(d^*) = \{2 : 40.475,\ 3 : 44.365,\ 4 : 53.687\}.$$

For producer buses, the critical price is defined using (2.28), which yields the marginal costs

$$\pi_b = c_b'((p_b^r)^*) \qquad \forall\, b \in N^+.$$

Hence, the candidate price vector for producer buses is

$$c'((p_b^r)^*) = \{1 : 30.0,\ 5 : 10.0\}$$

In summary, the complete candidate vector is

$$\hat{\pi} = \{1 : 30.0,\ 2 : 40.475,\ 3 : 44.365,\ 4 : 53.687,\ 5 : 10.0\}.$$

To verify the equilibrium, the TSO problem is solved at the candidate price vector $\hat{\pi}$, and the resulting optimizer is compared with the network variables obtained from the welfare problem. The TSO solution is essentially indistinguishable from the welfare-optimal solution, up to numerical tolerances. In particular, the average absolute deviation in the active line flows S^r is 3.11×10^{-4} p.u., with a maximum deviation of 7.10×10^{-4} p.u., while the reactive line flows S^c differ on average by only 3.58×10^{-5} p.u. The voltage variables are even closer: the average absolute deviation is 1.52×10^{-6} p.u. for the real voltage components V^r and 6.79×10^{-6} p.u. for the imaginary voltage components V^c. Reactive generation p^c also remains highly stable, with a maximum deviation of only 1.26×10^{-2} MVAr. Taken together, these discrepancies are negligible and can be attributed to numerical solver tolerances. Therefore, $y_{\text{TSO}}^{\text{WFP}}$ can be regarded, up to numerical tolerances, as a best response of the TSO to $\hat{\pi}$, which confirms that the welfare-optimal solution is indeed a market equilibrium for the considered test instance.

2.7 Conclusions

This chapter presents an analysis of the paper [39] by Grubël et al., complemented by extended proofs and a more detailed discussion of the main arguments. To test the framework proposed by Grubël et al. beyond the context considered in their paper, this chapter applies it to an ACOPF setting, which involves more intricate constraints and substantial modeling differences with respect to the DCOPF setting analyzed in that paper. In particular, ACOPF accounts for power losses in the network, thereby breaking the equivalence between injections and withdrawals across a transmission line. Even without modeling additional elements such as transformers or line charging susceptance, an adequate representation of the grid naturally relies on a directed graph in which each physical line is represented by a pair of antiparallel arcs. To embed ACOPF into the proposed framework, the players' problems are mapped explicitly to the framework components, so that the contribution of each player to the overall structure is made transparent. The TSO problem and the market-clearing conditions jointly encode the AC network physics and the interface between injections, withdrawals, and flows. The resulting formulation remains close in spirit to the original model, showing that the framework can be adapted to more complex settings. This extension comes at the cost of a deliberate modeling compromise, most notably in the specification of the TSO objective, adopted in order to preserve the theoretical properties required by the framework. It is shown that the argument underlying Theorem 4.1 in [39] can be replicated for the present case study, with the ACOPF TSO model as the only substantive modification. Since the original paper does not explicitly address this modeling step, the proposed example clarifies how to handle the interdependence of the variables when working with an electrical network representation. Moreover, the aforementioned loss of realism may not be critical for the present purpose, because the TSO and other actors are often subject to legal restrictions that limit their autonomy and impose additional hard constraints, potentially leading to non-optimal outcomes. Similarly, economic considerations may discourage withdrawal from production when generation assets are already owned. These aspects, however, lie beyond the scope of the present analysis and are not pursued further. Overall, the adaptation illustrates how the framework can be transferred to a different and more complex setting while preserving the main structural and theoretical guarantees targeted by the original approach.

Chapter 3

Accelerated Alternating Direction Method of Multipliers methods

3.1 Introduction

Many energy-related optimization problems require an explicit mathematical representation of the underlying physical network, as in DCOPF and ACOPF formulations. In this setting, some structural properties can be exploited to obtain solution methods that are more scalable and better aligned with practical requirements (e.g., limited information sharing and communication constraints). Two features are especially relevant. First, power networks induce sparse coupling patterns: each network constraint typically involves variables associated with a small neighborhood in the graph. Second, decision-making is often distributed across multiple actors (e.g., generators, loads, and aggregators), each with heterogeneous objectives and private local constraints.

As a consequence, centralized formulations can become large-scale, since each actor contributes local variables and constraints that are coupled through network relations. A widely used algorithmic approach in this setting is the Alternating Direction Method of Multipliers (ADMM), which can exploit these structural properties in a distributed and parallel manner. In particular, separability is exposed through a consensus (variable-splitting) reformulation, and ADMM leverages the resulting structure by alternating parallel local solves with coordination steps that enforce agreement on shared variables through consensus constraints. This decomposition is also attractive when information sharing is limited, since local models, data, and cost functions can remain private and only the quantities needed to enforce agreement on shared variables need to be exchanged. Examples of ADMM applications in this context include [77, 8, 23, 59].

Despite these advantages, distributed ADMM-based approaches have well-known limitations. First, achieving high accuracy and tight feasibility may require many iterations, and practical convergence can be sensitive to the choice of penalty parameters and stopping criteria. Second, the decomposition itself is not innocuous: the chosen partition determines the size of the coupling interface, the associated communication burden, and ultimately the overall computational performance. Therefore, unless exogenous considerations impose a specific partition, the decomposition should be treated as a design choice rather than an arbitrary modeling step.

Reducing the number of iterations required by ADMM to attain a target accuracy is therefore of practical interest. However, many acceleration schemes proposed in the literature either lack convergence guarantees in the ADMM setting or are analyzed under restrictive assumptions. To address this issue, safeguard and restart mechanisms have been proposed to decide whether an accelerated candidate should be accepted or rejected (see, e.g., [35]). ADMM is most commonly applied to convex problems, including many DCOPF-based formulations, while convergence results for nonconvex settings have also been established for specific classes of problems [47, 78]. Although the computational study in this chapter focuses on a DCOPF-based market-clearing problem, the broader motivation extends to more complex nonconvex settings such as ACOPF, where scalable decomposition methods and safeguarded iterative schemes remain relevant. In this context, convex relaxations and approximations play an important role; representative examples include Jabr's conic relaxation [48] and the linear cutting-plane relaxation approach by Bienstock and Villagra [10]; for further examples, see also [11].

Building on this context, this chapter studies a non-monotone acceptance framework for accelerated ADMM applied to the clearing of a day-ahead market with demand response and DCOPF network constraints. The proposed safeguard evaluates accelerated candidates through a combined residual merit function and adopts a sliding-window non-monotone acceptance rule, i.e.,

$$\gamma_{\mathrm{acc}}^{k+1} \leq \max_{j=0,\ldots,\min\{k,w\}} \{\gamma^{k-j}\},$$

where $\gamma_{\mathrm{acc}}^{k+1}$ denotes the combined residual at iteration $k+1$ and w is the window length. If the accelerated candidate is rejected, the algorithm falls back to the corresponding standard ADMM iterate. The goal is twofold: (i) to assess whether a non-monotone safeguard can improve practical performance by avoiding overly restrictive iteration-by-iteration acceptance conditions, and (ii) to provide a systematic comparison of multiple acceleration techniques under a common acceptance mechanism on the same application problem. In this sense, the chapter does not aim to establish the uniform dominance of a single acceleration strategy, but rather to evaluate robustness and practical gains across instances.

The computational study considers three test networks (5-, 30-, and 118-bus), each in two variants with either linear or quadratic objective costs. In addition, an ADMM variant with variable penalty parameters is included alongside the accelerated schemes. The comparison is conducted under a common stopping criterion, with iteration count as the primary performance indicator; the complete evaluation protocol is reported in Section 3.6. While the application setting is consistent with prior work on the same market-clearing problem [77], the purpose of this chapter is different. Rather than studying a single acceleration strategy with a problem-specific acceptance rule, the chapter introduces a common non-monotone safeguard framework and uses it to carry out a systematic comparison of multiple acceleration techniques.

The remainder of the chapter is organized as follows. Section 3.2 introduces the core concepts of ADMM. Section 3.3 reviews common ADMM variants. Section 3.4 presents the acceleration techniques considered in this work. Section 3.5 introduces the proposed non-monotone restart/acceptance framework. Section 3.6 describes the reformulation and the problem under study, and reports the experimental results on the test cases. Finally, Section 3.7 concludes the chapter.

3.2 Alternating Direction Method of Multipliers

In this section the Alternating Direction Method of Multipliers (ADMM) is introduced. First, the background is recalled by reviewing the two methods from which ADMM originates, namely dual ascent and the method of multipliers. Then, the algorithmic structure is presented together with its main convergence properties and practical stopping criteria. Finally, the generalized consensus formulation is discussed.

3.2.1 Background

To motivate the structure of ADMM, dual ascent and the method of multipliers are briefly reviewed. Unless otherwise stated, the exposition in this section follows [13].

Dual Ascent. Consider the convex optimization problem with equality constraints:

$$\begin{aligned} \min \quad & f(x) \\ s.t. \quad & Ax = b, \end{aligned} \tag{3.1}$$

with variable $x \in \mathbb{R}^n$, where $A \in \mathbb{R}^{m\times n}$ and $f : \mathbb{R}^n \to \mathbb{R}$ is convex. The Lagrangian associated with (3.1) is defined as

$$L(x, y) = f(x) + y^\top(Ax - b).$$

The dual function is

$$g(y) = \inf_x L(x, y),$$

where y is the dual variable. The dual problem is

$$\max_y \quad g(y). \tag{3.2}$$

The dual ascent method solves the dual problem by means of gradient ascent. In order to evaluate the gradient $\nabla g(y)$, assuming that g is differentiable, it holds that

$$\nabla g(y) = Ax^+ - b, \tag{3.3}$$

with $x^+ = \arg\min_x L(x, y^k)$. The method consists of iterating a minimization step (3.4) followed by a dual variable update (3.5):

$$x^{k+1} := \arg\min_x L(x, y^k), \tag{3.4}$$

$$y^{k+1} := y^k + \alpha^k(Ax^{k+1} - b), \tag{3.5}$$

where $\alpha^k > 0$ is the step size and k denotes the current iteration.

When the objective function of (3.1) is separable with respect to a splitting of the variables into subvectors, i.e., $f(x) = \sum_{i=1}^N f_i(x_i)$, and the constraint matrix is partitioned accordingly so that $Ax = \sum_{i=1}^N A_i x_i$ with $x = (x_1, \ldots, x_N)$, the x-minimization step can be decomposed into N separated problems.

Method of Multipliers. The method of multipliers can be obtained by applying the dual ascent to the problem

$$\begin{aligned} \min \quad & f(x) + \frac{\rho}{2}\|Ax - b\|^2 \\ s.t. \quad & Ax = b. \end{aligned} \tag{3.6}$$

Problem (3.6) is equivalent to (3.1), since the added term is equal to zero for every feasible x. The associated Lagrangian yields the augmented Lagrangian

$$L_\rho(x, y) = f(x) + y^\top (Ax - b) + \frac{\rho}{2}\|Ax - b\|^2, \tag{3.7}$$

where $\rho > 0$ is the penalty parameter. The associated dual function is

$$g_\rho(y) = \inf_x L_\rho(x, y), \tag{3.8}$$

which is differentiable under mild conditions on the original problem.

The method of multipliers consists of repeating the steps:

$$x^{k+1} := \arg\min_x L_\rho(x, y^k), \tag{3.9}$$

$$y^{k+1} := y^k + \rho(Ax^{k+1} - b). \tag{3.10}$$

In this scheme, ρ plays the role of the step size used in dual ascent. By optimality of the x-update and using the dual update, it follows that

$$\nabla f(x^{k+1}) + A^\top y^{k+1} = 0,$$

which is one optimality condition of (3.1). Primal feasibility, i.e., $Ax^k - b = 0$, is approached as the method proceeds. While this method converges under more general conditions than dual ascent, the decomposition property is lost, since the augmented Lagrangian is not separable.

3.2.2 Algorithm

Consider a problem of the form

$$\begin{aligned} \min_{x,z} \quad & f(x) + g(z) \\ \text{s.t.} \quad & Ax + Bz = c, \end{aligned} \tag{3.11}$$

with $x \in \mathbb{R}^n$ and $z \in \mathbb{R}^m$, $A \in \mathbb{R}^{p\times n}$, $B \in \mathbb{R}^{p\times m}$, and $c \in \mathbb{R}^p$. The functions $f : \mathbb{R}^n \to \mathbb{R}$ and $g : \mathbb{R}^m \to \mathbb{R}$ are convex.

The augmented Lagrangian of (3.11) reads

$$L_\rho(x, z, y) = f(x) + g(z) + y^\top (Ax + Bz - c) + \frac{\rho}{2}\|Ax + Bz - c\|_2^2, \tag{3.12}$$

where $\rho > 0$ is the penalty parameter.

ADMM alternates the following three updates:

$$x^{k+1} := \arg\min_x \; L_\rho(x, z^k, y^k), \tag{3.13}$$

$$z^{k+1} := \arg\min_z \; L_\rho(x^{k+1}, z, y^k), \tag{3.14}$$

$$y^{k+1} := y^k + \rho(Ax^{k+1} + Bz^{k+1} - c). \tag{3.15}$$

Steps (3.13) and (3.14) alternately update the primal variables x and z, while (3.15) updates the dual variable after the first two blocks.

Often, the algorithm state is expressed only through z^k and y^k, since x^k is treated as an intermediate quantity.

Stopping Criterion. At iteration k, the primal residual is defined as

$$r^k = Ax^k + Bz^k - c, \tag{3.16}$$

and the dual residual as

$$s^k = \rho A^\top B(z^k - z^{k-1}). \tag{3.17}$$

The primal residual (3.16) measures the violation of the constraint in (3.11), i.e. primal feasibility, while the dual residual (3.17) is associated with the dual optimality conditions.

Although not required by the algorithm, it is assumed for ease of exposition that f and g are differentiable. The dual optimality conditions then read as follows:

$$\nabla f(x^*) + A^\top y^* = 0, \tag{3.18}$$

$$\nabla g(z^*) + B^\top y^* = 0. \tag{3.19}$$

Recalling the update (3.15) and that z^{k+1} minimizes $L_\rho(x^{k+1}, z, y^k)$, it follows that

$$0 = \nabla g(z^{k+1}) + B^\top y^k + \rho B^\top (Ax^{k+1} + Bz^{k+1} - c) = \nabla g(z^{k+1}) + B^\top y^{k+1}. \tag{3.20}$$

Therefore, (3.19) is satisfied by z^{k+1} and y^{k+1}, and it remains to verify that (3.18) and primal feasibility are satisfied.

A possible stopping criterion is to require both residuals to be below chosen thresholds:

$$\|r^k\|_2 \leq \epsilon^{\text{primal}}, \tag{3.21}$$

$$\|s^k\|_2 \leq \epsilon^{\text{dual}}. \tag{3.22}$$

Convergence results. Consider the following assumptions.

Assumption 3.1. The (extended-real-valued) functions $f : \mathbb{R}^n \to \mathbb{R} \cup \{+\infty\}$ and $g : \mathbb{R}^m \to \mathbb{R} \cup \{+\infty\}$ are closed, proper, and convex.

Assumption 3.2. The non-augmented Lagrangian L_0 has a saddle point.

Under Assumptions 3.1 and 3.2, strong duality holds and ADMM iterations satisfy the following properties:

- Residual convergence: $r^k \to 0$ as $k \to \infty$.
- Objective convergence: $f(x^k) + g(z^k) \to p^*$ as $k \to \infty$.
- Dual variable convergence: $y^k \to y^*$ as $k \to \infty$, where y^* is a dual optimal point.

Furthermore, x^k and z^k do not need to converge to optimal values.

Other convergence results have been established in the literature, also for some non-convex cases [47, 78].

3.2.3 Generalized global variable consensus ADMM

In the global consensus setting, each subsystem optimizes its own local decision variables while enforcing agreement on a set of shared global variables. Consider local variables $x_i \in \mathbb{R}^{n_i}$ for $i = 1, \ldots, N$, and a separable objective function $\sum_{i=1}^{N} f_i(x_i)$. Consensus is imposed through a global variable $z \in \mathbb{R}^n$ whose components are shared among the subsystems.

In the generalized consensus setting, each local variable x_i contains only a subset of the components of z. Specifically, component j of x_i is associated with the component g of z via the mapping $g = \mathcal{G}(i, j)$, which maps a local index (i, j) to a global index $g \in \{1, \ldots, n\}$. Therefore, consensus can be written as

$$(x_i)_j = z_{\mathcal{G}(i,j)}, \quad i = 1, \ldots, N, \quad j = 1, \ldots, n_i. \tag{3.23}$$

A more in-depth discussion of consensus ADMM can be found in [13].
The generalized consensus problem can be formulated as

$$\begin{aligned} \min \quad & \sum_{i=1}^{N} f_i(x_i) \\ \text{s.t.} \quad & x_i - \tilde{z}_i = 0, \quad i = 1, \ldots, N, \end{aligned} \tag{3.24}$$

where $\tilde{z}_i \in \mathbb{R}^{n_i}$ collects, in the appropriate order, the components of z associated with x_i, i.e.,

$$(\tilde{z}_i)_j = z_{\mathcal{G}(i,j)} \quad j = 1, \ldots, n_i.$$

Let $x := (x_1, \ldots, x_N)$ and $y := (y_1, \ldots, y_N)$, where $y_i \in \mathbb{R}^{n_i}$ are the dual variables. The augmented Lagrangian associated with (3.24) is

$$L_\rho(x, z, y) = \sum_{i=1}^{N} \left(f_i(x_i) + y_i^\top (x_i - \tilde{z}_i) + \frac{\rho}{2} \|x_i - \tilde{z}_i\|_2^2 \right). \tag{3.25}$$

The ADMM iterations for (3.24) are:

$$x_i^{k+1} := \arg\min_{x_i} \left(f_i(x_i) + (y_i^k)^\top x_i + \frac{\rho}{2} \|x_i - \tilde{z}_i^k\|_2^2 \right), \qquad i = 1, \ldots, N, \tag{3.26}$$

$$z_g^{k+1} := \frac{1}{N_g} \sum_{(i,j)\,:\,\mathcal{G}(i,j)=g} (x_i)_j^{k+1}, \qquad g = 1, \ldots, n, \tag{3.27}$$

$$y_i^{k+1} := y_i^k + \rho \left(x_i^{k+1} - \tilde{z}_i^{k+1} \right), \qquad i = 1, \ldots, N. \tag{3.28}$$

Here, $\mathcal{I}_g := \{(i, j) : \mathcal{G}(i, j) = g\}$ denotes the set of local components associated with global component g, and $N_g := |\mathcal{I}_g|$. The z-update is obtained by minimizing the augmented Lagrangian with respect to z, which decomposes componentwise and results in the averaging step (3.27). Moreover, the x_i-updates in (3.26) can be computed in parallel across i, and the dual updates (3.28) can also be computed in parallel once z^{k+1} is available.

3.3 ADMM Variants

As already mentioned, ADMM can converge slowly, especially when high accuracy is required or when the problem is ill-conditioned. For this reason, several variants have been proposed in the literature to improve its computational efficiency. Many of these approaches provide substantial practical benefits and, in several cases, are supported by solid theoretical guarantees. In what follows, several variants of the standard algorithm are presented, namely: (i) ADMM with a variable penalty parameter ρ, (ii) inexact ADMM, (iii) over-relaxation, and (iv) symmetric ADMM. These methods modify the original scheme in different ways and may have a relevant impact on the algorithmic structure, implementation aspects, and overall performance.

3.3.1 Variable Penalty Parameter

The penalty parameter ρ can strongly affect the performance of ADMM, and a poor choice may lead to slow progress or numerical difficulties. To mitigate this sensitivity, several adaptive strategies have been proposed in the literature [43, 76, 13]. These approaches update ρ across iterations in response to the current balance between the primal and dual residuals.

A widely used update rule is:

$$\rho^{k+1} := \begin{cases} \tau^{\text{incr}}\rho^k, & \text{if } \|r^k\|_2 > \mu\|s^k\|_2, \\ \rho^k/\tau^{\text{decr}}, & \text{if } \|s^k\|_2 > \mu\|r^k\|_2, \\ \rho^k, & \text{otherwise,} \end{cases} \tag{3.29}$$

where $\mu > 1$, $\tau^{\text{incr}} > 1$, and $\tau^{\text{decr}} > 1$, and r^k and s^k denote the primal and dual residuals at iteration k. The parameter μ controls the maximum acceptable imbalance between the two residual norms before ρ is adjusted. Intuitively, ρ is increased to emphasize reduction of the primal residual when $\|r^k\|_2$ dominates, and decreased to emphasize reduction of the dual residual when $\|s^k\|_2$ dominates, while both residuals are driven to zero. Convergence results derived for a fixed ρ still apply whenever the sequence $\{\rho^k\}$ becomes constant after a finite number of iterations.

Other possible schemes have been proposed in the literature. For instance, in [71] the authors use the formula proposed in [15, 16]. Under the assumptions stated in [71], this variant of ADMM is shown to achieve a worst-case $\mathcal{O}(1/n^2)$ convergence rate.

3.3.2 Inexact

When the primal updates are performed using an iterative method, it may be beneficial to avoid exact minimization in the x- and z-minimization steps. The idea is to solve the minimization problems approximately at first, and then progressively increase the accuracy as the algorithm proceeds [13, 19]. This line of work has also been pursued in the literature on consensus ADMM as in [17].

3.3.3 Over-Relaxation

Another approach considered in the literature [19, 34, 13, 61] is over-relaxation. After computing x^{k+1}, the quantity Ax^{k+1} is replaced in the subsequent updates by the relaxed quantity

$$\alpha^k Ax^{k+1} - (1 - \alpha^k)(Bz^k - c) \tag{3.30}$$

where $\alpha^k \in (0, 2)$ is the relaxation parameter. Values $\alpha^k > 1$ correspond to over-relaxation, whereas $\alpha^k < 1$ yields an under-relaxation scheme.

In practice, the parameter α^k is usually chosen in the interval $[1.5, 1.8]$; however, values outside this range can also be beneficial [61]. When considering the generalized consensus problem (3.24), this modification can be naturally adapted to the local-variable updates. In this setting, the subset of constraints coupling the local variables x_i with the global variable $\tilde{z}$ takes the form

$$A_i x_i + B_i \tilde{z}_i = 0, \quad \forall\, i = 1, \ldots, N, \tag{3.31}$$

where $A_i \in \mathbb{R}^{n_i \times n_i}$ with $A_i = I$, $B_i \in \mathbb{R}^{n_i \times n_i}$, and $c = 0$.

3.3.4 Symmetric

An ADMM variant derived from the application of the Peaceman-Rachford splitting method to the dual problem of (3.11) [45] is Symmetric ADMM. Its main difference with respect to classical ADMM is the double update of the dual variable within each iteration, performed after each primal update. However, this modification alone has weaker convergence properties; therefore a relaxation parameter $\alpha \in (0, 1)$ is introduced to scale the Lagrange multiplier increments. Although this makes the dual update more conservative, it plays a crucial theoretical role in establishing global convergence and worst-case convergence rate under the standard assumptions stated for (3.11) [45]. Symmetric ADMM consists of the following steps:

$$x^{k+1} := \arg\min_x L_p(x, z^k, y^k) \tag{3.32a}$$

$$y^{k+\frac{1}{2}} := y^k + \alpha\rho(Ax^{k+1} + Bz^k - c), \tag{3.32b}$$

$$z^{k+1} := \arg\min_z L_p(x^{k+1}, z, y^{k+\frac{1}{2}}) \tag{3.32c}$$

$$y^{k+1} := y^{k+\frac{1}{2}} + \alpha\rho(Ax^{k+1} + Bz^{k+1} - c), \tag{3.32d}$$

Since reducing the dual step size is not desirable in practice, a different version is proposed in [44]. In line with the use of relaxation parameters in multiplier updates [29], He et al. introduce two parameters, τ and σ, for the two dual updates, with (τ, σ) restricted to $\mathcal{D}$ to ensure convergence.

$$x^{k+1} := \arg\min_x L_p(x, z^k, y^k) \tag{3.33a}$$

$$y^{k+\frac{1}{2}} := y^k + \tau\rho(Ax^{k+1} + Bz^k - c), \tag{3.33b}$$

$$z^{k+1} := \arg\min_z L_p(x^{k+1}, z, y^{k+\frac{1}{2}}) \tag{3.33c}$$

$$y^{k+1} := y^{k+\frac{1}{2}} + \sigma\rho(Ax^{k+1} + Bz^{k+1} - c), \tag{3.33d}$$

where

$$\mathcal{D} = \Big\{(\tau, \sigma) : \tau + \sigma > 0,\ |\tau| < 1 + \sigma - \sigma^2,\ |\sigma| < 1 + \tau - \tau^2\Big\} \tag{3.34}$$

Specifically, τ scales the intermediate dual update, whereas σ scales the final one. Note that setting $\tau = \sigma$ reduces the scheme to the relaxed symmetric ADMM (3.32).

3.4 Accelerated ADMM

In addition to the ADMM variants presented in Section 3.3, several acceleration methods have been proposed to improve the computational performance of the algorithm in practice. These methods often affect the structure of the algorithm in different ways, and may not possess the same theoretical guarantees as the original algorithm, or some of its variants. Past iterates can provide valuable information; therefore, many acceleration methods use a momentum-like term to speed up the algorithm. In what follows, different acceleration techniques are examined. Buccini et al. [14] present a framework for ADMM acceleration and a concise review of popular acceleration techniques. Other relevant reviews include [80, 40]. The notation adopted for the acceleration schemes follows Buccini et al., in order to simplify the exposition whenever possible. However, unlike in Buccini et al., where the acceleration formula is written in terms of non-accelerated ADMM outputs only, the formula used here also involves the value that was actually provided as input to the ADMM iteration. For this reason, the notation distinguishes between the non-accelerated ADMM output, denoted by $(\bar{z}^k, \bar{\lambda}^k)$, the accelerated proposal, denoted by $(\tilde{z}^k, \tilde{\lambda}^k)$, and the values retained at the end of iteration k, denoted by (z^k, λ^k), which are used as inputs to the subsequent ADMM iteration. This distinction is relevant because, within the acceptance framework presented in Section 3.5, the accelerated proposal is not necessarily the vector ultimately retained by the algorithm.

Unless otherwise specified, the adopted acceleration formula is

$$\tilde{v}^k = \bar{v}^k + \alpha^k \left(\bar{v}^k - v^{k-1}\right), \tag{3.35}$$

where v stands for either z or λ, and v^{k-1} denotes the value used as input to the ADMM iteration that produces $\bar{v}^k$.

The following subsections illustrate some popular acceleration techniques in more detail and present convergence results whenever possible and relevant.

3.4.1 Stationary acceleration

Referring to the general formula (3.35), the acceleration scheme in [18] uses a fixed value of α throughout the iterations. However, convergence results are established only for $\alpha < 1/3$.

3.4.2 Nesterov acceleration

Also referred to as Fast-ADMM in the literature [35, 56], this acceleration technique updates the parameter α^k following Nesterov's idea. Note that without modifications to the algorithm, such as the restart rule proposed by Goldstein et al. in [35], convergence is guaranteed only when both terms of the objective function are strongly convex. However, the restart rule guarantees convergence for weakly convex problems. The update rule is given by:

$$\tilde{v}^k = \bar{v}^k + \alpha^k \left(\bar{v}^k - \bar{v}^{k-1}\right), \tag{3.36}$$

where

$$\alpha^k = \frac{\beta^{k-1} - 1}{\beta^k}, \tag{3.37}$$

$$\beta^k = \frac{1 + \sqrt{1 + 4(\beta^{k-1})^2}}{2}, \tag{3.38}$$

with $\beta^0 = 1$.

3.4.3 Anderson acceleration

Originally introduced to accelerate fixed-point iterations, Anderson acceleration (AA) [2] can be applied to ADMM [57, 30, 75, 62, 81] by viewing one ADMM iteration as a mapping from the current iterate to the next. In the ADMM context, let v^k denote the iterate retained at the end of iteration k, i.e., the iterate that is used as input to the subsequent ADMM iteration, and let $\bar{v}^{k+1}$ be the corresponding unaccelerated ADMM output computed from v^k. AA constructs an extrapolated candidate $\tilde{v}^{k+1}$ by adding to $\bar{v}^{k+1}$ a linear combination of the most recent m unaccelerated differences. The coefficients are computed by solving the least-squares problem (3.40), which uses the recent history of fixed-point residuals to determine a suitable extrapolation direction. Intuitively, the least-squares problem looks for a combination of past residual variations that best compensates the current residual. In this way, Anderson acceleration uses the observed residual history to predict a correction that may reduce the fixed-point residual in the subsequent iterate. The resulting coefficients are then applied to the corresponding differences of the unaccelerated ADMM outputs to construct the accelerated candidate. Following [75], the accelerated vector is given by

$$\tilde{v}^{k+1} = \bar{v}^{k+1} + \sum_{i=0}^{m^k-1} \beta_i^{(k)} (\bar{v}^{k-i+1} - \bar{v}^{k-i}), \tag{3.39}$$

where $m^k = \min\{m, k\}$. The coefficients $\beta^{(k)} \in \mathbb{R}^{m^k}$ are obtained by solving the least-squares problem

$$\beta^{(k)} \in \arg\min_{\beta \in \mathbb{R}^{m^k}} \left\| w(v^k) + \sum_{i=0}^{m^k-1} \beta_i \big(w(v^{k-i}) - w(v^{k-i-1})\big) \right\|_2^2, \tag{3.40}$$

where

$$w(v^k) := v^k - \bar{v}^{k+1} \tag{3.41}$$

is the AA residual at iteration k, and $\beta_i^{(k)}$ denotes the i-th component of $\beta^{(k)}$. For linear problems, global convergence can be guaranteed if the fixed-point iteration is a contraction [72].

3.4.4 ν acceleration

The ν-type acceleration employed in this work should be regarded as a heuristic semi-iterative extrapolation inspired by the classical ν-method for Landweber iterations [41, 14]. However, unlike the ν-method, this acceleration does not possess established convergence guarantees. The corresponding update formula differs from the general formula in (3.35), and it is given by

$$\tilde{v}^k = \alpha^k \bar{v}^k + (1 - \alpha^k)\bar{v}^{k-1} + \beta^k(\bar{v}^k - \bar{v}^{k-1}) \tag{3.42}$$

where α^k and β^k are two parameters depending on k and on a constant $\nu \in \mathbb{R}$ with

$$\alpha^k = 1 + \frac{(k-1)(2k-3)(2k+2\nu-1)}{(k+2\nu-1)(2k+4\nu-1)(2k+2\nu-3)}, \tag{3.43}$$

$$\beta^k = \frac{4(2k+2\nu-1)(k+\nu-1)}{(k+2\nu-1)(2k+4\nu-1)}. \tag{3.44}$$

3.4.5 Automatic acceleration

Automatic acceleration is a parameter-free extrapolation strategy commonly used in the context of image restoration [12, 14]. It is defined by

$$g^{k-1} = \bar{v}^k - \tilde{v}^{k-1}, \tag{3.45}$$

$$g^{k-2} = \bar{v}^{k-1} - \tilde{v}^{k-2}, \tag{3.46}$$

$$\alpha^k = \frac{(g^{k-1})^\top g^{k-2}}{(g^{k-2})^\top g^{k-2}}. \tag{3.47}$$

For the first two iterations, α^k cannot be computed and is therefore set to $\alpha^0 = \alpha^1 = 0$. Furthermore, a clipping operation is applied such that $0 \leq \alpha^k \leq 1$, for all k.

3.5 Acceptance framework

Many acceleration schemes for ADMM have limited or no theoretical guarantees, especially when applied to problems that do not satisfy specific structural assumptions, such as strong convexity. In practice, an accelerated iterate is not guaranteed to improve convergence at every iteration and may even lead to divergence. For these reasons, several safeguard/restart frameworks have been proposed in the literature to assess the accelerated iterate and accept it only if a prescribed criterion is satisfied; see, e.g., [35, 14]. In these frameworks, the accelerated proposal is discarded whenever the acceptance test fails.

In the restart strategy of Goldstein et al. [35], originally proposed for weakly convex problems, a failed acceleration step is handled by reverting to the most recent non-accelerated ADMM iterate, which is then used as the input for the next iteration. In addition, the acceleration parameters may be reset; for instance, Goldstein et al. reinitialize the Nesterov parameter to its nominal value, $\beta_k = 1$. In the other acceleration schemes considered here, no parameter reset is performed when the accelerated iterate is rejected by the safeguard.

A commonly used criterion in the literature is the *combined residual*, defined for each subsystem s as

$$\gamma_s^k = (\rho^k)^{-1} \|\lambda_s^k - \lambda_s^{k-1}\|_2^2 + \rho^k \|\mathbf{z}_s^k - \mathbf{z}_s^{k-1}\|_2^2. \tag{3.48}$$

The combined residual is not the sum of the standard primal and dual residuals; however, it is related to both and provides a practical scalar metric for acceptance tests.

Goldstein et al. [35] employ a monotone acceptance criterion of the form

$$\gamma^k \leq \mu\,\gamma^{k-1}, \qquad 0 < \mu < 1. \tag{3.49}$$

The variant proposed and tested in the following section relaxes this requirement by adopting a *non-monotone* acceptance criterion based on the combined residual. The underlying idea is to allow temporary increases in the combined residual with respect to the previous iteration, while limiting them by the largest residual observed over a finite window of past iterations. Specifically, the accelerated proposal is accepted if

$$\gamma_{\mathrm{acc}}^{k+1} \leq \max_{j=0,\ldots,\min\{k,w-1\}} \{\gamma^{k-j}\}, \tag{3.50}$$

where $w \in \mathbb{N}$ is the safeguard window length.

For generalized consensus ADMM with multiple subsystems, the global combined residual is defined as

$$\gamma^k = \sum_{s\in\mathcal{S}} \gamma_s^k. \tag{3.51}$$

Algorithm 3 presents a generalized version of the safeguard mechanism described above.

Algorithm 3 Accelerated ADMM with non-monotone safeguard

Require: Augmented Lagrangian $L_\rho(x, z, y)$; initial (x^0, z^0, y^0); safeguard window length w.
Require: A stored fallback non-accelerated ADMM output $(\bar{z}^0, \bar{y}^0)$.
Require: Initialize skipRestart$^0 \leftarrow$ `false`.
for $k = 0, 1, 2, \ldots$ **do**
  (Unaccelerated ADMM step)
  $\bar{x}^{k+1} \leftarrow \arg\min_x \; L_\rho(x, z^k, y^k)$
  $\bar{z}^{k+1} \leftarrow \arg\min_z \; L_\rho(\bar{x}^{k+1}, z, y^k)$
  $\bar{y}^{k+1} \leftarrow y^k + \rho^k\big(A\bar{x}^{k+1} + B\bar{z}^{k+1} - c\big)$
  (Acceleration proposal)
  $(\tilde{z}^{k+1}, \tilde{y}^{k+1}) \leftarrow \mathrm{Accelerate}\big(\bar{z}^{k+1}, \bar{y}^{k+1}, \text{past iterates}\big)$
  (Safeguard test)
  $\gamma_{\mathrm{acc}}^{k+1} \leftarrow \sum_{s\in\mathcal{S}} \Big((\rho^k)^{-1}\, \|\tilde{y}_s^{k+1} - y_s^k\|_2^2 + \rho^k\, \|\tilde{\mathbf{z}}_s^{k+1} - \mathbf{z}_s^k\|_2^2\Big)$
  if $\gamma_{\mathrm{acc}}^{k+1} > \max_{j=0,\ldots,\min(k,w-1)}\{\gamma^{k-j}\}$ and skipRestart^k = `false` **then**
    (Reject / restart)
    $(z^{k+1}, y^{k+1}) \leftarrow (\bar{z}^k, \bar{y}^k)$ ▷ rollback to last stored non-accelerated ADMM output
    Optionally: reset/modify acceleration parameters
    skipRestart$^{k+1} \leftarrow$ `true` ▷ prevent consecutive rejection loops
  else
    (Accept acceleration)
    $(z^{k+1}, y^{k+1}) \leftarrow (\tilde{z}^{k+1}, \tilde{y}^{k+1})$
    (Update safeguard history) Update $\{\gamma^k\}$ for the next safeguard test
  end if
end for

3.6 Computational study

ADMM has been widely adopted in power system optimization, particularly for the Direct-Current Optimal Power Flow (DCOPF) problem, a linear approximation of the more complex Alternating-Current Optimal Power Flow (ACOPF) problem. This section investigates the empirical behavior of an ADMM-based distributed framework for an energy management problem subject to DCOPF network constraints.

The computational analysis focuses on comparing the baseline ADMM scheme, a variable-penalty ADMM variant, and several accelerated ADMM variants across the same problem instances, both with and without the non-monotone restart framework introduced in the previous section. In addition to comparing multiple acceleration strategies on several instances of the same market-clearing problem, the experiments assess the effect of enabling or disabling the safeguard framework, as well as the impact of different restart-parameter configurations.

The primary performance metric is the number of iterations required to satisfy the prescribed accuracy and feasibility tolerances. The final residual values are also reported to characterize convergence behavior and to highlight the effect of safeguarding, including cases in which all methods terminate under the same stopping criterion, such as reaching the maximum number of iterations. In addition, solution quality is assessed through an optimality indicator, defined by comparing the objective value returned by each method with the optimal objective value.

For each instance, the acceleration schemes are also evaluated under different restart/safeguard configurations.

3.6.1 Problem definition

Consider the following general structured formulation of the optimization problem:

$$
\begin{aligned}
\max_{\theta,\, y,\, w} \quad & F(y,w) = \sum_{v \in V} f_v(y_v) + \sum_{u \in U} c_u(w_u) && && \text{(3.52a)} \\
\text{s.t.} \quad & h_i(\theta) = y_i - w_i && \forall i \in N_1 && \text{(3.52b)} \\
& h_v(\theta) = y_v && \forall v \in N_2 && \text{(3.52c)} \\
& h_u(\theta) = -w_u && \forall u \in N_3 && \text{(3.52d)} \\
& g_j(\theta) \le d_j && \forall j \in J && \text{(3.52e)} \\
& y_v \in Y_v && \forall v \in V && \text{(3.52f)} \\
& w_u \in W_u && \forall u \in U && \text{(3.52g)} \\
& \theta^{\min} \le \theta \le \theta^{\max}, \quad \theta \in \mathbb{R}^{|N|}. && && \text{(3.52h)}
\end{aligned}
$$

Here, N is an index set partitioned into N_1, N_2, N_3 such that $N_1 \cup N_2 \cup N_3 = N$ and $N_a \cap N_b = \emptyset$ for all $a \neq b$. Define the index sets of decision variables as $V := N_1 \cup N_2$ and $U := N_1 \cup N_3$. Accordingly, $y = (y_v)_{v \in V}$ and $w = (w_u)_{u \in U}$ are decision variables, whereas $\theta \in \mathbb{R}^{|N|}$ is a system-level variable that appears only in the constraints. For each $v \in V$ and $u \in U$, the sets Y_v and W_u denote the feasible sets for y_v and w_u, respectively, and encode restrictions involving only the corresponding variable. Finally, $h_i : \mathbb{R}^{|N|} \to \mathbb{R}$ and $g_j : \mathbb{R}^{|N|} \to \mathbb{R}$ denote generic system-level constraint functions. When problem (3.52) is defined on a connected graph $\mathcal{G} = (N, J)$, N represents the nodes, J represents the edges, and the functions $h_i(\theta)$ and $g_j(\theta)$ model the network constraints, such as nodal balance relations and line-flow limits.

Decomposition (consensus reformulation). Let $\mathcal{S} = \{1, \dots, |\mathcal{S}|\}$ and consider a partition of the node set N into pairwise disjoint subsets $(N^s)_{s\in\mathcal{S}}$ such that $\bigcup_{s\in\mathcal{S}} N^s = N$.

The objective (3.52a) and the local feasibility constraints (3.52f)–(3.52g) are separable across subsystems. The nonseparability arises from the network constraints (3.52b)–(3.52e), because, for a connected graph and $|\mathcal{S}| > 1$, some of them necessarily involve variables associated with nodes belonging to different subsystems. To obtain a decomposable structure, the consensus, or variable-splitting, reformulation is applied:

1. Fix a partition $(N^s)_{s\in\mathcal{S}}$ and assign to each subsystem s the network constraints that refer to nodes in N^s and the line constraints that at least one one in N^s.
2. For each subsystem s, identify the set of *coupling indices*
$$\mathcal{B}^s := \{i \in N \setminus N^s \ : \ \theta_i \text{ appears in at least one constraint assigned to subsystem } s\}.$$
3. For each subsystem s, introduce local copies θ_i^s for all $i \in \mathcal{B}^s$ and replace each occurrence of θ_i in the constraints of subsystem s with the corresponding local copy θ_i^s.
4. Introduce a global *consensus variable* z_i for each index that is duplicated in at least one subsystem, i.e.,
$$\mathcal{B} := \bigcup_{s\in\mathcal{S}} \mathcal{B}^s, \qquad z := (z_i)_{i\in\mathcal{B}}.$$
5. Enforce consensus through
$$\begin{aligned} \theta_i^s &= z_i \qquad \forall s \in \mathcal{S},\ \forall i \in \mathcal{B}^s, \\ \theta_i &= z_i \qquad \forall s \in \mathcal{S},\ \forall i \in (N^s \cap \mathcal{B}). \end{aligned}$$

This yields a formulation in which, conditional on z, each subsystem can solve an independent local problem. ADMM then coordinates the subsystems by alternating local solves with a consensus update on z and dual updates associated with the constraints $\theta_i^s = z_i$.

Example. Consider the network in Figure 3.1, with node set $N = \{1, \dots, 8\}$ and partition
$$N^1 = \{6, 7, 8\}, \qquad N^2 = \{1, 4, 5\}, \qquad N^3 = \{2, 3\}.$$
The cut edges, shown as dashed lines in Figure 3.1, are
$$(6, 5),\ (6, 4),\ (7, 1),\ (1, 2),\ (2, 4).$$
Assume that subsystem s includes all network constraints indexed by nodes in N^s and all line constraints incident to N^s. Under this assignment, subsystem s requires the components θ_i associated with its own nodes and, for each cut edge incident to N^s, also the component associated with the external endpoint. Hence, the coupling index sets are
$$\mathcal{B}^1 = \{1, 4, 5\}, \qquad \mathcal{B}^2 = \{2, 6, 7\}, \qquad \mathcal{B}^3 = \{1, 4\},$$

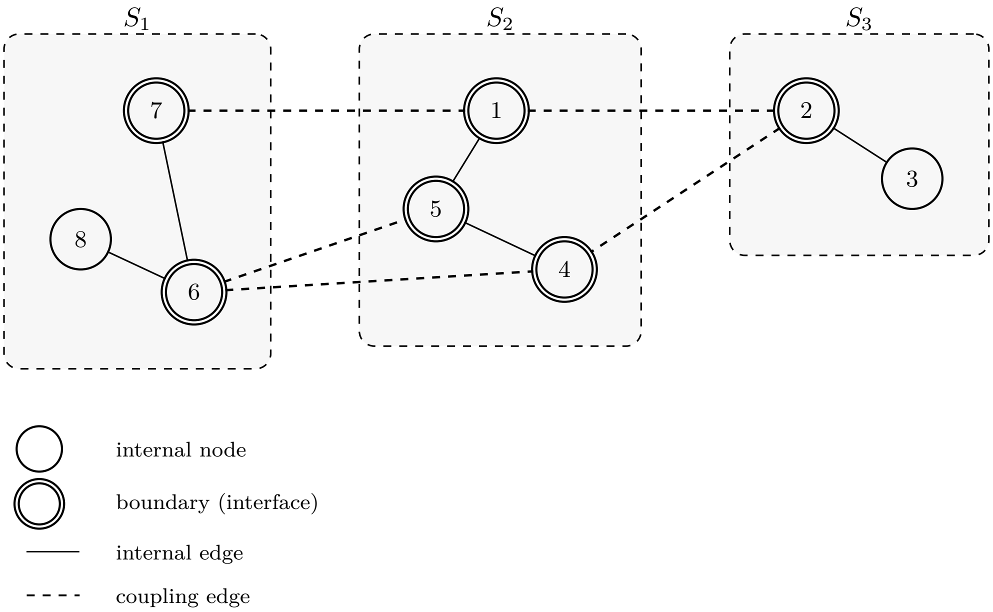

Figure 3.1. Partition of the example network into subsystems S_1–S_3, with internal edges and coupling edges.

and the set of duplicated indices is

$$\mathcal{B} = \bigcup_{s\in\{1,2,3\}} \mathcal{B}^s = \{1, 2, 4, 5, 6, 7\}.$$

Local duplicates of the system variable are introduced as follows:

$$S_1 : \ (\theta_1^1, \theta_4^1, \theta_5^1), \qquad S_2 : \ (\theta_2^2, \theta_6^2, \theta_7^2), \qquad S_3 : \ (\theta_1^3, \theta_4^3),$$

and each occurrence of θ_i with $i \in \mathcal{B}^s$ inside the constraints assigned to subsystem s is replaced by θ_i^s. A consensus variable z_i is introduced for each $i \in \mathcal{B}$, namely

$$z = (z_1, z_2, z_4, z_5, z_6, z_7).$$

Consensus is then enforced by the equalities

$$\begin{aligned} \theta_i^s &= z_i \qquad \forall s \in \{1,2,3\},\ \forall i \in \mathcal{B}^s, \\ \theta_i &= z_i \qquad \forall s \in \{1,2,3\},\ \forall i \in (N^s \cap \mathcal{B}). \end{aligned}$$

For this example, these equalities read explicitly as follows:

$S_1 :$	$\theta_1^1 = z_1$		$\theta_4^1 = z_4$	$\theta_5^1 = z_5$	$\theta_6 = z_6$	$\theta_7 = z_7$
$S_2 :$	$\theta_1 = z_1$	$\theta_2^2 = z_2$	$\theta_4 = z_4$	$\theta_5 = z_5$	$\theta_6^2 = z_6$	$\theta_7^2 = z_7$
$S_3 :$	$\theta_1^3 = z_1$	$\theta_2 = z_2$	$\theta_4^3 = z_4$			

Equivalently, each cut edge induces a duplication of θ at the external endpoint for each incident subsystem. For instance, edge $(6, 5)$ implies that subsystem S_1 uses θ_5^1 in place of θ_5 while subsystem S_2 uses θ_6^2 in place of θ_6, with both copies linked to z_5 and z_6, respectively, through the above consensus constraints.

Variable	Domain	Description
$\theta_{n,t}$	$\mathbb{R}$	Voltage angle at bus $n \in N$ in period $t \in T$.
$p_{g,t}$	$\mathbb{R}$	Power output of generator $g \in G$ in period $t \in T$.
$d_{i,t}$	$\mathbb{R}$	Served (elastic) demand at demand bus $i \in D$ in period $t \in T$.
$h^k_{i,t}$	$\mathbb{R}_{\geq 0}$	Demand allocated to segment $k \in K$ of the stepwise demand curve for bus $i \in D$ in period $t \in T$.

Table 3.1. Variables.

Set	Description
T	Set of discrete time periods in the planning horizon.
N	Set of network nodes (buses).
$D \subseteq N$	Set of demand buses.
$G \subseteq N$	Set of generation buses.
K	Set of segments (blocks) of the stepwise-linear demand function.
L	Set of transmission elements (branches), represented as ordered node pairs (b, j).

Table 3.2. Sets.

3.6.2 Test case

Below, a special case of Problem (3.52), introduced in [77], is considered. Following the approach of Wang et al., the model is reformulated and solved using the alternating direction method of multipliers (ADMM). Moreover, within the non-monotone acceptance framework, several ADMM variants and acceleration techniques are tested. The resulting formulation is a convex quadratic program with linear constraints. Compared with a standard day-ahead market-clearing model, it includes a demand-response mechanism that allows part of the load to be shifted across time periods, thereby increasing system flexibility. The network is represented using the DCOPF linearization. To simplify the exposition, each bus is assumed to host at most one generating unit. The generators are then identified with the buses at which they are located. No loss of generality is incurred, as the case of multiple generators per bus can be handled by aggregating their outputs at the nodal level.
Unless otherwise specified, vectors are denoted in boldface; a bold symbol indicates that the corresponding indexed variables are stacked over the omitted index, e.g. $\boldsymbol{\theta}_t := (\theta_{n,t})_{n \in N}$. Moreover, let $\mathbf{p}_t \in \mathbb{R}^{|N|}$ denote the nodal generation vector, with $(\mathbf{p}_t)_n = p_{n,t}$ for $n \in G$ and $(\mathbf{p}_t)_n = 0$ otherwise. Similarly, let $\mathbf{d}_t \in \mathbb{R}^{|N|}$ denote the nodal demand vector, with $(\mathbf{d}_t)_n = d_{n,t}$ for $n \in D$ and $(\mathbf{d}_t)_n = 0$ otherwise.

Before introducing the model, Table 3.1 shows the relevant variables, Table 3.2 the sets, and Table 3.3 the parameters.

The formulation used as a test case is shown below in (3.53).

Parameter	Domain	Description
$\mathbf{B}$	$\mathbb{R}^{\lvert N\rvert \times \lvert N\rvert}$	Nodal admittance matrix (DC model).
$b_{i,j}$	$\mathbb{R}$	Susceptance coefficient associated with a transmission element (i, j).
$F_{bj,t}^{\max}$	$\mathbb{R}$	Maximum admissible flow on transmission element (b, j) in period t.
$P_{g,t}^{\min}$	$\mathbb{R}$	Technical minimum output of generator g in period t.
$P_{g,t}^{\max}$	$\mathbb{R}$	Technical maximum output of generator g in period t.
P_g^{up}	$\mathbb{R}$	Ramp-up limit of generator g between two consecutive periods.
P_g^{down}	$\mathbb{R}$	Ramp-down limit of generator g between two consecutive periods.
$d_{i,t}^0$	$\mathbb{R}$	Minimum admissible demand at demand bus i in period t.
$d_{i,t}^{\max}$	$\mathbb{R}$	Maximum admissible demand at demand bus i in period t.
$d_{i,\mathrm{total}}$	$\mathbb{R}$	Total energy requirement of demand bus i over the horizon (demand conservation across T).
$\pi_{i,t}^k$	$\mathbb{R}$	Marginal willingness-to-pay (value) associated with segment k of the elastic demand at bus i in period t.
$l_{i,t}^k$	$\mathbb{R}$	Upper bound (width) of segment k in the stepwise demand representation at bus i in period t.
θ_n^{min}	$\mathbb{R}$	Lower bound of voltage angle at bus $n \in N$.
θ_n^{max}	$\mathbb{R}$	Upper bound of voltage angle at bus $n \in N$.
ref	N	Reference (slack) bus.
a_g^1	$\mathbb{R}$	Quadratic coefficient of the production cost function of generator g.
a_g^2	$\mathbb{R}$	Linear coefficient of the production cost function of generator g.
a_g^3	$\mathbb{R}$	Constant term of the production cost function of generator g.

Table 3.3. Parameters.

$$
\begin{aligned}
\max_{\theta,\mathbf{d},\mathbf{p},\mathbf{h}} \quad & \sum_{t\in T}\sum_{i\in D} g(d_{i,t}) - \sum_{t\in T}\sum_{g\in G} f_g(p_{g,t}) && && (3.53a)\\
\text{s.t.} \quad & \mathbf{B}\,\boldsymbol{\theta}_t = \mathbf{p}_t - \mathbf{d}_t && \forall t\in T && (3.53b)\\
& \theta_{b,t} - \theta_{j,t}\, b_{i,j} \le F_{bj,t}^{\max} && \forall (b,j)\in L,\ \forall t\in T && (3.53c)\\
& \theta_{j,t} - \theta_{b,t}\, b_{i,j} \le F_{bj,t}^{\max} && \forall (b,j)\in L,\ \forall t\in T && (3.53d)\\
& \theta_n^{min} \le \theta_{n,t} \le \theta_n^{max} && \forall n\in N,\ \forall t\in T && (3.53e)\\
& \theta_{n^{\mathrm{ref}},t} = 0 && \forall t\in T && (3.53f)\\
& P_{g,t}^{\min} \le p_{g,t} \le P_{g,t}^{\max} && \forall g\in G,\ \forall t\in T && (3.53g)\\
& p_{g,t} - p_{g,t-1} \le P_g^{\mathrm{up}} && \forall g\in G,\ \forall t\in T : t>1 && (3.53h)\\
& p_{g,t-1} - p_{g,t} \le P_g^{\mathrm{down}} && \forall g\in G,\ \forall t\in T : t>1 && (3.53i)\\
& d_{i,t}^0 \le d_{i,t} \le d_{i,t}^{\max} && \forall i\in D,\ \forall t\in T && (3.53j)\\
& \sum_{t\in T} d_{i,t} = d_{i,\mathrm{total}} && \forall i\in D && (3.53k)\\
& g(d_{i,t}) = \sum_{k\in K} \pi_{i,t}^k\, h_{i,t}^k && \forall i\in D,\ \forall t\in T && (3.53l)\\
& 0 \le h_{i,t}^k \le l_{i,t}^k && \forall i\in D,\ \forall t\in T,\ \forall k\in K && (3.53m)\\
& d_{i,t} = \sum_{k\in K} h_{i,t}^k && \forall i\in D,\ \forall t\in T && (3.53n)\\
& f_g(p_{g,t}) = a_g^1\,(p_{g,t})^2 + a_g^2\, p_{g,t} + a_g^3 && \forall g\in G,\ \forall t\in T. && (3.53o)
\end{aligned}
$$

The objective function (3.53a) maximizes the social surplus: the first term represents the total willingness to pay (gross utility) associated with elastic demand, whereas the second term accounts for generation costs. Quadratic or piecewise-linear convex approximations of generation costs are common in both the literature and practice. Additional cost components, such as start-up and shut-down costs, typically require different modeling choices and lead to mixed-integer formulations. The gross utility associated with elastic demand is modeled through the stepwise marginal willingness-to-pay parameters $\pi^k_{i,t}$ and the segment variables $h^k_{i,t}$; accordingly, the utility term $g(d_{i,t})$ is computed as in (3.53l). The served demand is restricted to the interval $[d^0_{i,t}, d^{\max}_{i,t}]$ by (3.53j).

Constraints (3.53b)–(3.53f) implement the DC power-flow approximation. In particular, constraints (3.53b) enforce the nodal power balance, constraints (3.53c) and (3.53d) impose the line-flow limits, constraints (3.53e) bound the voltage angles, and constraints (3.53f) fix the angle of the reference bus to zero. Note that the angle bounds in (3.53e) are not included in the original formulation of Wang et al. [77] and are introduced here to prevent unrealistic angle values. Constraints (3.53g) enforce generator capacity limits by bounding the power generated between the technical minimum and the maximum levels. Constraints (3.53h) and (3.53i) impose ramp-rate limits between consecutive periods. Finally, the demand-response mechanism is modeled through constraints (3.53j) and (3.53k), which allow the demand to shift over time while preserving total energy over the planning horizon.

3.6.3 Variants and acceleration techniques tested

The baseline method is the generalized consensus ADMM without acceleration and with a fixed penalty parameter ρ. For each test case, ρ is selected by evaluating a predefined range of values and choosing the one that yields the smallest number of iterations required to satisfy the stopping criterion. The baseline is compared with (i) the ADMM variant with variable penalty parameters described in Subsection 3.3.1, and (ii) the acceleration techniques introduced in Section 3.4, namely Stationary, Nesterov, Automatic, and Anderson acceleration. The ν-acceleration method is not included in the reported results, as it was not effective on the instances considered in preliminary experiments. For the variable-penalty variant, the parameters are set to $\mu = 10$ and $\tau^{\text{incr}} = \tau^{\text{decr}} = 2$, in line with the typical choices suggested in [13]. When an acceleration technique requires an additional parameter, namely α for Stationary acceleration and m for Anderson acceleration, this parameter is tuned over a predefined range, and the value yielding the smallest number of iterations is used in the global comparison.

Overall, the following methods are tested both with and without the safeguard mechanism:

- Standard ADMM (fixed ρ).
- ADMM with varying ρ.
- ADMM + Stationary acceleration (α).
- ADMM + Nesterov acceleration.
- ADMM + Automatic acceleration.
- ADMM + Anderson acceleration (m).

Table 3.4. Test instances considered in the experimental study. In the Cost column, Lin denotes linear costs, while Quad denotes quadratic costs.

Instance	Bus	Edge	Generators	Subsystems	Cost
`Case_5_base`	5	6	4	2	Lin
`Case_5_q`	5	6	4	2	Lin + Quad
`Case_30_base`	30	41	2	3	Lin
`Case_30_q`	30	41	2	3	Lin + Quad
`Case_118_base`	118	179	19	3	Lin
`Case_118_q`	118	179	19	3	Lin + Quad

3.6.4 Instances

To evaluate the proposed framework, six test instances derived from three networks with different sizes and topologies are considered. In particular: a 5-bus network, adapted from the MATPOWER [82] test, based on [53]; the 30-bus and 118-bus networks from the *IEEE PES Power Grid Library* [5]. The remaining parameters, such as the demand profile in the time period, ramp limits, and demand steps, have been generated accordingly to the original data.

For each network, two cost-model variants are analyzed: (i) a *base* formulation with linear generation costs only, and (ii) a Q formulation including additional quadratic generation costs. This setup allows us to assess the algorithmic behavior across problem classes with different curvature and conditioning. Table 3.4 presents the main characteristic of the instances.

3.6.5 Computational setup and implementation details

The experiments were conducted on a machine with an Intel Core i5-10210U processor, on eight cores with a clock speed of 1.60 GHz. The internal subproblems solution process is performed identically in all tests using Gurobi Optimizer version 13.0.0 through Python 3.12.3.

3.6.6 Results

This section presents the computational results. Each table caption reports the parameter values used in the corresponding experiment, along with the test case under analysis. The comparison is structured across three configurations: (i) no safeguard mechanism (i.e., all accelerated iterates are accepted), and (ii)–(iii) two safeguard-enabled configurations with different window lengths.

For each test case, two tables are reported. The first table shows the number of iterations required to converge (when convergence is achieved), the optimality gap expressed as a percentage with respect to the optimal objective value, the termination status, and the maximum primal and dual residuals across all subsystems, denoted by $\|r\|_\infty$ and $\|s\|_\infty$, respectively. The optimality gap is computed as

$$\text{Gap} = \frac{\text{Objective}^{\text{ADMM}} - \text{Objective}^*}{\text{Objective}^*} \cdot 100,$$

where $\text{Objective}^{\text{ADMM}}$ denotes the value of the objective function at the solution returned by ADMM, and Objective^* denotes the optimal objective value, obtained by solving the complete problem with Gurobi Optimizer in Python.

The second table reports the residual values at termination. In addition, three plots are provided for each test case, corresponding to the three safeguard configurations (SG OFF, SG ON with $w = 2$, and SG ON with $w = 3$). These plots show the evolution of the *Max Residual*, defined as

$$\textit{Max Residual} = \max(\|r_s\|_\infty,\ \|s\|_\infty)\,.$$

Aggregate overview. Before discussing the individual test cases, two aggregate heatmaps are used to summarize the main trends observed across all instances and acceleration strategies. Figure 3.2 reports the iteration count of each method relative to the best converged method for the same test case and safeguard configuration. This representation highlights the methods that are consistently close to the best observed performance, while also identifying configurations that reach the iteration limit. In particular, the heatmap provides a compact comparison of the three safeguard settings: SG OFF, SG ON with $w = 2$, and SG ON with $w = 3$.

Figure 3.4 focuses instead on the direct effect of the safeguard mechanism. For each method and test case, it reports the percentage variation in the number of iterations with respect to the corresponding SG OFF configuration. Negative values therefore indicate a reduction in the number of iterations, whereas positive values indicate a deterioration in terms of iteration count. The figure also distinguishes safeguarded runs that reach the iteration limit from cases in which the safeguard allows the prescribed convergence tolerance to be reached within the iteration budget, unlike the corresponding SG OFF run.

Overall, these aggregate results are intended to provide a qualitative overview of the main performance patterns before the case-by-case analysis. The detailed tables and residual plots reported in the following subsections are then used to interpret these trends more precisely for each individual test case.

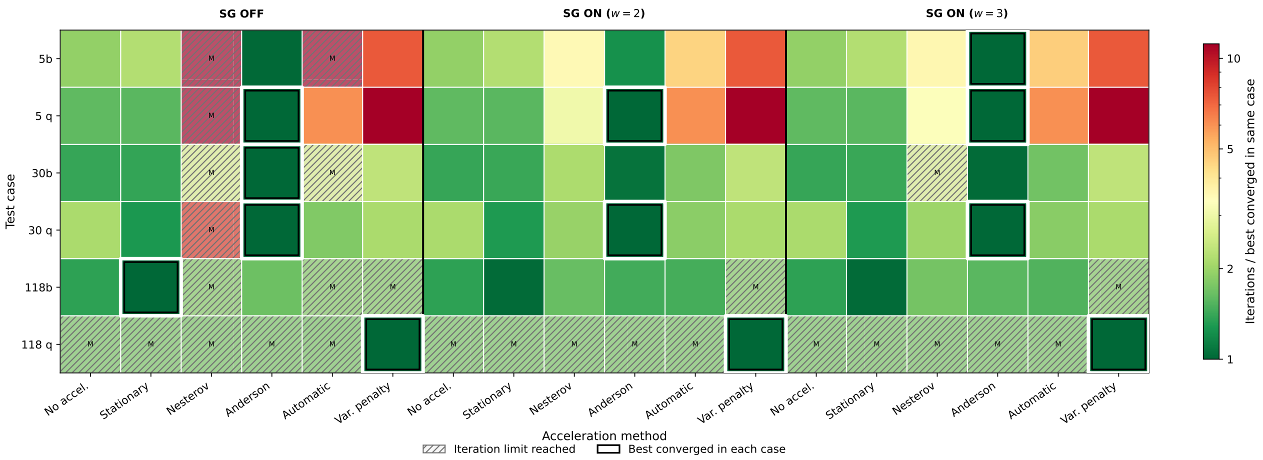

Figure 3.2. Relative number of iterations for each acceleration method, normalized by the lowest iteration count among the converged methods for the same test case and safeguard configuration. Hatched cells marked with M indicate runs that reached the maximum iteration budget. Black and white frames identify the best converged method in each test case and safeguard setting. Test cases labeled with b correspond to `Case_base`, while test cases labeled with q correspond to `Case_q`.

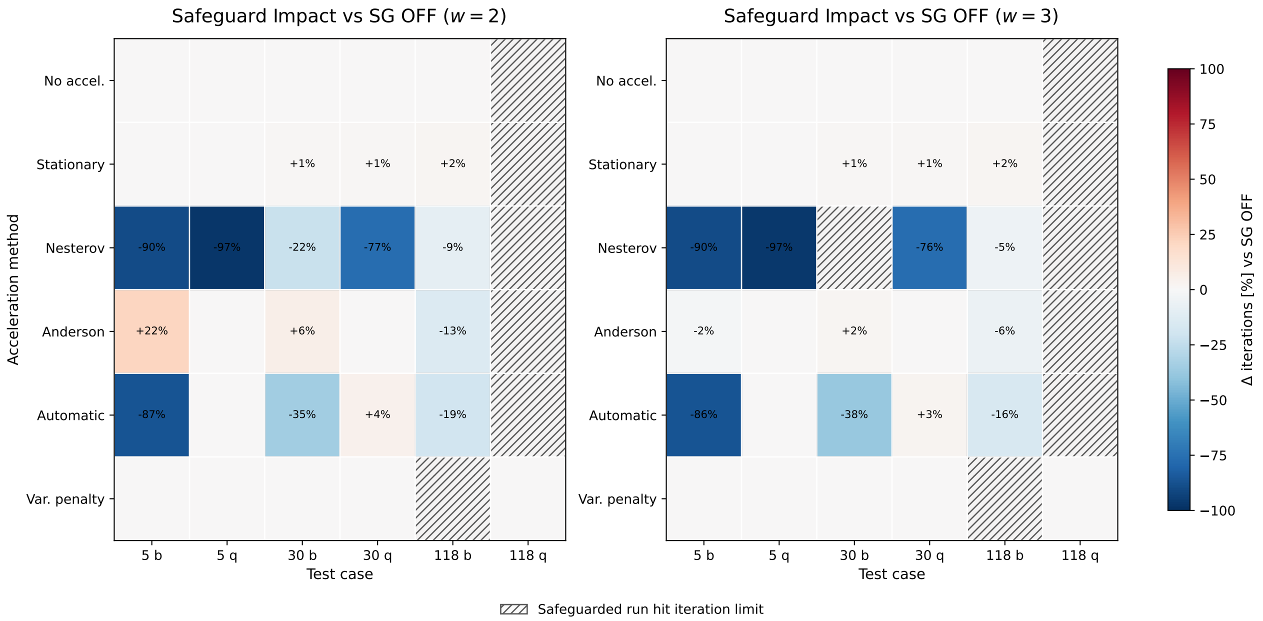

Figure 3.3. Safeguard impact

Figure 3.4. Percentage variation in the number of iterations induced by the safeguard mechanism with respect to the corresponding SG OFF run. Negative values indicate a reduction in iteration count, whereas positive values indicate an increase. The left and right panels correspond to SG ON with $w = 2$ and $w = 3$, respectively. Hatched cells denote safeguarded runs that reached the maximum iteration budget. Test cases labeled with b correspond to `Case_base`, while test cases labeled with q correspond to `Case_q`.

Case 5. The experiments on `Case_5_base` indicate that, on the 5-bus network, the safeguard mechanism primarily improves the robustness of the accelerated schemes by preventing divergence in otherwise unstable configurations. This effect is visible in Table 3.5, Table 3.6, and Figure 3.5. In particular, ADMM with Nesterov acceleration exhibits divergent behavior in the unsafeguarded setting (both in `Case_5_base` and `Case_5_q`), whereas it converges when the safeguard is enabled.

Automatic acceleration also benefits from the safeguard, which appears to reduce the acceptance of non-beneficial accelerated iterates. The most efficient convergent method is Anderson acceleration, with $m = 30$ for `Case_5_base` and $m = 7$ for `Case_5_q`. For Anderson acceleration, the effect of the safeguard depends on the window length w: performance is slightly worse for $w = 2$, but improves for $w = 3$. By contrast, for Nesterov acceleration, increasing the safeguard window from $w = 2$ to $w = 3$ does not improve performance and may slightly degrade it.

For `Case_5_q`, as shown in Table 3.7, Table 3.8, and Figure 3.6, the safeguard has no effect on the iteration count of any method other than Nesterov, since the combined residual never activates the restart mechanism (i.e., #SG = 0 for all those methods). Accordingly, the iteration counts remain unchanged for No Acceleration (91), Stationary acceleration (89), Anderson acceleration (57), Automatic acceleration (343), and Varying Penalty (637). By contrast, Nesterov acceleration reaches the iteration limit without the safeguard (6000 iterations) and converges only in the safeguarded configurations, requiring 174 iterations for $w = 2$ and 188 iterations for $w = 3$. The residuals in Table 3.8 confirm the same pattern. In the setting without the safeguard, Nesterov acceleration terminates with very large residuals ($\|r\|_\infty = 2.05 \times 10^2$, $\|s\|_\infty = 1.73 \times 10^5$), while with the safeguard enabled, both residuals are reduced below the prescribed tolerances. This indicates that, for `Case_5_q`, the safeguard acts primarily as a stabilization mechanism for Nesterov acceleration, with negligible impact on the other methods.

Table 3.5. Performance comparison for `Case_5_base` under three safeguard settings.

	Safeguard OFF			Safeguard ON ($w = 2$)				Safeguard ON ($w = 3$)			
Method	Iter.	Gap [%]	Status	Iter.	Gap [%]	Status	#SG	Iter.	Gap [%]	Status	#SG
No Acceleration	341	0.00	C	341	0.00	C	0	341	0.00	C	0
Stationary (α)	390	0.00	C	390	0.00	C	0	390	0.00	C	0
Nesterov	6000	−1.40	M	616	0.00	C	115	630	0.00	C	104
Anderson (m)	**180**	**0.00**	**C**	**219**	**0.00**	**C**	67	**177**	**0.00**	**C**	24
Automatic	6000	0.00	M	797	0.00	C	100	819	0.00	C	99
Varying Penalty	1315	0.00	C	1315	0.00	C	0	1315	0.00	C	0

Common parameters: $\rho = 400.0$, $\alpha = 0.5$, $m = 30$, $\varepsilon_r = 10^{-4}$, $\varepsilon_s = 10^{-4}$, max iter = 6000.
C = converged; **M** = iteration limit reached; #SG = number of safeguard activations.

Table 3.6. Residuals at termination for `Case_5_base` under three safeguard settings.

	Safeguard OFF		Safeguard ON ($w = 2$)		Safeguard ON ($w = 3$)	
Method	$\|r\|_\infty$	$\|s\|_\infty$	$\|r\|_\infty$	$\|s\|_\infty$	$\|r\|_\infty$	$\|s\|_\infty$
No Acceleration	1.80 e−6	7.11 e−5	1.80 e−6	7.11 e−5	1.80 e−6	7.11 e−5
Stationary (α)	3.71 e−6	6.54 e−5	3.71 e−6	6.54 e−5	3.71 e−6	6.54 e−5
Nesterov	2.08 e+2	1.09 e+5	7.45 e−7	8.91 e−5	5.22 e−6	9.49 e−5
Anderson (m)	**2.06e−7**	**8.23e−5**	**1.83e−7**	**8.70e−5**	**2.32e−7**	**9.79e−5**
Automatic	2.17 e−5	1.13 e−2	7.35 e−7	6.66 e−5	3.32 e−6	8.49 e−5
Varying Penalty	6.00 e−5	7.70 e−5	6.00 e−5	7.70 e−5	6.00 e−5	7.70 e−5

Residuals are reported at termination (convergence or stopping limit).
Scientific notation is aligned across the three safeguard settings for easier comparison.

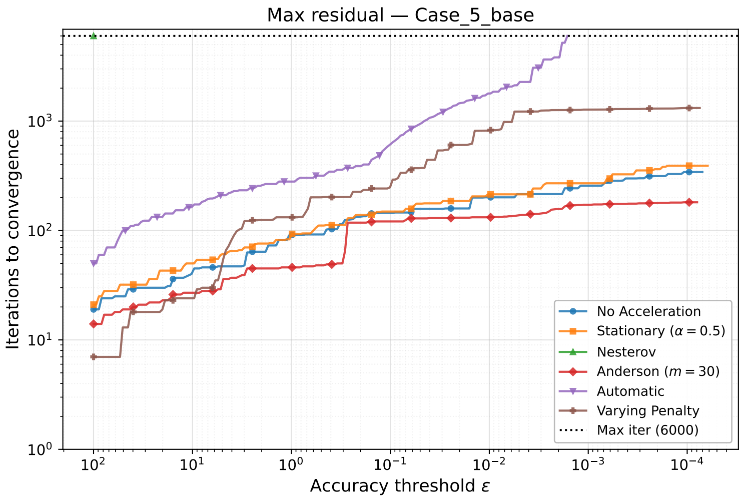

(a) No safeguard

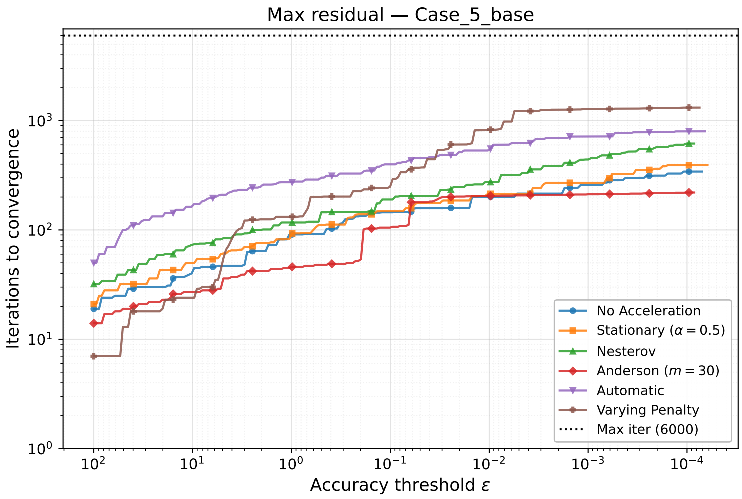

(b) Safeguard, $w = 2$

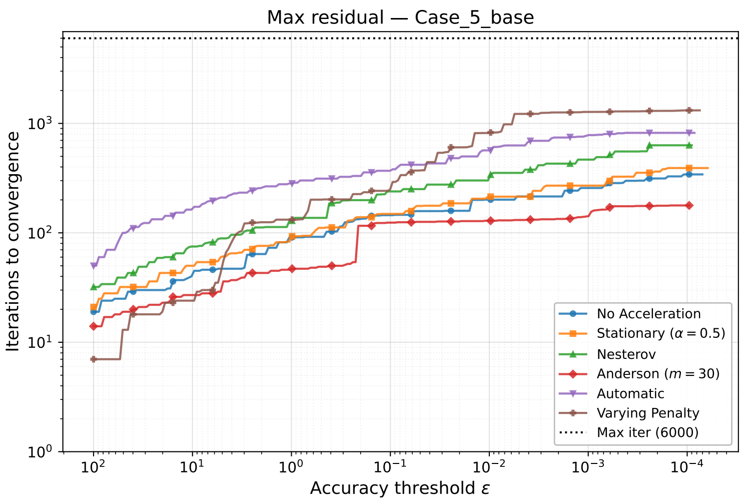

(c) Safeguard, $w = 3$

Figure 3.5. Comparison of the maximum residual for ADMM acceleration methods under three configurations (no safeguard, safeguard with $w = 2$, and safeguard with $w = 3$) for `Case_5_base`.

Table 3.7. Performance comparison for `Case_5_q` under three safeguard settings.

Method	Safeguard OFF			Safeguard ON ($w = 2$)				Safeguard ON ($w = 3$)			
	Iter.	Gap [%]	Status	Iter.	Gap [%]	Status	#SG	Iter.	Gap [%]	Status	#SG
No Acceleration	91	0.00	C	91	0.00	C	0	91	0.00	C	0
Stationary (α)	89	0.00	C	89	0.00	C	0	89	0.00	C	0
Nesterov	6000	2.44	M	174	0.00	C	28	188	0.00	C	29
Anderson (m)	**57**	**0.00**	**C**	**57**	**0.00**	**C**	0	**57**	**0.00**	**C**	0
Automatic	343	0.00	C	343	0.00	C	0	343	0.00	C	0
Varying Penalty	637	0.00	C	637	0.00	C	0	637	0.00	C	0

Common parameters: $\rho = 700.0$, $\alpha = 0.1$, $m = 7$, $\varepsilon_r = 10^{-4}$, $\varepsilon_s = 10^{-4}$, max iter = 6000.
C = converged; **M** = iteration limit reached; #SG = number of safeguard activations.

Table 3.8. Residuals at termination for `Case_5_q` under three safeguard settings.

Method	Safeguard OFF		Safeguard ON ($w = 2$)		Safeguard ON ($w = 3$)	
	$\|r\|_\infty$	$\|s\|_\infty$	$\|r\|_\infty$	$\|s\|_\infty$	$\|r\|_\infty$	$\|s\|_\infty$
No Acceleration	1.03 e−7	9.11 e−5	1.03 e−7	9.11 e−5	1.03 e−7	9.11 e−5
Stationary (α)	1.70 e−7	6.96 e−5	1.70 e−7	6.96 e−5	1.70 e−7	6.96 e−5
Nesterov	2.05 e+2	1.73 e+5	1.15 e−7	9.52 e−5	1.61 e−7	9.41 e−5
Anderson (m)	**8.95e−8**	**9.06e−5**	**8.95e−8**	**9.06e−5**	**8.95e−8**	**9.06e−5**
Automatic	4.11 e−7	9.78 e−5	4.11 e−7	9.78 e−5	4.11 e−7	9.78 e−5
Varying Penalty	9.85 e−5	7.62 e−5	9.85 e−5	7.62 e−5	9.85 e−5	7.62 e−5

Residuals are reported at termination (convergence or stopping limit).
Scientific notation is aligned across safeguard settings for easier comparison.

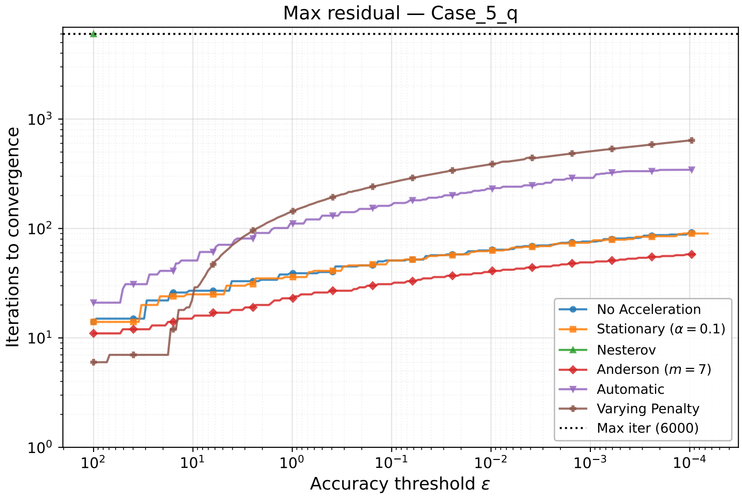

(a) No safeguard

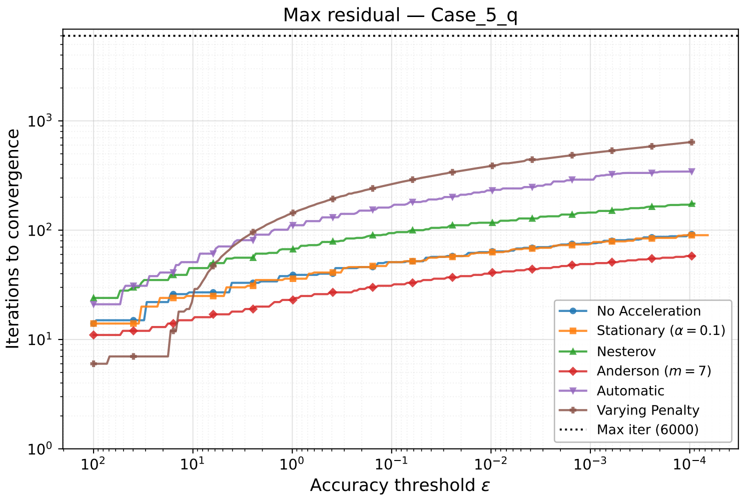

(b) Safeguard, $w = 2$

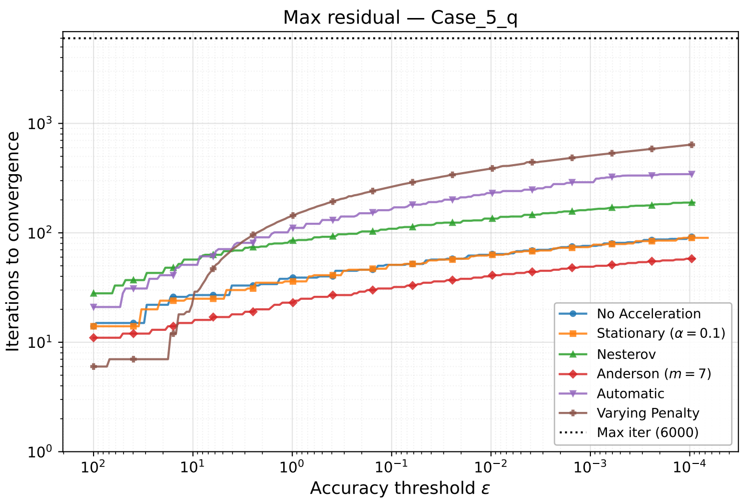

(c) Safeguard, $w = 3$

Figure 3.6. Comparison of the maximum residual for ADMM acceleration methods under three configurations (no safeguard, safeguard with $w = 2$, and safeguard with $w = 3$) for `Case_5_q`.

Case 30. The results on the 30-bus network show that the safeguard has a non-uniform effect across the acceleration schemes.

For `Case_30_base` (Tables 3.9–3.10 and Figure 3.7), the most efficient convergent method overall is ADMM with Anderson acceleration, which converges in 2191 iterations (compared with 3059 for the non-accelerated baseline). When the safeguard is enabled, Anderson acceleration remains the best-performing variant, converging in 2321 iterations for $w = 2$ and 2240 iterations for $w = 3$.

The safeguard also has a marked effect on Nesterov acceleration. Without the safeguard, Nesterov does not converge within the iteration limit and terminates with very large residuals ($\|r\|_\infty = 9.21 \times 10^2$, $\|s\|_\infty = 5.41 \times 10^3$). With the safeguard enabled and $w = 2$, it converges in 4666 iterations, whereas for $w = 3$ it again reaches the iteration limit. However, even in the latter case, the residuals ($\|r\|_\infty = 7.35 \times 10^{-4}$, $\|s\|_\infty = 7.23 \times 10^{-3}$) remain much smaller than in the unsafeguarded setting, indicating improved numerical stability despite not reaching the prescribed tolerances within the iteration limit.

Stationary acceleration is only marginally affected by the safeguard, with a slight increase in iteration count ($3046 \to 3089$ for $w = 2$, 3079 for $w = 3$). By contrast, Automatic acceleration benefits substantially: it does not converge without the safeguard (reaching 6000 iterations), but converges in 3897 iterations for $w = 2$ and 3730 iterations for $w = 3$. The Varying Penalty variant is independent of the safeguard and converges in 5082 iterations in all configurations.

For `Case_30_q` (Tables 3.11–3.12 and Figure 3.8), Anderson acceleration is the most efficient method in all safeguard configurations, converging in 719 iterations in each case. In this instance, the safeguard mainly affects Nesterov acceleration: without the safeguard, Nesterov reaches the iteration limit with large residuals ($\|r\|_\infty = 8.86 \times 10^2$, $\|s\|_\infty = 1.07 \times 10^4$), whereas with the safeguard it converges in 1408 iterations ($w = 2$) and 1440 iterations ($w = 3$).

By contrast, the safeguard provides limited benefit to the other methods. Stationary acceleration requires slightly more iterations ($923 \to 934/932$), and Automatic acceleration also becomes slightly slower ($1292 \to 1348/1328$). The non-accelerated ADMM and the Varying Penalty variants are unchanged (1518 iterations in all settings). Overall, `Case_30_q` is less sensitive to the safeguard than `Case_30_base`, except for the stabilization of Nesterov acceleration.

Table 3.9. Performance comparison for `Case_30_base` under three safeguard settings.

	Safeguard OFF			Safeguard ON ($w = 2$)				Safeguard ON ($w = 3$)			
Method	Iter.	Gap [%]	Status	Iter.	Gap [%]	Status	#SG	Iter.	Gap [%]	Status	#SG
No Acceleration	3059	0.00	C	3059	0.00	C	0	3059	0.00	C	0
Stationary (α)	3046	0.00	C	3089	0.00	C	39	3079	0.00	C	30
Nesterov	6000	-2.76	M	4666	0.00	C	854	6000	0.00	M	1049
Anderson (m)	**2191**	**0.00**	**C**	**2321**	**0.00**	**C**	218	**2240**	**0.00**	**C**	202
Automatic	6000	0.00	M	3897	0.00	C	1082	3730	0.00	C	916
Varying Penalty	5082	0.00	C	5082	0.00	C	0	5082	0.00	C	0

Common parameters: $\rho = 5.0$, $\alpha = 0.1$, $m = 20$, $\varepsilon_r = 10^{-4}$, $\varepsilon_s = 10^{-4}$, max iter = 6000.
C = converged; **M** = iteration limit reached; #SG = number of safeguard activations.

Table 3.10. Residuals at termination for `Case_30_base` under three safeguard settings.

	Safeguard OFF		Safeguard ON ($w = 2$)		Safeguard ON ($w = 3$)	
Method	$\|r\|_\infty$	$\|s\|_\infty$	$\|r\|_\infty$	$\|s\|_\infty$	$\|r\|_\infty$	$\|s\|_\infty$
No Acceleration	9.84 e−5	8.08 e−5	9.84 e−5	8.08 e−5	9.84 e−5	8.08 e−5
Stationary (α)	9.48 e−5	9.40 e−5	9.44 e−5	8.09 e−5	9.44 e−5	8.60 e−5
Nesterov	9.21 e+2	5.41 e+3	9.53 e−5	9.55 e−5	7.35 e−4	7.23 e−3
Anderson (m)	**2.07e−5**	**9.13e−5**	**4.75e−6**	**1.00e−4**	**1.33e−5**	**9.74e−5**
Automatic	9.32 e−3	9.84 e−2	7.80 e−5	9.35 e−5	7.79 e−5	8.72 e−5
Varying Penalty	9.80 e−5	9.28 e−5	9.80 e−5	9.28 e−5	9.80 e−5	9.28 e−5

Residuals are reported at termination (convergence or stopping limit).
Scientific notation is aligned across the three safeguard settings for easier comparison.

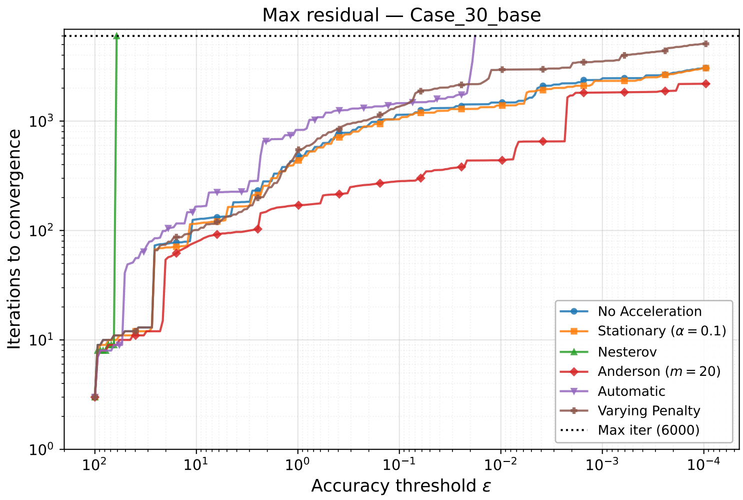

(a) No safeguard

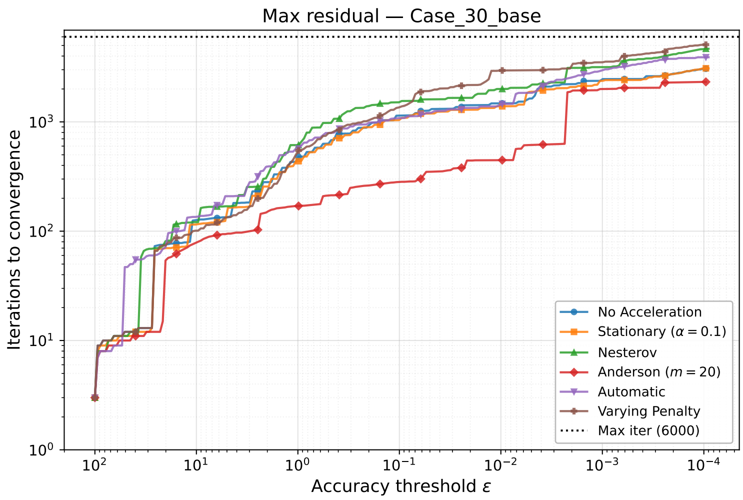

(b) Safeguard, $w = 2$

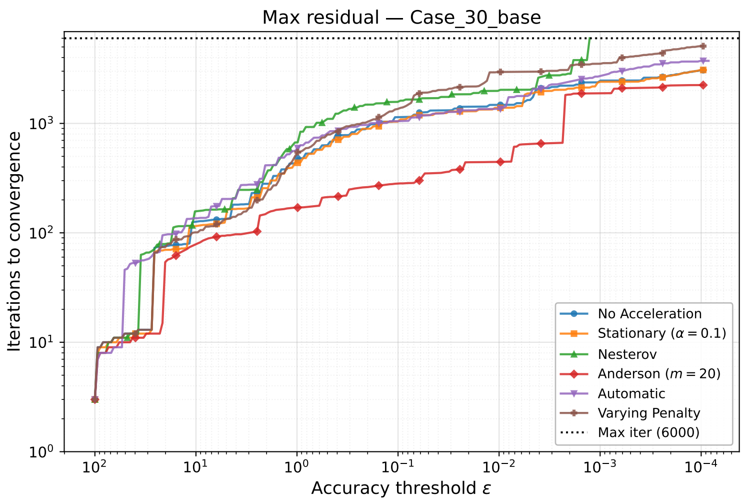

(c) Safeguard, $w = 3$

Figure 3.7. Comparison of the maximum residual for ADMM acceleration methods under three configurations (no safeguard, safeguard with $w = 2$, and safeguard with $w = 3$) for `Case_30_base`.

Table 3.11. Performance comparison for `Case_30_q` under three safeguard settings.

	Safeguard OFF			Safeguard ON ($w = 2$)				Safeguard ON ($w = 3$)			
Method	Iter.	Gap [%]	Status	Iter.	Gap [%]	Status	#SG	Iter.	Gap [%]	Status	#SG
No Acceleration	1518	0.00	C	1518	0.00	C	0	1518	0.00	C	0
Stationary (α)	923	0.00	C	934	0.00	C	8	932	0.00	C	6
Nesterov	6000	5.09	M	1408	0.00	C	214	1440	0.00	C	218
Anderson (m)	**719**	**0.00**	**C**	**719**	**0.00**	**C**	0	**719**	**0.00**	**C**	0
Automatic	1292	0.00	C	1348	0.00	C	330	1328	0.00	C	313
Varying Penalty	1518	0.00	C	1518	0.00	C	0	1518	0.00	C	0

Common parameters: $\rho = 10.0$, $\alpha = 0.7$, $m = 10$, $\varepsilon_r = 10^{-4}$, $\varepsilon_s = 10^{-4}$, max iter = 6000.
C = converged; **M** = iteration limit reached; #SG = number of safeguard activations.

Table 3.12. Residuals at termination for `Case_30_q` under three safeguard settings.

	Safeguard OFF		Safeguard ON ($w = 2$)		Safeguard ON ($w = 3$)	
Method	$\|r\|_\infty$	$\|s\|_\infty$	$\|r\|_\infty$	$\|s\|_\infty$	$\|r\|_\infty$	$\|s\|_\infty$
No Acceleration	8.20 e−5	9.98 e−5	8.20 e−5	9.98 e−5	8.20 e−5	9.98 e−5
Stationary (α)	7.34 e−5	9.21 e−5	7.20 e−5	9.08 e−5	7.18 e−5	9.62 e−5
Nesterov	8.86 e+2	1.07 e+4	7.36 e−5	9.26 e−5	7.23 e−5	9.47 e−5
Anderson (m)	**8.07e−5**	**9.93e−5**	**8.07e−5**	**9.93e−5**	**8.07e−5**	**9.93e−5**
Automatic	1.25 e−5	1.00 e−4	9.98 e−5	8.31 e−5	9.97 e−5	9.52 e−5
Varying Penalty	8.20 e−5	9.98 e−5	8.20 e−5	9.98 e−5	8.20 e−5	9.98 e−5

Residuals are reported at termination (convergence or stopping limit).
Scientific notation is aligned across safeguard settings for easier comparison.

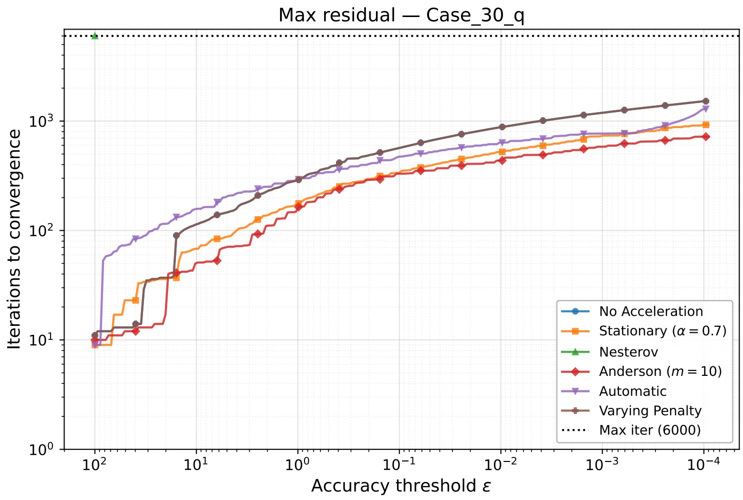

(a) No safeguard

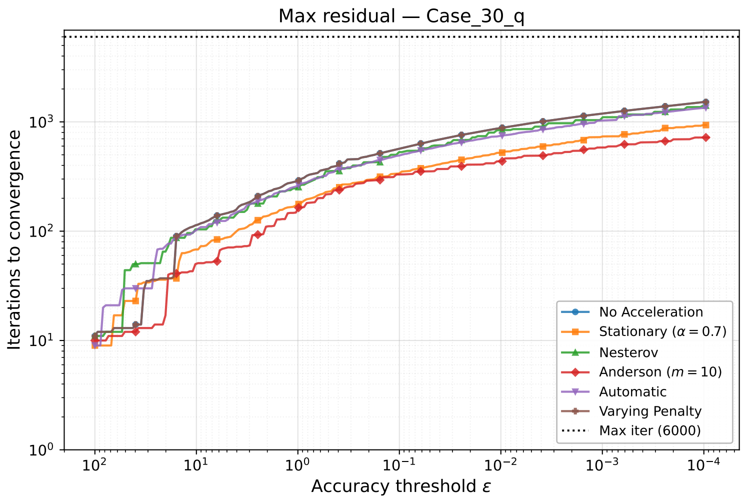

(b) Safeguard, $w = 2$

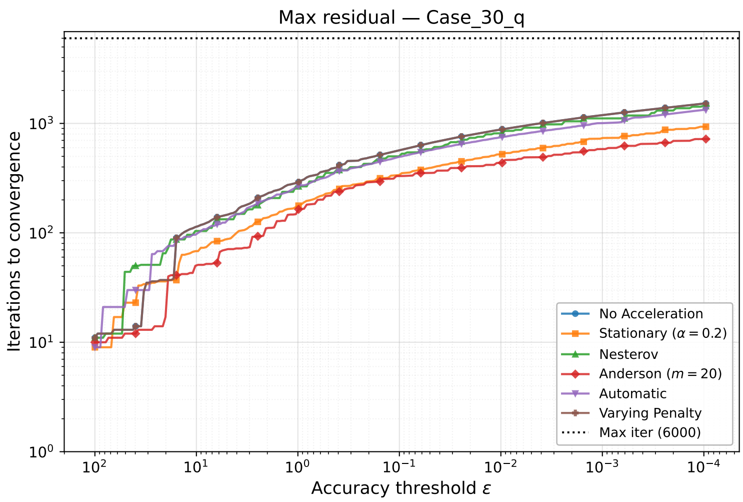

(c) Safeguard, $w = 3$

Figure 3.8. Comparison of the maximum residual for ADMM acceleration methods under three configurations (no safeguard, safeguard with $w = 2$, and safeguard with $w = 3$) for `Case_30_q`.

Case 118. The results for the 118-bus network indicate a substantially more challenging regime than the previous test cases, as several methods fail to satisfy the stopping criteria within the maximum iteration limit, which is set to 8000 iterations due to the higher complexity of this test case.

For `Case_118_base`, as shown in Tables 3.13– 3.14 and in Figure 3.9, Stationary acceleration without safeguard is the most efficient convergent method, requiring 4415 iterations, compared with 7378 for Anderson acceleration and 5992 for the non-accelerated baseline. When the safeguard is enabled, Stationary acceleration remains the best-performing convergent variant, but with a slight increase in iteration count (4512 for $w = 2$ and 4500 for $w = 3$).

The safeguard has a strong stabilizing effect on the other accelerated schemes in `Case_118_base`. Without the safeguard, Nesterov acceleration exhibits divergent behavior and reaches the iteration limit, with residuals at termination of $\|r\|_\infty = 7.42 \times 10^2$ and $\|s\|_\infty = 5.56 \times 10^3$. With the safeguard enabled, Nesterov converges in 7277 iterations for $w = 2$ and 7566 iterations for $w = 3$, with both residuals reduced below the prescribed tolerances. Anderson acceleration also remains convergent in the safeguarded configurations, requiring 6398 iterations for $w = 2$ and 6940 iterations for $w = 3$, while Automatic acceleration changes from non-convergent (8000 iterations) to convergent (6450 and 6720 iterations for $w = 2$ and $w = 3$, respectively). By contrast, the Varying Penalty variant does not converge in any safeguard configuration.

For `Case_118_q`, Tables 3.15 3.16 and Figure 3.10 show that the ADMM variant with the variable penalty parameter is the only method that converges, reaching the prescribed tolerances in 4583 iterations.

The residuals in Table 3.16 show that the dominant difficulty is the reduction of the dual residual. Several methods attain very small primal residuals (often well below the prescribed threshold), but the dual residual remains above tolerance. For example, the Automatic method with the safeguard enabled and $w = 3$ reaches $\|r\|_\infty = 3.46 \times 10^{-9}$ while stopping at $\|s\|_\infty = 1.20 \times 10^{-4}$, i.e., slightly above the target threshold. The safeguard also mitigates the unstable behavior of Nesterov acceleration in `Case_118_q`: without the safeguard, it terminates with very large residuals ($\|r\|_\infty = 1.48 \times 10^3$, $\|s\|_\infty = 5.69 \times 10^4$), whereas with the safeguard the primal residual is drastically reduced, although the dual residual remains above tolerance and convergence is not achieved.

Table 3.13. Performance comparison for `Case_118_base` under three safeguard settings.

	Safeguard OFF			Safeguard ON ($w = 2$)				Safeguard ON ($w = 3$)			
Method	Iter.	Gap [%]	Status	Iter.	Gap [%]	Status	#SG	Iter.	Gap [%]	Status	#SG
No Acceleration	5992	0.00	C	5992	0.00	C	0	5992	0.00	C	0
Stationary (α)	**4415**	**0.00**	**C**	**4512**	**0.00**	**C**	73	**4500**	**0.00**	**C**	64
Nesterov	8000	−1.62	M	7277	0.00	C	1305	7566	0.00	C	1274
Anderson (m)	7378	0.00	C	6398	0.00	C	159	6940	0.00	C	149
Automatic	8000	0.00	M	6450	0.00	C	2201	6720	0.00	C	2046
Varying Penalty	8000	0.00	M	8000	0.00	M	0	8000	0.00	M	0

Common parameters: $\rho = 5.0$, $\alpha = 0.5$, $m = 20$, $\varepsilon_r = 10^{-4}$, $\varepsilon_s = 10^{-4}$, max iter = 8000.
C = converged; **M** = iteration limit reached; #SG = number of safeguard activations.

Table 3.14. Residuals at termination for `Case_118_base` under three safeguard settings.

	Safeguard OFF		Safeguard ON ($w = 2$)		Safeguard ON ($w = 3$)	
Method	$\|r\|_\infty$	$\|s\|_\infty$	$\|r\|_\infty$	$\|s\|_\infty$	$\|r\|_\infty$	$\|s\|_\infty$
No Acceleration	4.84 e−5	9.96 e−5	4.84 e−5	9.96 e−5	4.84 e−5	9.96 e−5
Stationary (α)	**9.93e−5**	**8.85e−5**	**9.57e−5**	**8.96e−5**	**9.63e−5**	**9.00e−5**
Nesterov	7.42 e+2	5.56 e+3	9.92 e−5	7.78 e−5	9.58 e−5	8.66 e−5
Anderson (m)	6.00 e−5	9.99 e−5	9.59 e−5	9.95 e−5	6.20 e−5	9.94 e−5
Automatic	2.62 e−3	1.41 e−2	2.63 e−5	9.97 e−5	2.88 e−5	9.92 e−5
Varying Penalty	1.19 e−3	4.85 e−3	1.19 e−3	4.85 e−3	1.19 e−3	4.85 e−3

Residuals are reported at termination (convergence or stopping limit).
Scientific notation is aligned across the three safeguard settings for easier comparison.

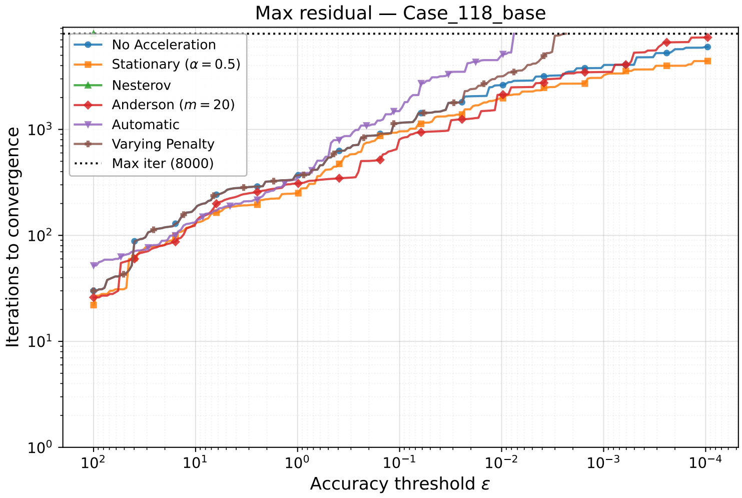

(a) No safeguard

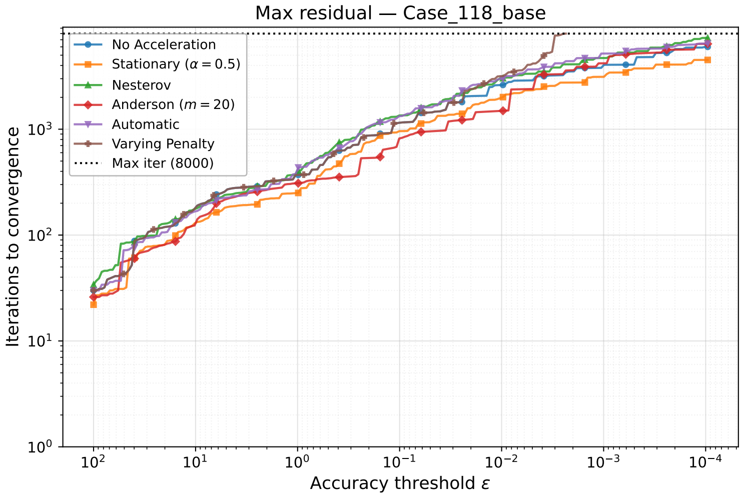

(b) Safeguard, $w = 2$

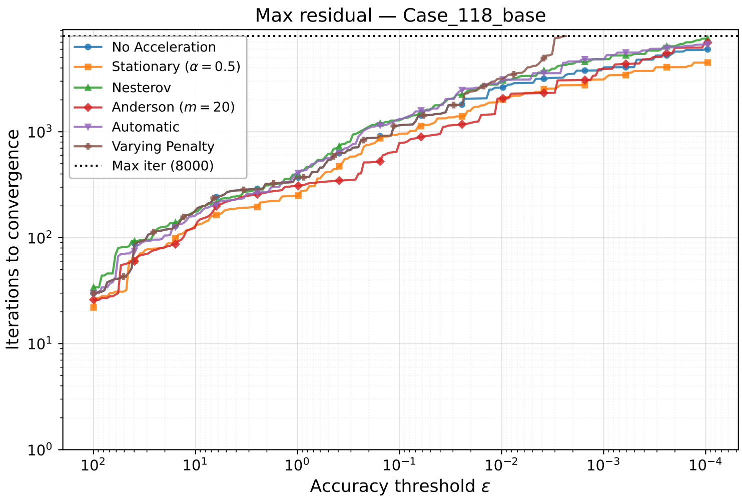

(c) Safeguard, $w = 3$

Figure 3.9. Comparison of the maximum residual for ADMM acceleration methods under three configurations (no safeguard, safeguard with $w = 2$, and safeguard with $w = 3$) for `Case_118_base`.

Table 3.15. Performance comparison for `Case_118_q` under three safeguard settings.

	Safeguard OFF			Safeguard ON ($w = 2$)				Safeguard ON ($w = 3$)			
Method	Iter.	Gap [%]	Status	Iter.	Gap [%]	Status	#SG	Iter.	Gap [%]	Status	#SG
No Acceleration	8000	0.00	M	8000	0.00	M	0	8000	0.00	M	0
Stationary (α)	8000	0.00	M	8000	0.00	M	422	8000	0.00	M	407
Nesterov	8000	−5.04	M	8000	0.00	M	1176	8000	0.00	M	1137
Anderson (m)	8000	0.00	M	8000	0.00	M	710	8000	0.00	M	729
Automatic	8000	0.00	M	8000	0.00	M	2925	8000	0.00	M	1535
Varying Penalty	**4583**	**0.00**	**C**	**4583**	**0.00**	**C**	0	**4583**	**0.00**	**C**	0

Common parameters: $\rho = 60.0$, $\alpha = 0.4$, $m = 7$, $\varepsilon_r = 10^{-4}$, $\varepsilon_s = 10^{-4}$, max iter = 8000.
C = converged; **M** = iteration limit reached; #SG = number of safeguard activations.

Table 3.16. Residuals at termination for `Case_118_q` under three safeguard settings.

	Safeguard OFF		Safeguard ON ($w = 2$)		Safeguard ON ($w = 3$)	
Method	$\|r\|_\infty$	$\|s\|_\infty$	$\|r\|_\infty$	$\|s\|_\infty$	$\|r\|_\infty$	$\|s\|_\infty$
No Acceleration	3.75 e−8	4.94 e−4	3.75 e−8	4.94 e−4	3.75 e−8	4.94 e−4
Stationary (α)	2.50 e−8	3.33 e−4	1.52 e−5	7.93 e−4	5.48 e−6	6.48 e−4
Nesterov	1.48 e+3	5.69 e+4	1.61 e−7	2.16 e−4	2.03 e−7	2.31 e−4
Anderson (m)	1.04 e−7	2.65 e−4	1.12 e−5	5.48 e−4	1.14 e−7	1.79 e−4
Automatic	2.87 e−5	1.39 e−3	7.84 e−9	1.28 e−4	3.46 e−9	1.20 e−4
Varying Penalty	**1.85e−5**	**1.00e−4**	**1.85e−5**	**1.00e−4**	**1.85e−5**	**1.00e−4**

Residuals are reported at termination (convergence or stopping limit).
Scientific notation is aligned across the three safeguard settings for easier comparison.

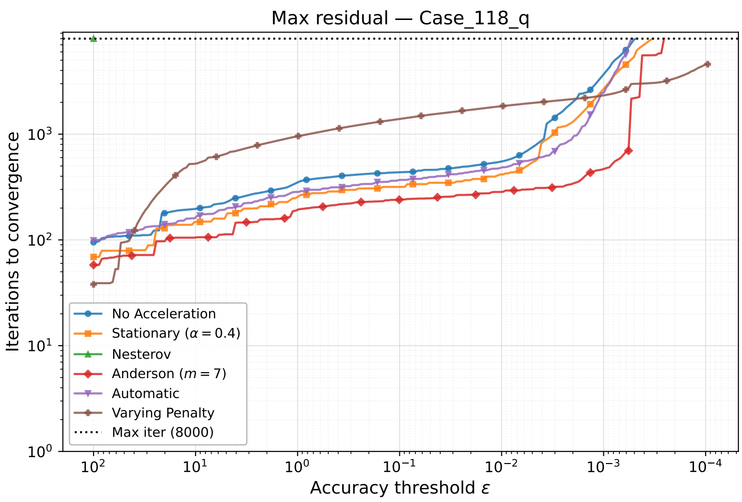

(a) No safeguard

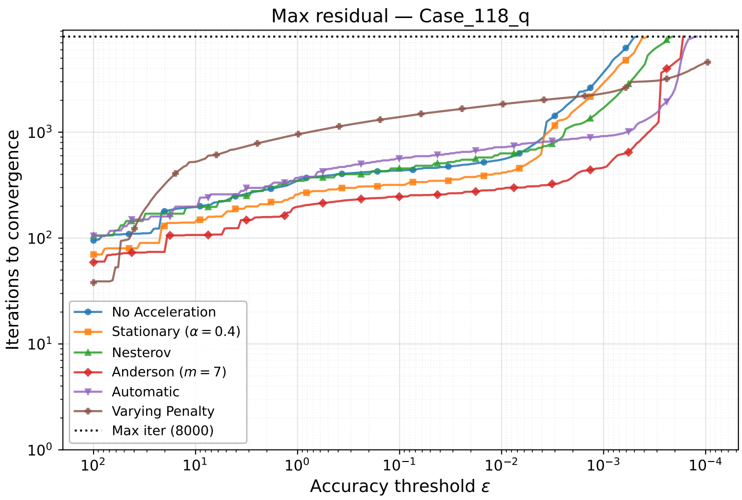

(b) Safeguard, $w = 2$

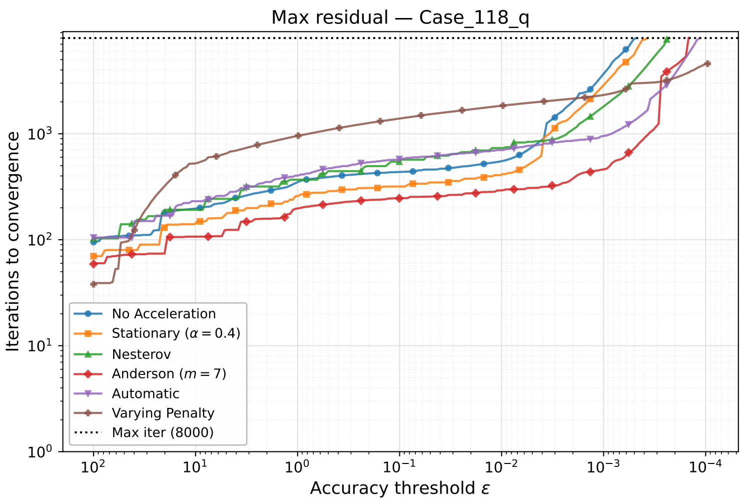

(c) Safeguard, $w = 3$

Figure 3.10. Comparison of the maximum residual for ADMM acceleration methods under three configurations (no safeguard, safeguard with $w = 2$, and safeguard with $w = 3$) for `Case_118_q`.

3.7 Conclusions

This chapter presented an analysis of a non-monotone acceptance safeguard with restart for accelerated ADMM, applied to the market-clearing problem of a Day-Ahead Market with demand response and DCOPF network constraints. Several acceleration strategies were evaluated on six test instances derived from three networks of increasing size, namely 5-bus, 30-bus, and 118-bus systems. Unless otherwise specified, performance is discussed in terms of the number of iterations among converged runs.

The computational results reveal a heterogeneous behavior across acceleration schemes, both with respect to the safeguard mechanism and to the choice of the safeguard window length w. Overall, Anderson acceleration emerges as the best-performing method in four out of six instances, namely, all the 5-bus and 30-bus cases. In the remaining two instances, the best performance is attained by Stationary acceleration in `Case_118_base` and by the ADMM variant with a varying penalty parameter in `Case_118_q`.

Among the tested methods, Nesterov acceleration is the one most strongly dependent on the safeguard mechanism. In the absence of the safeguard, it frequently exhibits unstable behavior, often reaching the iteration limit with residuals well above the prescribed tolerances. When the safeguard is activated, convergence is restored in several instances, and even when convergence is not achieved, the terminal residuals are substantially reduced. A similar, although less uniform, pattern is observed for Automatic acceleration: in several cases, the safeguard restores convergence, while in others it primarily improves numerical stability through lower final residuals. By contrast, Stationary acceleration is the method that benefits least from restart. Its performance is generally only marginally affected by safeguard activation and, in some instances, the safeguard leads to a slight deterioration in iteration count or terminal residuals.

The impact of the safeguard is also influenced by the structure of the underlying instance. For the smaller quadratic-cost cases, `Case_5_q` and `Case_30_q`, most methods are only mildly affected by the safeguard, while Nesterov constitutes the main exception, showing a substantial improvement when the safeguard is enabled. In `Case_118_q`, none of the accelerated schemes with the restart framework satisfies the stopping criteria within the iteration limit; however, the safeguard still reduces the terminal residuals for some methods, most notably Nesterov and Automatic, whereas its effect is weaker or unfavorable for others, such as Stationary. In this instance, the only method that achieves convergence is the ADMM variant with the varying penalty parameter.

For the linear-cost instances, Stationary acceleration remains robust but may become slightly slower when the safeguard is activated. Nesterov consistently performs better with $w = 2$ than with $w = 3$, suggesting that a shorter safeguard window is more effective for this method. The effect of the safeguard on Anderson acceleration is instance-dependent. In some cases, the safeguarded variants improve upon the non-safeguarded one, whereas in others they lead to no clear benefit or to slightly worse performance. More generally, the computational evidence suggests that the safeguard window length controls a non-trivial trade-off between aggressiveness and stability, and therefore requires instance-dependent tuning.

Overall, the computational results show that the effectiveness of acceleration depends significantly on the specific method, the instance considered, and the safeguard configuration, with marked differences in both convergence performance and robustness. From a practical perspective, Anderson and Stationary acceleration appear to be the most reliable default choices, with the former offering the best performance on smaller instances and the latter showing greater robustness in the more demanding 118-bus case. The safeguard mechanism is essential when employing Nesterov acceleration and is often beneficial when using Automatic acceleration, both in terms of convergence robustness and residual reduction.

Chapter 4

From Zonal Representation to Nodal Feasibility: Recovery Models and Redispatch in Electricity Markets

4.1 Introduction

The Italian electricity market framework is organized into sequential market stages through which operating schedules are progressively refined as real-time operations approach. In the energy markets (e.g., day-ahead and intraday), market participants submit bids and offers to a centralized clearing mechanism that determines commercial injection/withdrawal schedules and market prices. Following the clearing of the day-ahead and intraday markets, Terna, the Italian Transmission System Operator (TSO), ensures the secure and technically feasible operation of the power system through the Balancing and Redispatch framework (*Mercato per il Bilanciamento e il Ridispacciamento* – MBR). The MBR is not aimed at commercial energy trading; rather, it focuses on the procurement and activation of dispatching resources needed to manage network constraints, maintain adequate reserves, and correct imbalances close to real time. Conceptually, energy markets determine economically efficient commercial schedules, whereas the MBR determines the secure and feasible physical adjustments (e.g., up/down regulation, reserve activation, and redispatch actions) required by the TSO to operate the system within security limits. However, dispatching arrangements and the provision of ancillary services vary significantly across countries, even within regional coordination frameworks such as the European one. A key design dimension is whether the system follows a central-dispatch or a self-dispatch approach, i.e., whether schedules and dispatch decisions for dispatchable facilities are determined by the TSO within an integrated scheduling process or by market participants (or their scheduling agents). Within the European regulatory framework, Commission Regulation (EU) 2017/2195 [25] provides formal definitions of the two models, while their advantages and disadvantages are analyzed in [1]. The choice between these systems may be driven by several factors, including the need to ensure system security and minimize the cost of energy delivery to end users [22]. In a central-dispatch system (CDS), producers submit detailed cost data to the market, and the TSO determines the output level of each facility, jointly defining scheduling and dispatch deci-

[0]This chapter is based on a joint work with Dr. Claudio Gentile (Istituto di Analisi dei Sistemi ed Informatica “Antonio Ruberti”, C.N.R.)

sions within an integrated process. In contrast, in a self-dispatch system (SDS), scheduling decisions are determined by market participants, subject to market rules and system constraints. Within self-dispatching systems, a further distinction is commonly drawn between portfolio-based and unit-based models. In a portfolio-based system, scheduling decisions are taken at the portfolio level by the entity responsible for balancing the portfolio, whereas in a unit-based system each generating unit and demand facility follow its own generation or consumption schedule [64]. Within this framework, two key roles for balancing responsibility and service provision are the Balance Responsible Party (BRP) and the Balancing Service Provider (BSP). The BRP is the entity (a market participant or its representative) responsible for the financial settlement of its imbalances, while the BSP is a market participant that provides balancing energy and/or balancing capacity to the TSO [26]. Depending on the market design, the same entity may act as both a BRP and a BSP; conceptually, the BRP relates to imbalance exposure and settlement, whereas the BSP relates to the provision of resources that may be activated within the MBR.

In practice, the activation of balancing and redispatch resources is constrained by the physical transmission network. Therefore, the way network constraints are represented in market models directly affects the feasibility and cost of the adjustments that must ultimately be implemented within the MBR. Often, models representing a single phase of the electricity market adopt a zonal network representation, in which the grid is aggregated into zones and only inter-zonal transfer limits are modeled, rather than enforcing line-by-line (nodal) transmission constraints. This choice simplifies the solution process by avoiding the technical complexities associated with a full network-constrained formulation (e.g., detailed power-flow and security constraints). However, it may leave intra-zonal congestion unresolved, thereby shifting the task of finding a feasible dispatch on the physical network to later stages. When nodal transmission constraints are explicitly considered, the resulting market outcomes, in terms of dispatch, congestion patterns, and prices, can differ significantly from those obtained under a zonal representation.

The main objective of this chapter is to evaluate the effectiveness of an electricity redispatch model that incorporates nodal network constraints using Direct Current (DC) power flow conditions, while also accounting for secondary reserve requirements. Specifically, this chapter investigates whether this model can be economically advantageous compared with a zonal approach without significantly increasing computational costs.
To this end, two market models are introduced:

- **Base model** – A zone-based formulation that accounts only for zonal network constraints.
- **DC model** – A model that incorporates nodal network constraints through DC power flow equations.

The formulations of these two problems differ only in their transmission constraints, and both take the same solution from the previous market stage as input. However, since the Base model solution may be infeasible with respect to intra-zonal constraints, the outcomes obtained from these two models are not directly comparable. Recovering network-feasible solutions from the Base model outcomes requires an additional step, which may also incorporate fairness criteria to limit deviations from market results. To this end, two recovery models are proposed to adapt Base model solutions so that they satisfy nodal transmission constraints.

- **Recovery model 1 (R1)** minimizes the *number of changes* to the initial solution, considering profile modifications (upward/downward bids), generator status changes, and start-up actions. This approach emphasizes maintaining similarity to the original solution.
- **Recovery model 2 (R2)** minimizes the *total magnitude of changes in power output* across all generators, without considering the type or reason for each change.

These recovery models are designed to transform an infeasible solution, originally obtained through a zonal model or computed under different demand conditions, into a feasible one satisfying nodal network constraints. Their objective is to minimize deviations from the initial configuration in order to preserve market outcomes, penalizing both the removal of previously selected generators and the introduction of new generators whose bids had not previously been accepted, as such changes could compromise market fairness.

All models in this study are built upon a simulator developed by *Ricerca sul Sistema Energetico* (RSE S.p.A.) [27]. Compared with the original simulator, the proposed formulations introduce additional modeling features through new constraints, and the DC model and recovery models explicitly include network constraints.
A set of computational experiments was conducted to compare the Base and DC market models and to evaluate the behavior of the proposed recovery formulations under different post-processing strategies. First, both the Base and DC models were solved for the reference scenario, and then feasible dispatches were computed by applying the two recovery models, R1 and R2, to the Base-model outcomes. To further investigate the interaction between recovery objectives and economic performance, two alternative formulations were considered. The refining approach is implemented as a second optimization stage: starting from a solution obtained with a recovery model (within a given time limit), the value of the recovery objective is fixed and the problem is re-optimized with a cost-based objective, in order to identify a less expensive solution that preserves the same recovery performance. By contrast, the penalty approach is formulated as a single-stage recovery model. In this case, an additional cost-related term is included in the recovery objective to promote economically preferable solutions, while still prioritizing the original recovery objective. The relative weight of the penalty term governs the trade-off between recovery performance and cost, without explicitly enforcing equality of the primary objective value. Finally, an additional robustness analysis compares the recovery of Base and DC solutions across perturbed demand scenarios. In particular, starting from solutions obtained at the reference demand, recovery was evaluated using R1 and R2 with increased and decreased demand levels, to assess whether DC-based solutions exhibit greater robustness and retain their economic advantage when adjustments are required.

Results indicate that directly integrating network constraints (DC model) provides better economic outcomes without significantly increasing computational complexity. Among recovery models, R1 generally yields more expensive solutions and is more difficult to solve, whereas R2 is computationally tractable. However, the Refined R1 solutions outperform those obtained with R2.

The remainder of the chapter is organized as follows. Section 4.2 introduces the Base and DC models, followed by the recovery formulations in Section 4.3. Section 4.4 presents the numerical results, and Section 4.5 concludes the chapter.

4.1.1 Literature review

Attention is now directed to the literature on alternative dispatching systems and market models. Several contributions investigate the role of network constraints in electricity market design and performance. However, apart from the previously cited RSE simulator [27], no modeling frameworks with a scope directly comparable to that of the model proposed in this paper were identified. For instance, Galatoire et al. [31] examine the differences between nodal and zonal markets, as well as centralized versus decentralized structures with strategic behavior. The authors propose a novel approach to identify locational price signals in a decentralized market with zonal pricing and subsequent redispatch. Applied to the Spanish system, their method is expected to enable informed investment decisions and reduce redispatch costs, without requiring major structural changes to the market. A complementary perspective is provided by Matin et al. [58], whose study analyzes increment–decrement gaming and other forms of strategic behavior in international electricity markets with market-based redispatch. Focusing on California, Great Britain and Denmark, the study shows how market power can influence market performance, but also that these issues have been acknowledged and addressed in practice by regulators. In a related contribution, the authors of [66] compare zonal and nodal models in a strategic setting. They contrast two zonal two-stage frameworks, one based on the Available Transfer Capacity (ATC) system and the other on Flow-Based Market Coupling (FBMC), with a nodal model, all relying on a formulation based on Power Transfer Distribution Factors (PTDF). To deal with Nash equilibria and optimality conditions, their linear programming approach simplifies the representation of the market by excluding bid management details and generators' technical constraints. Their numerical experiments confirm the inefficiencies of ATC, especially under increment–decrement (inc-dec) gaming. Rancilio et al. [64] focus instead on the evolution of ancillary services markets and associated regulatory trade-offs. Considering the perspective of both Balancing Service Providers and System Operators, their paper evaluates the impact of market modifications. They also present a survey, updated to 2022, of developments in European ancillary service markets, covering Italy, the United Kingdom, Germany, and Denmark. A different market mechanism is analyzed by Ehrhart et al. [20], who investigate a capacity-based redispatch mechanism. In this model, market participants are compensated for their availability to participate in the redispatch process, rather than for actual activation. The main objective of this design is to prevent inc-dec gaming or other forms of strategic behavior. However, the authors find that the proposed mechanism is not effective in improving redispatch efficiency, as it fails to distinguish between beneficial and undesirable participants, even when mitigation strategies are implemented. Another analysis of redispatch market design is provided by [37], in which the authors compare cost-based redispatch (CBR) with market-based redispatch (MABR), following a uniform-price day-ahead market in the presence of line congestion. They argue that the minimization of redispatch cost by the TSO would reduce efficiency under MABR, while yielding efficient outcomes under CBR. In [50], the authors propose a unit commitment model for the co-optimization of wholesale energy and ancillary services markets, considering standard European market products. Their framework explicitly incorporates multiple flexibility service providers, such as energy storage systems, electric vehicles, and demand response programs, in order to assess the benefits of their integration into power system operations. The model accounts for a wide range of operational constraints and shows that the participation of flexibility providers enhances system performance, reducing operational costs while improving overall system flexibility. In [74], the authors analyze the redispatching process that follows a day-ahead market clearing in which nodal transmission constraints are not considered. The study focuses on quantifying how different parameters affect redispatch quantities and costs. Their framework separates the day-ahead and redispatch phases: the former is modeled as a unit commitment problem, while the latter minimizes the redispatching cost for the TSO, accounting for production adjustments, start-up costs, renewable curtailment, and load shedding. The network is represented through a DC power flow formulation using PTDF. Although the objective and market structure differ from those considered in this work, the study similarly interprets redispatching, accounting for the difference in generation levels between the two optimization stages. A stochastic optimization approach can be found in [28]. In their work, the authors propose a two-stage stochastic model for the self-scheduling of a virtual power plant, which includes a wind farm and a battery, and a deterministic model for redispatch.

4.2 Market models

This section introduces the two primary market models: the Base model, which adopts a zonal representation of transmission constraints, and the DC model, which instead adopts a nodal representation.

4.2.1 Base model with zonal constraints

The Base model is presented first and formulated as a redispatch model with a zonal network representation. It includes the generator start-up profile, time windows limiting the number of start-ups, upward and downward bid management, secondary reserve scheduling, technical constraints on generator status, and a compensation mechanism for deviations from the previous market.

The main objective of this model is to adjust the schedule obtained from the previous market to the updated demand conditions, incorporate transmission constraints that more accurately reflect the actual transmission system, and limit possible congestion.
With regard to the start-up process, additional constraints are introduced to preserve generators' operational flexibility while ensuring consistency between the current and previous operating states. During the start-up process, a generator can use ω^g increasing thresholds, which define the upper bounds on the power offered to the market up to its maximum power output, without requiring this level to be reached. This mechanism can be used only in periods in which the generator is turned off in the previous market's solution (Intraday Market, MI), since in such cases it needs to submit offers to modify its production schedule. In particular, constraints (4.9) provide the general equations of the start-up process, while constraints (4.10) govern the initial periods.

With respect to the model presented in [27], the present formulation differs in both the system dynamics considered and the mathematical representation of the constraints. In particular, (i) a start-up profile mechanism is introduced, according to which a generator progressively makes capacity available during the start-up phase, thereby preventing technically infeasible dispatch requests and expanding the feasible operating region; (ii) boundary-time constraints are properly defined for both $t < \omega_g - 1$ and $t \geq \omega_g - 1$, with $g \in G$, where G denotes the set of generators, and never refer to periods outside the planning horizon, i.e., $t < 0$ or $t > T^{\max}$, where T denotes the set of time periods, with $T = \{0, \dots, T^{\max}\}$; (iii) constraints (4.14) are added to forbid the simultaneous acceptance, for the same generator and at the same time instant, of both upward and downward bids; and (iv) the production constraints are revised to incorporate the start-up profile and the parameter $S^{MI}_{t,g}$, thereby removing the need for explicit conditional expressions. For ease of exposition, variables and constraints related to hydroelectric units, storage systems, tertiary reserves, the automatic acceptance mechanism for renewable generation, and essential facilities are omitted, although all such components can be reintroduced if required. The same simplification applies to the mutual-exclusivity constraint between the start-up and shut-down variables, i.e., $s^{on}_{t,g} + s^{off}_{t,g} \leq 1$, as well as to the variables representing unmet reserve capacity, unmet demand, and excess power.

Variables. Table 4.1 introduces the variables for the Base model.

Table 4.1. Decision variables.

Name	Domain	Description
$p_{t,g}$	$\mathbb{R}_{\geq 0}$	Active power produced by generator g in period t.
$p^{on}_{t,g}$	$\mathbb{R}_{\geq 0}$	Power contribution associated with the start up of generator g at time t (startup power).
$dp^{u}_{t,g,k}$, $dp^{d}_{t,g,k}$	$\mathbb{R}_{\geq 0}$	Upward / downward incremental bid quantities of generator g for bid segment k at time t.
$\delta^{1}_{t,g,k}$, $\delta^{2}_{t,g,k}$	$\{0,1\}$	Binary activation indicators for upward / downward bid segment k of generator g at time t.
$s^{MBR}_{t,g}$	$\{0,1\}$	On/off status of generator g in the MBR schedule at time t.
$s^{on}_{t,g}$, $s^{off}_{t,g}$	$\{0,1\}$	Startup and shutdown event indicators for generator g at time t.
Δs^{u}_{g}	$\mathbb{Z}_{\geq 0}$	Non-negative integer measuring excess startups of unit g across the horizon.
$\Delta p^{2,u}_{t,g_{R2}}$, $\Delta p^{2,d}_{t,g_{R2}}$	$\mathbb{R}_{\geq 0}$	Upward / downward secondary-reserve contribution (R2) provided by qualified unit g at time t.
κ_{t,z,z_2}	$\{0,1\}$	Auxiliary binary variable for the inter-zonal line connecting z and z_2 at time t.
f_{t,z,z_2}	$\mathbb{R}$	Net z_1, z_2 inter-zonal flow variable at time t; the sign indicates direction.

Table 4.2. Sets.

Set	Description
N	Network nodes (all buses).
G	Generators.
T	Time periods.
N_z	Nodes in zone z; $\bigcup_{z\in Z} N_z = N$ and $N_{z_1} \cap N_{z_2} = \emptyset$ for $z_1 \neq z_2$.
N_a	Nodes in area a.
G^{MI}	Generators selected in MI.
G^{R2}	Generators eligible for secondary reserve.

Sets and parameters. Table 4.2 and Table 4.3 present the sets and parameters used in the following section. Unless otherwise stated, indices refer to $g \in G$, $t \in T$, $n \in N$, $a \in A$, $z, z_2 \in Z$, and $k \in K$.

Table 4.3. Parameters.

Parameter	Domain	Description
$\overline{L}^{max}_{t,z,z_2}$	$\mathbb{R}_{\geq 0}$	Maximum transfer capacity between zones z and z_2 at t.
$\overline{P}_{j,g}$	$\mathbb{R}_{\geq 0}$	Maximum output of generator g, j periods after start-up.
$\overline{P}^{min}_{g}$	$\mathbb{R}_{\geq 0}$	Minimum output of g.
$\overline{P}^{max}_{g}$	$\mathbb{R}_{\geq 0}$	Maximum output of g.
$\overline{\pi}^{su}_{t,g}$	$\mathbb{R}_{\geq 0}$	Start-up bid price of g at t.
$\overline{\pi}^{sd}_{t,g}$	$\mathbb{R}_{\geq 0}$	Shut-down bid price of g at t.
$\overline{\pi}^{step,u}_{t,g,k}$	$\mathbb{R}_{\geq 0}$	Upward bid prices at step k for g at t.
$\overline{\pi}^{step,d}_{t,g,k}$	$\mathbb{R}_{\geq 0}$	Downward bid prices at step k for g at t.
$S^{MI}_{t,g}$	$\{0,1\}$	1 if g participates in MI at t, 0 otherwise.
$S^{MI,on}_{t,g}$	$\mathbb{R}_{\geq 0}$	Number of start-ups of g scheduled in MI at t.
$\overline{R2}^{u}_{t,g}$, $\overline{R2}^{d}_{t,g}$	$\mathbb{R}_{\geq 0}$	Upward/downward secondary reserve offered by $g \in G^{R2}$ at t.
$\overline{R}^{2,u}_{t,a}$, $\overline{R}^{2,d}_{t,a}$	$\mathbb{R}_{\geq 0}$	Minimum upward/downward secondary reserve requirement for area a at t.
$d^{N}_{t,n}$	$\mathbb{R}_{\geq 0}$	Demand at node n at t.
ω_g	$\mathbb{N}$	Start-up window length of g.
τ^u_g, τ^d_g	$\mathbb{N}$	Length of minimum up/down time for g.
ω_g	$\mathbb{N}$	Start-up window length of g.
$\overline{GA}_g$	$\mathbb{R}_{\geq 0}$	Excess-start-up penalty-token price of g.

Bounds. Upper bounds are imposed on selected variables.

The power generated by generator g in each time period t cannot exceed its maximum capacity:

$$p_{t,g} \leq \overline{P}^{max}_{g} \qquad g \in G. \tag{4.1}$$

The secondary reserve contribution of generator g, when eligible to participate in the reserve market, shall not exceed the quantity offered to the market at each time t:

$$\Delta p^{2,u}_{t,g} \leq \overline{R2}^{u}_{t,g} \qquad g \in G^{R2}, \tag{4.2}$$

$$\Delta p^{2,d}_{t,g} \leq \overline{R2}^{d}_{t,g} \qquad g \in G^{R2}. \tag{4.3}$$

The accepted upward and downward bids of generator g at time t are bounded by the size of step k, denoted by $\overline{DP}^{u}_{t,g,k}$ and $\overline{DP}^{d}_{t,g,k}$, respectively, which represent the quantities offered at the corresponding prices:

$$dp^{u}_{t,g,k} \leq \overline{DP}^{u}_{t,g,k} \qquad t \in T, g \in G, k \in K, \tag{4.4}$$

$$dp^{d}_{t,g,k} \leq \overline{DP}^{d}_{t,g,k} \qquad t \in T, g \in G, k \in K. \tag{4.5}$$

For generators not eligible to provide secondary reserve, the accepted reserve is set to zero:

$$\Delta p^{2,u}_{t,g} = 0 \qquad g \in G \setminus G^{R2}, \tag{4.6}$$

$$\Delta p^{2,d}_{t,g} = 0 \qquad g \in G \setminus G^{R2}. \tag{4.7}$$

Constraints
The constraints that characterize the model are described in detail below.

Power generated. The power produced by a generator can be expressed as the sum of four components, as shown in (4.8). The first term, $P^0_{t,g}$ accounts for the previous schedule, creating a baseline for the redispatch process; the second term, $p^{on}_{t,g} \cdot (1 - S^{MI}_{t,g})$ represents the power produced during the switching-on period, when $S^{MI}_{t,g} = 0$, i.e. the generator was not scheduled for production; the third term, $-\overline{P}^{min}_g \cdot (1 - s^{MBR}_{t,g}) \cdot S^{MI}_{t,g}$, modifies the baseline when $(1 - s^{MBR}_{t,g}) \cdot S^{MI}_{t,g} = 1$, i.e. when the generator exits from the schedule after being set for production in the previous market; the last term, $\sum_{k \in K} (dp^u_{t,g,k} - dp^d_{t,g,k}) \cdot S^{MI}_{t,g}$, accounts for the upwards and downwards bids submitted by generator g, when $S^{MI}_{t,g} = 1$, i.e. the generator was part of the initial schedule. If the generator g was scheduled, i.e., if $S^{MI}_{t,g} = 1$, then $P^0_{t,g} > 0$. In order to reach the status $s^{MBR}_{t,g} = 0$, or equivalently $p_{t,g} = 0$, all downward bids have to be accepted. In fact, since generators are required to offer their full capacity, it holds that $P^0_{t,g} = \overline{P}^{min}_g + \sum_{k \in K} dp^d_{t,g,k} \quad \forall t \in T, g \in G$. The general constraints related to power generated read as follows:

$$\begin{aligned} p_{t,g} = P^0_{t,g} + p^{on}_{t,g}\,(1 - S^{MI}_{t,g}) - \overline{P}^{min}_g\,(1 - s^{MBR}_{t,g})\,S^{MI}_{t,g} + \\ + \sum_{k \in K} (dp^u_{t,g,k} - dp^d_{t,g,k})\,S^{MI}_{t,g}, \qquad t \in T,\ g \in G. \end{aligned} \tag{4.8}$$

Start-up profile. The general equation for the start-up profile (4.9) consists of two terms. The first term represents the quantity produced if the generator has been switched-on during the ω_g time periods preceding t ; the second term allows the start-up power to remain at its maximum level.
Constraints (4.10) cover the initial ω_g periods. Constraints (4.11) force the startup power to zero if the generator was selected in the previous market.
This mechanism uses ω_g increasing upper bounds to allow greater flexibility while preventing excessive increases in generated power. It is worth noting that ramp-up and ramp-down constraints are not considered in the proposed model, as this represents more an offer mechanism than the technical requirement. The constraints corresponding to the start-up profile are formulated as:

$$p^{on}_{t,g} \leq \sum_{j=0}^{\omega_g - 1} \overline{P}_{j,g}\, s^{on}_{t-j,g} + \overline{P}^{max}_g \Big(s^{MBR}_{t,g} - \sum_{j=0}^{\omega_g - 1} s^{on}_{t-j,g} \Big) \qquad t \in T:\ t \geq \omega_g - 1, \tag{4.9}$$

$$p^{on}_{t,g} \leq \sum_{j=0}^{t} \overline{P}_{j,g}\, s^{on}_{t-j,g} \qquad t \in T:\ t < \omega_g - 1, \tag{4.10}$$

$$p^{on}_{t,g} \leq 0 \qquad g \in G^{MI},\ t \in T:\ S^{MI}_{t,g} = 1. \tag{4.11}$$

Bids. BRPs or generators participating in the market submit upward and downward bids. The following constraints prevent $dp^u_{t,g,k}$ and $dp^d_{t,g,k}$ from being positive at the same time. It should be noted that these constraints may be unnecessary in practice, since the relationship between the prices in the previous market and those in the MBR, and between $\overline{\pi}^{step\_u}_{t,g,k}$ and $\overline{\pi}^{step\_d}_{t,g,k}$, may be sufficient to yield a solution in which is not profitable for both quantities to be positive simultaneously. However, it may occur that $\overline{\pi}^{step\_u}_{t,g,k} \leq \overline{\pi}^{step\_d}_{t,g,k}$; in such a case, without constraints (4.12)–(4.14), the values assigned to these variables would no longer be valid. The constraints are therefore formulated as follows:

$$dp^u_{t,g,k} \leq \overline{DP}^u_{t,g,k} \cdot \delta^1_{t,g,k} \qquad t \in T, g \in G^{MI}, k \in K, \tag{4.12}$$

$$dp^d_{t,g,k} \leq \overline{DP}^d_{t,g,k} \cdot \delta^2_{t,g,k} \qquad t \in T, g \in G^{MI}, k \in K, \tag{4.13}$$

$$\delta^1_{t,g,k} + \delta^2_{t,g,k} \leq S^{MI}_{t,g} \qquad t \in T, g \in G^{MI}, k \in K. \tag{4.14}$$

Under normal circumstances, $\overline{\pi}^{step\_d}_{t,g,k} \leq \overline{\pi}^{MI}_t$, where $\overline{\pi}^{MI}_t$ is the market clearing price in the previous market, is expected to hold, since the acceptance of this offer would allow the generator to obtain a profit without actually producing power. The relationship between $\overline{\pi}^{step\_u}_{t,g,k}$ and $\overline{\pi}^{MI}_t$, depends on the participant's bidding strategy. Nonetheless, it is reasonable to assume that since the upward bids were not fully accepted in the previous market, their price was higher than the market-clearing price [31]. Consequently, $\overline{\pi}^{step\_u}_{t,g,k} \geq \overline{\pi}^{MI}_t$ is expected to hold. Taken together, these assumptions lead to the following relationship:

$$\overline{\pi}^{step\_d}_{t,g,k} \leq \overline{\pi}^{MI}_{t,g} \leq \overline{\pi}^{step\_u}_{t,g,k} \qquad t \in T,\ g \in G.$$

Status changes. These constraints govern status changes. Thus, if a generator changes its status from off to on, or vice versa, a powering-on or powering-off event is considered to have occurred and must be accounted for in the corresponding variables.
It is not necessary to include a constraint forcing at most one of the variables $s^{on}_{t,g}$ and $s^{off}_{t,g}$ to be equal to one, because by (4.15), this would imply that $s^{MBR}_{t,g}$ did not change. Status changes are modeled by the following expression:

$$s^{MBR}_{t,g} - s^{MBR}_{t-1,g} = s^{on}_{t,g} - s^{off}_{t,g} \qquad t \in T,\ g \in G. \tag{4.15}$$

Minimum up-time and minimum down-time. Minimum up-time and down-time constraints aim to prevent generators from being switched on and off within a limited time interval, thereby reflecting actual technical constraints that often involve expensive operations over multiple time periods. In practice, these constraints create windows of τ^u_g and τ^d_g periods in which the variable can be equal to one at most once by linking $s^{on}_{t,g}$ and $s^{off}_{t,g}$ to the status variable $s^{MBR}_{t,g}$. This requirement is given by:

$$\sum_{t1=t-\tau_g^u+1}^{t} s_{t1,g}^{on} \leq s_{t,g}^{MBR} \qquad t \in T : t \geq \tau_g^u + 1,\ g \in G \tag{4.16}$$

$$\sum_{t1=t-\tau_g^d+1}^{t} s_{t1,g}^{off} \leq 1 - s_{t,g}^{MBR} \qquad t \in T : t \geq \tau_g^d + 1,\ g \in G \tag{4.17}$$

Excess start-ups in the MBR. The total number of generator start-ups in the MBR is compared with the expected number based on the previous market. If the actual count exceeds the expected value, the generator is rewarded with a token for each excess start-up. This can be written as:

$$\Delta s_g^u \geq \sum_{t \in T} s_{t,g}^{on} - S_{t,g}^{MI,on} \qquad g \in G \tag{4.18}$$

Production feasibility. When accounting for reserve, it is important to ensure that the planned flexibility is immediately available without further changes. The following two constraints act in this direction and limit the maximum and minimum power generated when the generator is on, while accounting for the scheduled reserve. Note that if additional reserves are considered, they should be included as well. In the present case, the constraints are given by:

$$p_{t,g} + \Delta p_{t,g_R 2}^{2,u} \leq \overline{P}_{t,g}^{max} \cdot s_{t,g}^{MBR} \qquad t \in T,\ g \in G \tag{4.19}$$

$$p_{t,g} - \Delta p_{t,g_R 2}^{2,d} \geq \overline{P}_{t,g}^{min} \cdot s_{t,g}^{MBR} \qquad t \in T,\ g \in G \tag{4.20}$$

Secondary reserve needed level. In each area, a certain amount of reserve must be accounted for and provided by the generators. An upper bound is also imposed on the reserve that a generator can offer, despite the requirement that each generator submit its entire capacity to the market. Let $G_z^{R2} \subseteq G^{R2}$ denote the set of generators providing secondary reserve and located in zone z. The constraints read as follow:

$$\sum_{z \in a} \sum_{g \in G_z^{R2}} \Delta p_{t,g}^{2,u} \geq \overline{R}_{t,a}^{2,u} \qquad t \in T,\ a \in A \tag{4.21}$$

$$\sum_{z \in a} \sum_{g \in G_z^{R2}} \Delta p_{t,g}^{2,d} \geq \overline{R}_{t,a}^{2,d} \qquad t \in T,\ a \in A \tag{4.22}$$

Zonal balance. In each zone, the balance between generated and demanded power is enforced through a network-related constraint, which accounts for congestion management and reduces the number of adjustments required to obtain a feasible solution. In this case, the model adopts a simplified network representation by aggregating adjacent nodes into zones and considering only the total transfer capacity of each inter-zonal line.

$$\sum_{g\in z} p_{t,g} + \sum_{z_2\in Z: z_2\neq z} f_{t,z_2,z} = \sum_{n\in N_z} d^N_{t,n} \qquad t\in T,\ z\in Z \tag{4.23}$$

Furthermore, upper and lower bounds are imposed on the power flow through the virtual line connecting the two zones, based on the connection capacity.

$$f_{t,z,z_2} \leq \overline{L}^{max}_{t,z,z_2} \qquad \forall t\in T,\ \forall(z,z_2): z, z_2\in Z, z\neq z_2 \tag{4.24}$$

$$f_{t,z,z_2} \geq -\overline{L}^{max}_{t,z,z_2} \qquad \forall t\in T,\ \forall(z,z_2): z, z_2\in Z, z\neq z_2 \tag{4.25}$$

Objective function. The objective is to minimize the cost associated with the redispatch solution. This cost consists of several terms, which are described as follows. The first term represents the cost of the power produced by newly committed generators that were not scheduled in that period and are remunerated at their offered prices. The second term represents the savings obtained when generators are switched off; it provides a negative contribution to the cost, since these units buy back their previous commitments. Given that the shutdown price is lower than the downward step prices, i.e., $\overline{\pi}^{sd}_{t,g} \leq \overline{\pi}^{step,d}_{t,g,k}$ for all k, a unit can be switched off only after its downward step bids have been accepted, with the shutdown offer priced at $\overline{\pi}^{sd}_{t,g}$ being accepted last. The third term model the cost of accepting upward and downward bids at different steps. The final term penalizes any excess number of start-ups relative to the MI outcome by charging a token cost for each additional start-up. Overall, the objective function is given by:

$$\begin{aligned}\sum_{t\in T}\Bigg[&\sum_{g\in G: S^{MI}_{t,g}=0} (\overline{\pi}^{su}_{t,g}\cdot p^{on}) - \sum_{g\in G: S^{MI}_{t,g}=1} (\overline{\pi}^{sd}_{t,g}\cdot \overline{P}^{min}_{t,g}\cdot (1-s^{MBR}_{t,g}))+ \\ &+ \sum_{g\in G^{MI}} \sum_{k\in K} (\overline{\pi}^{step,u}_{t,g,k}\cdot dp^u_{t,g,k} - \overline{\pi}^{step,d}_{t,g,k}\cdot dp^d_{t,g,k})\Bigg] + \quad + \sum_{g\in G} \Delta s^u_g \cdot \overline{GA}_g.\end{aligned} \tag{4.26}$$

4.2.2 The Direct Current Model

In the DC model, the DC power flow approximation is introduced to account for all inter-node connections, as well as for technical variables such as nodal phase angles and line power flows. These constraints allow the model to represent, albeit approximately, the technical challenges associated with balancing a network of nodes characterized by different injections and withdrawals. Moreover, the position of each node within the network and its interconnections become relevant, as they directly affect power flows and the overall system balance.

Since the secondary reserve must also be considered, feasibility is required to hold even under full reserve activation. To this end, an additional set of phase angle variables and DC constraints is introduced, making it possible to compute the corresponding network variables without directly affecting the other decision variables of the model. By combining the results obtained for the zero-activation and full-activation cases, the phase angles, together with the corresponding line flows, associated with any intermediate reserve activation level can be obtained by linear interpolation, without re-solving the optimization model, provided that the network topology and the reserve activation pattern remain fixed.

Variables. In addition to the variables already listed in Table 4.1, this model incorporates new sets of variables, presented in Table 4.4. It should also be noted that the flows f_{t,z,z_2} and κ_{t,z,z_2} are excluded from the present formulation.

Table 4.4. Decision variables of the DC formulation.

Name	Domain	Description
$\theta_{n,t}$	$\mathbb{R}$	Phase angle at network node n during period t.
$\theta^{\text{res}}_{n,t}$	$\mathbb{R}$	Phase angle at network node n during period t considering the reserves activation.

Sets and parameters. In addition to the elements defined in Section 4.2.1, this model employs further parameters and a set, which are presented in Table 4.5 and Table 4.6.

Table 4.5. Sets of the DC formulation.

Symbol	Description
Lines	Set of network connection lines (branches) between nodes.

Table 4.6. Parameters of the DC formulation.

Symbol	Domain	Description
$\overline{F}^{max}_{t,j,k}$	$\mathbb{R}_{\geq 0}$	Maximum transmission capacity of the line between nodes j and k in period t.
$\mathbf{B}$	$\mathbb{R}^{\lvert N \rvert \times \lvert N \rvert}$	Network susceptance matrix used in the DC power-flow linearization.
$b_{j,k}$	$\mathbb{R}_{>0}$	Susceptance of line (j,k).

Constraints

The constraints of the DC model are introduced below. To avoid redundancy, the constraints in (4.8)–(4.22) are not restated, although they remain included in the present formulation.

Direct Current constraints. The main elements of the DC model are the following constraints, which ensure that the power injected into or withdrawn from each node is feasible with respect to the network topology and the associated voltage phase angles. In particular, (4.27) and (4.28) enforce nodal balance under zero secondary reserve activation and full reserve activation, respectively. Constraints (4.29) and (4.30) impose upper bounds on the power transmitted through the lines, based on the corresponding technical parameters.

In the DC approximation, the active power flow on a line connecting nodes i and j is proportional to the voltage phase-angle difference between its endpoints, i.e. $b_{i,j}(\theta_i - \theta_j)$.

Therefore, depending on how $\overline{F}^{\max}_{t,j,k}$ is defined, the line-transmission constraints can be interpreted in two equivalent ways: either as limits on the transmitted power or as limits on the absolute voltage phase-angle difference. Conversely, imposing a constraint on the phase angle difference directly yields a bound on the maximum power that can flow through the line. Note that $b_{i,j} \neq \mathbf{B}_{i,j}$ by construction of the matrix $\mathbf{B}$. In what follows, whenever an index is suppressed, the corresponding collection of variables is represented in vector form and denoted in boldface. Zonal balance constraints have been removed from the model, as they are inherently satisfied by the DC power flow equations; see Appendix A. Formally, the constrains reads as follows:

$$\mathbf{B}\boldsymbol{\theta}_t = \mathbf{p}_t - \overline{\mathbf{d}}_t \qquad t \in T, \tag{4.27}$$
$$\mathbf{B}\boldsymbol{\theta}^{res}_t = \mathbf{p}_t - \overline{\mathbf{d}}_t + \Delta p^{u,r2}_t - \Delta p^{d,r2}_t \qquad t \in T, \tag{4.28}$$
$$b_{j,k}\left|\theta_{j,t} - \theta_{k,t}\right| \leq \overline{F}^{\max}_{t,j,k} \qquad t \in T,\ (j,k) \in Lines, \tag{4.29}$$
$$b_{j,k}\left|\theta^{res}_{j,t} - \theta^{res}_{k,t}\right| \leq \overline{F}^{\max}_{t,j,k} \qquad t \in T,\ (j,k) \in Lines, \tag{4.30}$$

Linearized angles constraints. Since constraints (4.29) and (4.30) involve the absolute value of the phase-angle difference, they are reformulated as the following equivalent linear constraints.

$$(\theta_{j,t} - \theta_{k,t}) \cdot b_{j,k} \leq \overline{F}^{max}_{t,j,k} \qquad t \in T,\ (j,k) \in Lines \tag{4.31}$$
$$(\theta_{k,t} - \theta_{j,t}) \cdot b_{j,k} \leq \overline{F}^{max}_{t,j,k} \qquad t \in T,\ (j,k) \in Lines \tag{4.32}$$
$$(\theta^{res}_{j,t} - \theta^{res}_{k,t}) \cdot b_{j,k} \leq \overline{F}^{max}_{t,j,k} \qquad t \in T,\ (j,k) \in Lines \tag{4.33}$$
$$(\theta^{res}_{k,t} - \theta^{res}_{j,t}) \cdot b_{j,k} \leq \overline{F}^{max}_{t,j,k} \qquad t \in T,\ (j,k) \in Lines \tag{4.34}$$

$$b_{j,k}(\theta_{j,t} - \theta_{k,t}) \leq \overline{F}^{\max}_{t,j,k} \qquad t \in T,\ (j,k) \in Lines \tag{4.35}$$
$$b_{j,k}(\theta_{k,t} - \theta_{j,t}) \leq \overline{F}^{\max}_{t,j,k} \qquad t \in T,\ (j,k) \in Lines \tag{4.36}$$
$$b_{j,k}(\theta^{reserve}_{j,t} - \theta^{reserve}_{k,t}) \leq \overline{F}^{\max}_{t,j,k} \qquad t \in T,\ (j,k) \in Lines \tag{4.37}$$
$$b_{j,k}(\theta^{reserve}_{k,t} - \theta^{reserve}_{j,t}) \leq \overline{F}^{\max}_{t,j,k} \qquad t \in T,\ (j,k) \in Lines \tag{4.38}$$

Objective function
The objective function is identical to that in (4.26) and is therefore omitted for brevity.

Summary of the DC model Overall, the DC model reads as follows:

$$\begin{aligned} &\min && (4.26) \\ &\text{s.t.} && (4.8)-(4.22),\ (4.27),\ (4.28),\ (4.35)-(4.38). \end{aligned}$$

4.3 Recovery models

Two recovery models are now introduced. Each model takes as input an initial solution that, in general, is not guaranteed to satisfy the DC power flow constraints. The purpose of these models

is to construct a DC-feasible solution that remains as close as possible to the initial one according to two alternative criteria: (i) minimizing the number of modifications with respect to the initial solution, and (ii) minimizing the total power variation with respect to the initial profile.
Maintaining proximity to the initial solution helps minimize the impact on prior market outcomes, thereby preserving the original generation schedules of the units and avoiding unnecessary operational adjustments.
Both recovery models share a common core of constraints, corresponding to those of the DC model. In addition, each model includes further constraints, which are detailed in the following sections. The main differences between the two formulations therefore concern both the objective function and the additional constraints introduced to reflect the respective proximity criterion.

For clarity of notation, variables marked with a tilde (e.g., $\tilde{dp^u}_{t,g,k}$) denote fixed parameters corresponding to the values obtained in the solution of the Base model, and are therefore treated as constants in the recovery formulations.

4.3.1 R1: Minimizing the number of changes

In this model, the number of modifications applied to the initial solution, which, in general, is not guaranteed to satisfy the nodal network constraints, is quantified. Specifically, start-up and shutdown events, changes in the acceptance of upward and downward bids, and variations in start-up power are accounted for separately. A modification is recorded only if the numerical difference exceeds a predefined threshold, whose magnitude directly affects the total number of detected changes and, consequently, the outcome of the model. To avoid double-counting the penalty associated with the same modification, changes in unit status and start-up power are captured by the same variable. Moreover, since the objective function is not cost-driven, the selection of accepted bids may otherwise be influenced by factors unrelated to economic efficiency, potentially resulting in a solution that is not practically implementable. To address this issue, an additional set of constraints is introduced to embed economic logic into the model.
Along with the set, parameters, variables and constraints defined in Subsection 4.2.2, the additional elements in Tables 4.7 and 4.8 are introduced.

Status changes. The number of generator status changes is tracked through the binary variable $\psi_{t,g}$. Start-up and shutdown events are captured by the same variable to avoid penalizing the same deviation twice, namely through the simultaneous activation of both the penalty associated with status changes and the penalty for exceeding the threshold on the difference $\left|\tilde{p}^{on}_{t,g} - p^{on}_{t,g}\right|$.

$$\psi_{t,g} \geq \tilde{s}^{\mathrm{MBR}}_{t,g} - s^{\mathrm{MBR}}_{t,g} \qquad t \in T,\ g \in G, \tag{4.39}$$

$$\psi_{t,g} \geq s^{\mathrm{MBR}}_{t,g} - \tilde{s}^{\mathrm{MBR}}_{t,g} \qquad t \in T,\ g \in G. \tag{4.40}$$

Table 4.7. Decision variables of the R1 formulation.

Variable	**Domain**	**Description**
$\gamma_{t,g,k}$	$\{0,1\}$	Equals 1 if the difference in the acceptance of the k-th step of upward bids from generator g at time t exceeds $Q^u_{t,g,k}$; equals 0 otherwise.
$\xi_{t,g,k}$	$\{0,1\}$	Equals 1 if the difference in the acceptance of the k-th step of downward bids from generator g at time t exceeds $Q^d_{t,g,k}$; equals 0 otherwise.
$\psi_{t,g}$	$\{0,1\}$	Equals 1 if the operational status of generator g changes at time t; equals 0 otherwise.
$\Phi_{t,g}$	$\{0,1\}$	Equals 1 if the ignition power difference exceeds the threshold $W_{t,g}$; equals 0 otherwise.
$\iota^u_{t,g}$	$\{0,1\}$	Equals 1 if the first step of the upward bid of generator g is fully accepted at time t; equals 0 otherwise.
$\beta^u_{t,g}$	$\{0,1\}$	Equals 1 if the second step of the upward bid of generator g is fully accepted at time t; equals 0 otherwise.
$\iota^d_{t,g}$	$\{0,1\}$	Equals 1 if the first step of the downward bid of generator g is fully accepted at time t; equals 0 otherwise.
$\beta^d_{t,g}$	$\{0,1\}$	Equals 1 if the second step of the downward bid of generator g is fully accepted at time t; equals 0 otherwise.
$u^1_{t,g,k}, u^2_{t,g,k}$	$\mathbb{R}_{\geq 0}$	Variables representing the positive and negative components of the absolute value of the upward bid constraints for generator g at time t.
$r^1_{t,g,k}, r^2_{t,g,k}$	$\mathbb{R}_{\geq 0}$	Variables representing the positive and negative components of the absolute value of the downward bid constraints for generator g at time t.
$h^1_{t,g}, h^2_{t,g}$	$\mathbb{R}_{\geq 0}$	Variables representing the positive and negative components of the absolute value of the start-up power constraints for generator g at time t.

Table 4.8. Parameters of the R1 formulation.

Parameter	**Domain**	**Description**
$Q^u_{t,g,k}$	$\mathbb{R}_{\geq 0}$	Threshold to count upward changes for step k, generator g at time t.
$Q^d_{t,g,k}$	$\mathbb{R}_{\geq 0}$	Threshold to count downward changes for step k, generator g at time t.
$W_{t,g}$	$\mathbb{R}_{\geq 0}$	Threshold to count ignition difference for generator g at time t.
ϵ	$\mathbb{R}_{>0}$	Small positive value.

Accepted bid changes. The main idea is to enforce $\gamma_{t,g,k} = 1$ (or $\xi_{t,g,k} = 1$) when the difference between the original value and the updated one exceeds a predefined threshold $Q^u_{t,g,k}$ (or$Q^d_{t,g,k}$). Conversely, if this threshold is not exceeded, the corresponding binary variable must be equal to zero. This representation requires specifying an upper bound on the difference to allow the variable to vary correctly. In this case, there is no need to introduce a large constant, since the maximum attainable value is known. In particular, for the bids, the maximum value is defined as the larger of the absolute difference between the initial bid ($\overline{DP}^u_{t,g,k}$ or $\overline{DP}^d_{t,g,k}$) and the bid accepted in the Base model solution ($\tilde{dp}^u_{t,g,k}$ or $\tilde{dp}^d_{t,g,k}$), and the accepted bid itself. For each $t \in T$, $g \in G^{MI}$, and $k \in K$, let $\Lambda^u_{t,g,k} := \max\{\overline{DP}^u_{t,g,k} - \tilde{dp}^u_{t,g,k}, \tilde{dp}^u_{t,g,k}\}$, and $\Lambda^d_{t,g,k} := \max\{\overline{DP}^d_{t,g,k} - \tilde{dp}^d_{t,g,k}, \tilde{dp}^d_{t,g,k}\}$.

$$\left|\tilde{dp^u}_{t,g,k} - dp^u_{t,g,k}\right| \leq \gamma_{t,g,k}\Lambda^u_{t,g,k} + (1-\gamma_{t,g,k})Q^u_{t,g,k} \qquad t \in T,\ g \in G^{MI},\ k \in K, \tag{4.41}$$
$$\left|\tilde{dp^u}_{t,g,k} - dp^u_{t,g,k}\right| \geq \gamma_{t,g,k}Q^u_{t,g,k} \qquad t \in T,\ g \in G^{MI},\ k \in K, \tag{4.42}$$

$$\left|\tilde{dp^d}_{t,g,k} - dp^d_{t,g,k}\right| \leq \xi_{t,g,k}\Lambda^d_{t,g,k} + (1-\xi_{t,g,k})Q^d_{t,g,k} \qquad t \in T,\ g \in G^{MI},\ k \in K, \tag{4.43}$$
$$\left|\tilde{dp^d}_{t,g,k} - dp^d_{t,g,k}\right| \geq \xi_{t,g,k}Q^d_{t,g,k} \qquad t \in T,\ g \in G^{MI},\ k \in K, \tag{4.44}$$

To eliminate the absolute-value terms, the model is reformulated by introducing three auxiliary variables, namely two continuous variables and one binary variable, together with one additional constraint for each absolute-value term. A penalty term could also be added to the objective function to discourage the two continuous variables from being simultaneously strictly positive. However, this would increase the computational complexity without providing meaningful information, since the exact values of the variables $u^1, u^2, r^1, r^2, h^1, h^2$ are not relevant for the present purposes,the penalty does not depend on whether both variables in each pair are positive.

The absolute-value terms are removed, and constraints (4.41)–(4.44) are replaced by the following set of constraints:

$$u^1_{t,g,k} + u^2_{t,g,k} \leq \gamma_{t,g,k}\Lambda^u_{t,g,k} + (1-\gamma_{t,g,k})Q^u_{t,g,k} \qquad t \in T,\ g \in G^{MI},\ k \in K \tag{4.45}$$
$$u^1_{t,g,k} + u^2_{t,g,k} \geq \gamma_{t,g,k}Q^u_{t,g,k} \qquad t \in T,\ g \in G^{MI},\ k \in K \tag{4.46}$$
$$u^1_{t,g,k} - u^2_{t,g,k} = \tilde{dp^u}_{t,g,k} - dp^u_{t,g,k} \qquad t \in T,\ g \in G^{MI},\ k \in K \tag{4.47}$$

$$r^1_{t,g,k} + r^2_{t,g,k} \leq \xi_{t,g,k}\Lambda^d_{t,g,k} + (1-\xi_{t,g,k})Q^d_{t,g,k} \qquad t \in T,\ g \in G^{MI},\ k \in K \tag{4.48}$$
$$r^1_{t,g,k} + r^2_{t,g,k} \geq \xi_{t,g,k}Q^d_{t,g,k} \qquad t \in T,\ g \in G^{MI},\ k \in K \tag{4.49}$$
$$r^1_{t,g,k} - r^2_{t,g,k} = \tilde{dp^d}_{t,g,k} - dp^d_{t,g,k} \qquad t \in T,\ g \in G^{MI},\ k \in K \tag{4.50}$$

Start-up power differences. Excessive changes in start-up power are penalized. In particular, if the absolute value of the difference between the variable $p^{on}_{t,g}$ and $\tilde{p}^{on}_{t,g}$ is larger than a selected

threshold $W_{t,g}$, then $\Phi_{t,g} = 1$. Since the status change is already penalized, an additional constraint is introduced to account for all changes through a single variable and avoid double penalizing the same phenomenon. Similarly to the previous case, the maximum attainable value of the difference is known and corresponds to the maximum between $\overline{P}^{max}_{t,g} - \tilde{p}^{on}$ and $\tilde{p}^{on}$.
For each $t \in T$ and $g \in G$, let $\Lambda^{on}_{t,g} := \max\{\overline{P}^{max}_{g} - \tilde{p}^{on}_{t,g}, \tilde{p}^{on}_{t,g}\}$.

Constraints (4.51) and (4.52) penalize excessive deviations in start-up power, while constraint (4.53) assigns the corresponding penalty to the variable $\psi_{t,g}$.

$$\left|\tilde{p}^{on}_{t,g} - p^{on}_{t,g}\right| \leq \Phi_{t,g}\Lambda^{on}_{t,g} + (1 - \Phi_{t,g})W_{t,g} \qquad t \in T,\ g \in G \tag{4.51}$$
$$\left|\tilde{p}^{on}_{t,g} - p^{on}_{t,g}\right| \geq \Phi_{t,g}W_{t,g} \qquad t \in T,\ g \in G \tag{4.52}$$
$$\psi_{t,g} \geq \Phi_{t,g} \qquad t \in T,\ g \in G \tag{4.53}$$

The absolute value is removed using the same technique described earlier, and the following constraints (4.54)–(4.56) replace (4.51)–(4.52):

$$h^1_{t,g} + h^2_{t,g} \leq \Phi_{t,g}\Lambda^{on}_{t,g} + (1 - \Phi_{t,g})W_{t,g} \qquad t \in T,\ g \in G \tag{4.54}$$
$$h^1_{t,g} + h^2_{t,g} \geq \Phi_{t,g}W_{t,g} \qquad t \in T,\ g \in G \tag{4.55}$$
$$h^1_{t,g} - h^2_{t,g} = \tilde{p}^{on}_{t,g} - p^{on}_{t,g} \qquad t \in T,\ g \in G \tag{4.56}$$

Economic logic. This model does not account for the economic aspect; therefore, bid acceptance must be enforced step by step to better mimic the actions of a decision-maker. Specifically, when three steps are considered, the first step must be accepted before the second, and the second before the third. The following constraints ensure that the model operates in an economically rational manner. This scheme can be easily extended to any number of steps by repeating the same pattern.

$$dp^u_{t,g,1} \geq \overline{DP}^u_{t,g,1}\iota^u_{t,g} \qquad t \in T,\ g \in G^{MI}, \tag{4.57}$$
$$dp^u_{t,g,2} \leq \overline{DP}^u_{t,g,2}\iota^u_{t,g} \qquad t \in T,\ g \in G^{MI}, \tag{4.58}$$
$$dp^u_{t,g,2} \geq \overline{DP}^u_{t,g,2}\beta^u_{t,g} \qquad t \in T,\ g \in G^{MI}, \tag{4.59}$$
$$dp^u_{t,g,3} \leq \overline{DP}^u_{t,g,3}\beta^u_{t,g} \qquad t \in T,\ g \in G^{MI}. \tag{4.60}$$

$$dp^d_{t,g,1} \geq \overline{DP}^d_{t,g,1}\iota^d_{t,g} \qquad t \in T,\ g \in G^{MI}, \tag{4.61}$$
$$dp^d_{t,g,2} \leq \overline{DP}^d_{t,g,2}\iota^d_{t,g} \qquad t \in T,\ g \in G^{MI}, \tag{4.62}$$
$$dp^d_{t,g,2} \geq \overline{DP}^d_{t,g,2}\beta^d_{t,g} \qquad t \in T,\ g \in G^{MI}, \tag{4.63}$$
$$dp^d_{t,g,3} \leq \overline{DP}^d_{t,g,3}\beta^d_{t,g} \qquad t \in T,\ g \in G^{MI}. \tag{4.64}$$

Objective function

The objective function comprises several terms: the number of status changes and the power variations during the start-up process ($\psi_{t,g}$), and the binary variables that track differences in the generator bids ($\gamma_{t,g,k}$ and $\xi_{t,g,k}$).

$$\sum_{t \in T} \sum_{g \in G} \left(\psi_{t,g} + \sum_{k \in K} (\gamma_{t,g,k} + \xi_{t,g,k}) \right) \tag{4.65}$$

Summary of the R1 model. In summary, the R1 model is defined as follows:

$$\begin{aligned} \min \quad & (4.65) \\ \text{s.t.} \quad & (4.8) - (4.22),\ (4.27),\ (4.28),\ (4.35) - (4.40) \\ & (4.45) - (4.50),\ (4.53) - (4.64) \end{aligned}$$

4.3.2 R2: Minimizing changes in nodal output

The second recovery model aims to limit variations in the output of each generator. A single additional non-negative continuous variable is introduced, which represents the deviation of a generator's production from its previous profile in each time period. The model also includes the constraints associated with economically rational behavior. The following constraints extend the core model described above.

In addition to the sets, parameters, variables, and constraints defined in Subsection 4.2.2, Table 4.9 presents the additional variable used in the R2 formulation.

Table 4.9. Decision variables of the R2 formulation.

Name	Domain	Description
$\Omega_{t,g}$	$\mathbb{R}_{\geq 0}$	Power-output deviation of generator g from its previous profile in time period t.

Differences in power produced. These two constraints assign the positive difference in each generator's output profile to the variable $\Omega_{t,g}$.

$$\Omega_{t,g} \geq \tilde{p}_{t,g} - p_{t,g} \qquad t \in T,\ g \in G \tag{4.66}$$

$$\Omega_{t,g} \geq p_{t,g} - \tilde{p}_{t,g} \qquad t \in T,\ g \in G \tag{4.67}$$

Objective function

The objective function penalizes deviations in each generator's output between the two solutions, regardless of the underlying causes of these changes.

$$\sum_{t \in T} \sum_{g \in G} \Omega_{t,g} \tag{4.68}$$

Summary of the R2 model For completeness, the R2 model can be compactly written as:

$$\begin{aligned} \min \quad & (4.68) \\ \text{s.t.} \quad & (4.8) - (4.22),\ (4.27),\ (4.28),\ (4.35) - (4.38) \\ & (4.66) - (4.67) \end{aligned}$$

4.4 Results

This section describes the test instances and reports the computational results obtained for the proposed formulations.

4.4.1 Instances

The proposed models were tested on two networks from the *IEEE PES Power Grid Library* [5], each considered under two demand configurations, denoted as summer and winter. Since the original data do not fully match the present modeling requirements (e.g., they refer to a single time period), the available data on network topology, generator linear marginal costs, maximum generation capacities, and peak demand were used as reported for each case study, while the remaining parameters were adapted accordingly. The main characteristics of each network, which provide an indication of the overall system scale, are reported in Table 4.10.

Table 4.10. Description of instances in terms of number of buses, edges and generators

	Buses	**Edges**	**Generators**
IEEE118	118	179	19
IEEE300	300	409	57

The number of zones and areas is fixed for each network and does not depend on the demand configuration. Each demand profile follows a typical daily pattern, characterized by two main peaks around 12:00 and 20:00, with seasonal differences. These patterns are based on generic Italian demand data for August and January and are shown in Figure 4.1. To introduce variability while preserving the overall shape, a 2% noise term was added to each demand profile.
For each instance, 24 time periods were considered, although the model can be straightforwardly extended to shorter imbalance intervals, such as the recent 15-minute ones.

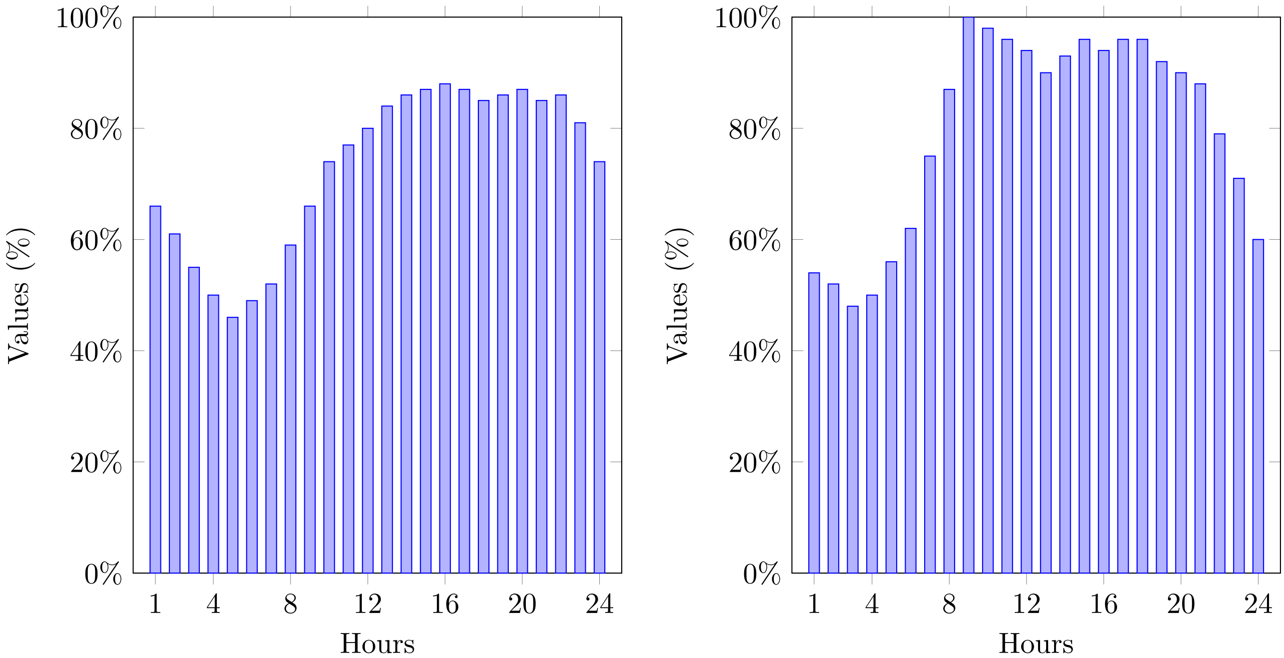

(a) Demand profile - Summer

(b) Demand profile - Winter

Figure 4.1. Comparison of daily demand profiles for Summer and Winter.

Generators in MI. To define an initial market state given by a previous market solution, a simplified unit commitment model was solved. The model included generator technical constraints, such as ramping limits, was solved under a reduced demand level, and did not include network constraints.

Zones and Areas. To determine the zonal partitioning, a criterion based on minimizing the number of connections between nodes belonging to different zones was adopted. For the instances derived from the IEEE 118-bus network, the partitioning was taken from the literature [77]. For the remaining networks, the zonal partitioning was computed using the greedy modularity algorithm available in the NetworkX library (*networkx.community.greedy_modularity_communities(G)*). The zones were then aggregated into k areas by grouping zones with stronger mutual connectivity.

Bid specifications. The bids submitted by generators to increase or decrease their power output were modeled using a three-step structure. For upward bids, bid prices increase from one step to the next, whereas for downward bids they decrease. Moreover, the step sizes decrease progressively. To construct these steps, the difference between the generator's current output $P^0_{t,g}$ and its upper or lower technical limit was considered, ensuring that only feasible power adjustments were offered. This available range was then divided into $k = 3$ steps of unequal size, corresponding to the percentages [0.45, 0.35, 0.20]. Bid prices were derived from the generator's linear marginal production cost, which was used as a reference value and adjusted through step-dependent percentage increments for upward bids or decrements for downward bids.

Prices. The start-up and shutdown prices, $\overline{\pi}^{su}_{t,g}$ and $\overline{\pi}^{sd}_{t,g}$, respectively, were derived from the linear marginal production cost a_2. Specifically, the following values were used:

$$\overline{\pi}^{su}_{t,g} = 1.10 \cdot a_2, \qquad \overline{\pi}^{sd}_{t,g} = 0.99 \cdot a_2.$$

Lines data. Since the models do not consider parallel lines, duplicate transmission lines between the same pair of nodes in the original data were removed. The maximum power flow on each line was defined based on the maximum admissible phase-angle difference between the connected nodes and was computed as

$$F^{\max}_{i,j} = \Delta\theta^{\max} b_{i,j}.$$

This value was assumed to be constant across all time periods.
The Base model does not represent individual transmission lines within a zone-to-zone connection; hence, all lines between two zones were aggregated into a single equivalent connection. The total transfer capacity between two zones, z_1 and z_2, was therefore obtained by summing the maximum flow limits of all lines whose endpoints belong to the two zones:

$$F^{\max,tot}_{z_1,z_2} = \sum_{\substack{(i,j)\in L: \\ (i\in z_1, j\in z_2) \\ \vee \\ (j\in z_1, i\in z_2)}} F^{\max}_{i,j}. \tag{4.69}$$

Generator start-up process. Each generator g reaches its maximum production level after ω_g periods from start-up. During this ramping phase, the maximum allowable output increases according to the following schedule, expressed as a percentage of the generator's nominal maximum output $P^{\max}$:

$$\overline{P}_{\cdot,g} = [50\%,\ 60\%,\ 75\%,\ 100\%].$$

Reserve. The secondary reserve requirement was set to at least 7% of the total hourly demand in each area.

Bid-change thresholds. Parameters $W_{t,g}$, $Q^u_{t,g,k}$, and $Q^d_{t,g,k}$ are set equal to 5% of $(\overline{P}^{max}_g - \overline{P}^{min}_g)$, $\overline{DP}^u_{t,g,k}$, and $\overline{DP}^d_{t,g,k}$, respectively.

Summary. Table 4.11 summarizes the main features of each instance.

Table 4.11. Summary of instances. **# A** indicates the number of Areas, **# Z** indicates the number of Zones, **T** the time periods.

	Network	**Demand**	**# A**	**# Z**	**T**
Case 1	IEEE118	Winter	2	4	24
Case 2	IEEE118	Summer	2	4	24
Case 3	IEEE300	Winter	2	4	24
Case 4	IEEE300	Summer	2	4	24

4.4.2 Computational results

The results obtained from solving the instances with the different models are summarized in the following tables. The model without network constraints is denoted as **B**, the DC model as **DC**, and the two recovery models as **R1**, which minimizes the number of changes, and **R2**, which minimizes deviations in the generation profile.
The experiments were conducted on a machine with an Intel Core i9-13900K processor, on four cores with a clock speed of 4.3 GHz. All optimization models were solved using Gurobi Optimizer 13.0.0 through Python 3.12.3, with the *TimeLimit* parameter set to 1800 seconds.

Table 4.12 presents the results in terms of economic cost for the Base model and the DC model. Table 4.13 reports a comparison between the DC model and the two recovery models, R1 and R2. Since the objective functions differ, the comparison is based on the DC solution cost as returned by the solver, whereas the costs of the R1 and R2 solutions are computed *ex post* under the Base and DC cost function (4.26). Both recovery models consistently yield higher costs than the DC model. The additional cost ranges from 22.16% to 39.62% for R1, and from 12.66% to 35.21% for R2. In all test cases, R2 is systematically less expensive than R1.

Moreover, the computational time required to solve R1 is higher than that required for the DC model and for model R2 in each test case. When compared to the DC model, R2 shows a case-dependent behavior, yielding lower computational times in Cases 2 and 4, and higher computational times in Cases 1 and 3. The same results are true considering also the time needed for solving the Base model. Finally, the DC model is solved to optimality in all cases, while the optimality gap for R1 is relevant in some instances, most notably in Cases 3 and 4.

Table 4.12. Comparison between the Base and DC-constrained models.

Case	**Objective Function**		**Time (s)**	
	B	**DC**	**B**	**DC**
Case 1	223,396	228,005	0.55	6.28
Case 2	205,104	211,472	1.10	19.82
Case 3	1,086,767	1,157,794	9.74	25.20
Case 4	933,576	995,952	9.72	163.86

Table 4.13. Comparison between constrained and recovery models in terms of costs, computational time, and optimality gap. Objective function values for R1 and R2 are computed *ex post* using the Base and DC objective functions.

Case	**Cost**			**Time (s)**			**Gap (%)**		
	DC	**R1**	**R2**	**DC**	**R1**	**R2**	**DC**	**R1**	**R2**
Case 1	228,005	312,151	278,940	6.28	374.99	9.44	0.0	0.0	0.0
Case 2	211,472	295,250	285,935	19.82	859.05	2.25	0.0	0.0	0.0
Case 3	1,157,794	1,421,328	1,304,391	25.20	1803.74	66.62	0.0	16.67	0.0
Case 4	995,952	1,311,407	1,202,712	163.86	1803.41	82.37	0.0	10.91	0.0

Solution refining. Both models R1 and R2 may admit multiple feasible solutions that attain the same optimal value of the primary objective function while differing in their associated economic costs. Therefore, after identifying the best objective value found within the imposed time limit, an additional optimization step was performed to select the minimum-cost solution among those satisfying the requested objective level. For model R1, after solving the problem and obtaining the best value R_1^*, the formulation was augmented with the constraint

$$\sum_{t\in T}\sum_{g\in G}\left(z_{t,g}^1+\psi_{t,g}+\sum_{k\in K}\left(\gamma_{t,g,k}+\xi_{t,g,k}\right)\right)\leq R_1^*. \tag{4.70}$$

The original objective function (4.65) was then replaced with the cost-minimization objective of the Base (DC) model (4.26), and the resulting model was solved again.

For model R2, after obtaining a solution with objective value R_2^*, the constraint

$$\sum_{t\in T}\sum_{g\in G}\Omega_{t,g}\leq\kappa\,R_2^* \tag{4.71}$$

was introduced, where $\kappa\geq 1$ is a relaxation parameter. Unlike R_1^*, which is an integer value representing the number of discrete changes with respect to a reference configuration, R_2^* is a continuous measure that captures differences in generation profiles. Therefore, the parameter κ was introduced to allow limited deviations from the value R_2^*, in order to potentially obtain solutions with a lower overall economic cost. As in the R1 case, the original objective function (4.68) was replaced with the cost-minimization objective (4.26).
In addition, to assess whether the "best" solution could be obtained directly, a modified version of the previously presented models was also tested. In this variant, a weighted cost term is added to the objective function. Since the primary goal remains to identify the closest feasible solution, the parameter ϵ must be chosen carefully to avoid selecting a solution with a worse value of the primary objective than the one obtained without the weighted cost term. Specifically, the following term was added to the objective functions of models R1 and R2:

$$\epsilon\cdot\text{Cost}, \tag{4.72}$$

where the auxiliary cost function is defined as (4.26).

In what follows, Table 4.14 reports, for each test instance, the objective values of the solutions obtained through the different procedures described above, namely those found within the prescribed time window ("Found"), those obtained via the refinement procedure ("Refined"), and those produced by the penalized objective function ("Penalty"). It is worth noting that the refinement procedure requires solving a second optimization problem, even though it is initialized with the solution obtained in the first stage. Consequently, its total computational time may exceed the time limit imposed on a single run of the other approaches.

Overall, the refined solutions consistently exhibit lower costs than those obtained directly within the time window, for both models R1 and R2. However, the magnitude of the improvement is higher for model R1, while it is negligible for R2. This overall improvement is expected, as the recovery models do not explicitly minimize the economic cost of the solution in their objective functions. The solutions obtained through the penalized objective function generally outperform those found directly within the time window for R1, although they remain more expensive than the refined ones. The penalization approach proves less effective, or even ineffective, for R2. Model R2, on the other hand, is solved to proven optimality for all tested instances, under both the refined and penalized approaches. As further highlighted in Table 4.15, model R2 also exhibits substantially better computational performance, achieving a zero optimality gap within significantly shorter computational times than model R1. Finally, Table 4.16 compares the DC solution cost with the costs associated with the Refined and penalty-augmented formulations of R1 and R2. In particular, the results show that the solutions obtained with R1 now yield costs ranging from 0.73% to 35.04% above the DC solution, whereas no significant variations are observed for model R2.

Table 4.14. Comparison of the incumbent solution cost (Found), the refined solution (Refined), and the solution obtained with an additional cost-based penalty term in the objective function (Penalty) for recovery models R1 and R2 ($\kappa = 1$). The value of the primary objective is identical across the three solution strategies; thus, the reported values of the secondary objective are directly comparable.

Case	**R1**			**R2**		
	Found	**Refined**	**Penalty**	**Found**	**Refined**	**Penalty**
Case 1	312,151	282,673	307,891	278,940	278,922	279,397
Case 2	295,250	213,026	222,769	285,935	285,668	285,934
Case 3	1,421,328	1,274,636	1,336,082	1,304,391	1,304,391	1,305,249
Case 4	1,311,407	1,174,847	1,190,044	1,202,712	1,201,738	1,202,427

Table 4.15. Percentage gap of the secondary objective and total computational time (s).

Case	**R1**				**R2**			
	Refined		**Penalty**		**Refined**		**Penalty**	
	Gap	**Time**	**Gap**	**Time**	**Gap**	**Time**	**Gap**	**Time**
Case 1	16.34	2179.70	0.00	1535.09	0.00	15.96	0.00	2.92
Case 2	0.00	1464.97	8.85	1803.10	0.00	7.74	0.00	2.45
Case 3	2.59	3606.20	19.28	1800.39	0.00	870.37	0.00	83.74
Case 4	11.00	3602.51	12.61	1802.86	0.00	996.58	0.00	216.21

Table 4.16. Comparison of the DC solution, the refined solution (Refined), and the solution obtained by adding the penalty cost term (Penalty) for recovery models R1 and R2 ($\kappa = 1$). Since the value of the primary objective is the same for the Refined and Penalty solution strategies, the reported values of the secondary objective are directly comparable.

Case	**DC**	**R1**		**R2**	
		Refined	**Penalty**	**Refined**	**Penalty**
Case 1	228,005	282,673	307,891	278,922	279,397
Case 2	211,472	213,026	222,769	285,668	285,934
Case 3	1,157,794	1,274,636	1,336,082	1,304,391	1,305,249
Case 4	995,952	1,174,847	1,190,044	1,201,738	1,202,427

Differences between solutions. The focus now shifts to the results obtained from the two recovery models, evaluated according to the following two criteria: (i) the number of changes and (ii) the total deviation in nodal output. To compute the values reported in the tables, the same comparison procedures used to derive the R1 and R2 recovery solutions were applied to the solutions obtained with all models (Base, DC, R1, and R2). Specifically, the R1 and R2 recovery solutions were obtained by measuring, respectively, the number of changes and the global profile deviation with respect to the Base solution. The remaining entries in Tables 4.17–4.20 report the pairwise distances between the solutions produced by the different models, computed according to the two criteria. In the following, the results obtained under both criteria are discussed and reported side by side for each instance. The left-hand side of each table presents the number of changes, decomposed into distinct categories and their total, while the right-hand side reports the corresponding global profile differences. When considering the number of changes, reported in the left part of , the smallest number of changes from the Base model is achieved by the first recovery model (R1), as expected by construction. Similarly, when focusing on the global profile changes (right part), the solution provided by the second recovery model (R2) is the closest to the Base model. These findings confirm that each recovery model behaves consistently with its design objective: R1 minimizes the number of modifications, whereas R2 minimizes deviations in the overall profile. Moreover, the entries in the "DC" row indicates that the closest feasible solution to the Base model solution, according to either criterion, may still differ substantially from the optimal DC solution.

	Number of changes					Profile differences
Pair	**dp**	**status**	**p_on**	**=**	**Tot**	
B–DC	66	21	9	=	96	4,252.68
B–R1	12	18	0	=	30	4,256.50
B–R2	31	17	1	=	49	2,374.06
DC–R1	59	31	23	=	113	5,189.35
DC–R2	61	24	21	=	106	3,101.17
R1–R2	26	7	16	=	49	2,768.38

Table 4.17. Comparison of unit-status changes and dispatch profile differences across configurations (Case 1).

Note: "Number of changes" counts component-wise deviations in (bids `dp` , `status`, start-up offers `p_on`); "Tot" is their sum per pair. "Profile differences" represent the distance calculated as the L_1 norm.

	Number of changes					Profile differences
Pair	**dp**	**status**	**p_on**	**=**	**Tot**	
B–DC	57	15	2	=	74	3,056.43
B–R1	15	10	0	=	25	2,847.53
B–R2	21	13	0	=	34	1,493.15
DC–R1	60	23	15	=	98	4,615.94
DC–R2	74	28	15	=	117	4,411.12
R1–R2	28	5	10	=	43	2,899.37

Table 4.18. Comparison of unit-status changes and dispatch profile differences across configurations (Case 2).

Note: Definitions as in Table 4.17.

	Number of changes					Profile differences
Pair	**dp**	**status**	**p_on**	**=**	**Tot**	
B–DC	179	48	44	=	271	27,754.48
B–R1	30	23	1	=	54	30,576.16
B–R2	107	49	9	=	165	19,013.27
DC–R1	178	61	49	=	288	45,349.69
DC–R2	193	85	45	=	323	29,667.10
R1–R2	107	62	31	=	200	37,757.28

Table 4.19. Comparison of unit-status changes and dispatch profile differences across configurations (Case 3).

Note: Definitions as in Table 4.17.

	Number of changes					Profile differences
Pair	**dp**	**status**	**p_on**	**=**	**Tot**	
B–DC	122	62	59	=	243	33,317.48
B–R1	32	23	0	=	55	33,742.62
B–R2	94	55	5	=	154	19,568.96
DC–R1	115	85	71	=	271	57,545.95
DC–R2	134	95	69	=	298	39,529.80
R1–R2	90	78	27	=	195	45,262.55

Table 4.20. Comparison of unit-status changes and dispatch profile differences across configurations (Case 4).

Note: Definitions as in Table 4.17.

Additional recovery. To further validate the models, an additional experiment was conducted in which the solutions obtained by the Base and DC models under the original demand were re-optimized using the recovery models R1 and R2 after perturbing the demand. Two settings were considered: a 5% demand decrease and a 5% demand increase. The recovered solutions were then compared to assess whether directly embedding the DC constraints in the model provides greater robustness than recovering feasibility *ex post*.

The results reported in Tables 4.21–4.22, which refer to the reduced-demand experiments, show a balanced picture: for both R1 and R2, there are two instances in which starting from a DC-feasible solution is advantageous and four in which it is not. However, in many cases, the computational time required when starting from a DC-feasible solution is significantly lower.

When demand increases, Tables 4.23–4.24 show that, for R1, the DC-feasible starting point is preferable in three out of four cases. For R2, by contrast, there is no clear preference from an economic perspective. In terms of computational time, the DC-feasible starting point is always faster for R2, whereas for R1 the Base model performs better in only one case; in the remaining cases, both starting points reach the time limit.

Table 4.21. Comparison between R1(b) and R1(DC), with demand reduced by 5% with respect to the original case.

	Cost		Time (s)		Gap (%)	
Case	**R1(b)**	**R1(DC)**	**R1(b)**	**R1(DC)**	**R1(b)**	**R1(DC)**
Case 1	158,183	164,609	1031.91	307.35	0.00	0.00
Case 2	155,489	150,790	1057.18	601.63	0.00	0.00
Case 3	844,804	959,647	1803.39	1803.48	18.97	34.88
Case 4	803,932	738,279	1800.58	1802.59	21.21	38.64

Table 4.22. Comparison between R2(b) and R2(c), with demand reduced by 5% with respect to the original case.

	Cost		Time (s)		Gap (%)	
Case	**R2(b)**	**R2(DC)**	**R2(b)**	**R2(DC)**	**R2(b)**	**R2(DC)**
Case 1	163,154	176,856	2.39	2.99	0.00	0.00
Case 2	155,137	145,471	2.48	1.75	0.00	0.00
Case 3	675,686	680,648	17.39	5.09	0.00	0.00
Case 4	663,088	527,761	16.10	4.66	0.00	0.00

Table 4.23. Comparison between R1(b) and R1(DC), with demand increased by 5% with respect to the original case.

	Cost		Time (s)		Gap (%)	
Case	**R1(b)**	**R1(DC)**	**R1(b)**	**R1(DC)**	**R1(b)**	**R1(DC)**
Case 1	467,864	432,115	1800.23	1800.21	12.07	12.82
Case 2	330,762	342,233	1584.04	1803.70	0.00	16.67
Case 3	2,250,804	2,099,285	1800.57	1800.64	27.27	18.18
Case 4	2,010,233	1,849,552	1803.61	1800.69	19.12	12.12

Table 4.24. Comparison between R2(b) and R2(c), with demand increased by 5% with respect to the original case.

	Cost		Time (s)		Gap (%)	
Case	**R2(B)**	**R2(DC)**	**R2(B)**	**R2(DC)**	**R2(B)**	**R2(DC)**
Case 1	495,858	524,128	10.84	9.76	0.00	0.00
Case 2	514,472	437,083	2.50	2.48	0.00	0.00
Case 3	2,172,552	2,279,194	45.19	9.53	0.00	0.00
Case 4	2,097,681	1,897,283	82.82	21.23	0.00	0.00

4.5 Conclusions

In this chapter, alternative redispatch approaches in a centralized electricity market are examined, with the aim of assessing the benefits of incorporating nodal constraints directly into the optimization process. As a first step, two modified versions of an existing simulator of the Italian redispatch market are developed. These versions explicitly include secondary reserve requirements and introduce a new mechanism for handling generator offers during start-up periods. The two formulations differ in their network representation: the Base model adopts zonal constraints, whereas the DC model relies on Direct Current (DC) power flow constraints.

In addition, two recovery models are introduced to compute DC-feasible solutions with minimal deviations from a given starting point. In this case, the starting point is the solution obtained from the Base model. These recovery models enable a fair comparison between the DC and Base models, as they emulate an *ex-post* feasibility adjustment process that preserves, as far as possible, the characteristics of the initial solution.

The computational experiments presented in Section 4.4 show that the DC model is economically advantageous and does not lead to a significant increase in computation time. The recovery model that minimizes the number of deviations from the Base solution (R1) yields higher system costs than the model that minimizes deviations in generation profiles (R2), and is generally more computationally demanding. When the solution refinement process is carried out through a second optimization stage aimed at obtaining the most economically efficient solution among those with the same value of the original objective function, R1 often leads to cheaper solutions than R2, which is mostly unaffected by this process. A penalization approach applied to both the R1 and R2 models shows that introducing a weighted cost term in the objective function often leads to better results, in terms of both final cost and computational time, than the original models. However, this approach requires an accurate choice of the penalty parameter. In particular, while the economic performance of R2 is less affected, the penalized formulation yields a significant reduction in computational time.

To further evaluate the robustness of the proposed approaches, additional recovery experiments were conducted under demand perturbations of $\pm 5\%$. The results show that the relative performance of the recovery strategies depends on both the direction of the demand variation and the specific recovery formulation considered. In the reduced-demand setting, no systematic economic advantage can be identified for either starting point, although the DC-feasible starting point is often associated with lower computational times. Under increased demand, the DC-feasible starting point appears to be more favorable for R1, whereas no clear economic preference emerges for R2; however, it remains computationally advantageous in terms of solution time. Overall, these findings suggest that, while the economic benefits of a DC-feasible starting point are not uniform across all operating conditions, its adoption may still offer relevant computational advantages.

Appendix A

Supplement to Chapter 4

Remark A.1. Direct Current equations include Zonal Balance

Proof. Let $t \in T$ be fixed. Consider

$$B \cdot \theta_t = p_t - d_t \tag{A.1}$$

which can be written componentwise as

$$\sum_{m \in \delta_n} (\theta_{t,n} - \theta_{t,m}) \cdot b_{n,m} = p_{t,n} - d_{t,n} \quad \forall n \in N \tag{A.2}$$

Let z be a fixed zone, and let N_z denote the set of nodes in z.

Summing (A.2) over all nodes $n \in N_z$ yields

$$\sum_{n \in N_z} \sum_{m \in \delta_n} (\theta_{t,n} - \theta_{t,m}) \cdot b_{n,m} = \sum_{n \in N_z} (p_{t,n} - d_{t,n}) \tag{A.3}$$

For links whose endpoints both belong to the same zone, the corresponding terms cancel out, i.e.,

$$\sum_{n \in N_z} \sum_{\substack{m \in \delta_n \\ m \in N_z}} (\theta_{t,n} - \theta_{t,m}) \cdot b_{n,m} = 0 \tag{A.4}$$

Since an orientation convention is adopted and the set of links contains only one arc for each pair of nodes, (A.3) can be rewritten by retaining only the terms associated with nodes connected to nodes outside the zone: After cancellation of the terms associated with links internal to N_z, only the boundary links remain, i.e.,

$$\sum_{\substack{(n,m) \in L: \\ (n \in N_z,\, m \notin N_z) \text{ or } (m \in N_z,\, n \notin N_z)}} (\theta_{t,n} - \theta_{t,m})\, b_{n,m} = \sum_{n \in N_z} (p_{t,n} - d_{t,n}). \tag{A.5}$$

Partitioning the boundary links according to the adopted arc orientation yields

$$\sum_{\substack{(n,m) \in L: \\ n \in N_z,\, m \notin N_z}} (\theta_{t,n} - \theta_{t,m})\, b_{n,m} - \sum_{\substack{(j,k) \in L: \\ j \notin N_z,\, k \in N_z}} (\theta_{t,j} - \theta_{t,k})\, b_{j,k} = \sum_{n \in N_z} (p_{t,n} - d_{t,n}). \tag{A.6}$$

Rearranging terms, one obtains

$$\sum_{n \in N_z} p_{t,n} + \sum_{\substack{(j,k) \in L: \\ j \notin N_z,\, k \in N_z}} (\theta_{t,j} - \theta_{t,k})\, b_{j,k} - \sum_{\substack{(n,m) \in L: \\ n \in N_z,\, m \notin N_z}} (\theta_{t,n} - \theta_{t,m})\, b_{n,m} = \sum_{n \in N_z} d_{t,n}. \tag{A.7}$$

□

Bibliography

[1] Victor Ahlqvist, Pär Holmberg, and Thomas P Tangerås. *Central-versus self-dispatch in electricity markets*. JSTOR, 2018.

[2] Donald G Anderson. “Iterative procedures for nonlinear integral equations”. In: *Journal of the ACM (JACM)* 12.4 (1965), pp. 547–560.

[3] Arera. *Testo Integrato del Dispacciamento Elettrico*. [In Italian]. 2024. URL: `https://www.arera.it/fileadmin/allegati/docs/25/227-2025-R-eel-ALLEGATO_A.pdf`.

[4] Autorità Regolazione per Energia Reti e Ambiente (ARERA). *Superamento del prezzo unico nazionale e modifiche al Testo integrato del dispacciamento elettrico (TIDE) funzionali alla sua entrata in operatività all’1 gennaio 2025, 304/2024/R/eel*. [in Italian]. URL: `https://www.arera.it/fileadmin/allegati/docs/24/304-2024-R-eel.pdf`.

[5] Sogol Babaeinejadsarookolaee et al. “The power grid library for benchmarking ac optimal power flow algorithms”. In: *arXiv preprint arXiv:1908.02788* (2019).

[6] Mokhtar S Bazaraa, Hanif D Sherali, and Chitharanjan M Shetty. *Nonlinear programming: theory and algorithms*. John wiley & sons, 2006.

[7] Yasmine Beck, Ivana Ljubić, and Martin Schmidt. “A survey on bilevel optimization under uncertainty”. In: *European Journal of Operational Research* 311.2 (2023), pp. 401–426.

[8] David Biagioni et al. “Learning-accelerated ADMM for distributed DC optimal power flow”. In: *IEEE Control Systems Letters* 6 (2020), pp. 1–6.

[9] Daniel Bienstock and Abhinav Verma. “Strong NP-hardness of AC power flows feasibility”. In: *Operations Research Letters* 47.6 (2019), pp. 494–501.

[10] Daniel Bienstock and Matías Villagra. “Accurate linear cutting-plane relaxations for ACOPF”. In: *Mathematical Programming Computation* (2025), pp. 1–55.

[11] Daniel Bienstock et al. “Mathematical programming formulations for the alternating current optimal power flow problem”. In: *Annals of Operations Research* 314.1 (2022), pp. 277–315.

[12] David SC Biggs and Mark Andrews. “Acceleration of iterative image restoration algorithms”. In: *Applied optics* 36.8 (1997), pp. 1766–1775.

[13] Stephen Boyd et al. “Distributed optimization and statistical learning via the alternating direction method of multipliers”. In: *Foundations and Trends® in Machine learning* 3.1 (2011), pp. 1–122.

[14] Alessandro Buccini, Pietro Dell’Acqua, and Marco Donatelli. “A general framework for ADMM acceleration”. In: *Numerical Algorithms* 85 (2020), pp. 829–848.

[15] Antonin Chambolle and Thomas Pock. “A first-order primal-dual algorithm for convex problems with applications to imaging”. In: *Journal of mathematical imaging and vision* 40.1 (2011), pp. 120–145.

[16] Antonin Chambolle and Thomas Pock. “On the ergodic convergence rates of a first-order primal–dual algorithm”. In: *Mathematical Programming* 159.1 (2016), pp. 253–287.

[17] Tsung-Hui Chang, Mingyi Hong, and Xiangfeng Wang. “Multi-agent distributed optimization via inexact consensus ADMM”. In: *IEEE Transactions on Signal Processing* 63.2 (2014), pp. 482–497.

[18] Caihua Chen et al. “Inertial proximal ADMM for linearly constrained separable convex optimization”. In: *SIAM Journal on Imaging Sciences* 8.4 (2015), pp. 2239–2267.

[19] Jonathan Eckstein and Dimitri P Bertsekas. “On the Douglas—Rachford splitting method and the proximal point algorithm for maximal monotone operators”. In: *Mathematical programming* 55.1 (1992), pp. 293–318.

[20] Karl-Martin Ehrhart et al. “Analysis of a capacity-based redispatch mechanism”. In: *Energy Economics* (2025), p. 108751.

[21] Anselm Eicke and Tim Schittekatte. “Fighting the wrong battle? A critical assessment of arguments against nodal electricity prices in the European debate”. In: *Energy Policy* 170 (2022), p. 113220.

[22] ENTSO-E. *Supporting document for the network code on electricity balancing.* 6 August 2014. 2014. URL: `https://www.acer.europa.eu/sites/default/files/documents/Recommendations_annex/140806_NCEB_Supporting_Document.pdf` (visited on 06/09/2025).

[23] Tomaso Erseghe. “Distributed optimal power flow using ADMM”. In: *IEEE transactions on power systems* 29.5 (2014), pp. 2370–2380.

[24] European Commission. *COMMISSION REGULATION (EU) 2015/1222 of 24 July 2015.* Official Journal of the European Union, L 197/24. 2015. URL: `http://data.europa.eu/eli/reg/2015/1222/oj` (visited on 06/09/2025).

[25] European Commission. *Commission Regulation (EU) 2017/2195 of 23 November 2017.* Official Journal of the European Union, L 312/6, 28.11.2017. 2017. URL: `https://eur-lex.europa.eu/legal-content/EN/ALL/?uri=CELEX:32017R2195` (visited on 06/09/2025).

[26] European Commission. *Commission Regulation (EU) 2019/943 of 5 June 2019.* Official Journal of the European Union, L 158/54. 2019. URL: `https://eur-lex.europa.eu/legal-content/EN/ALL/?uri=CELEX:32017R2195` (visited on 06/09/2025).

[27] I. Serra F. Davò D. Siface. *Aggiornamento dei modelli matematici e delle metodologie per la simulazione dei mercati energetici.* Tech. rep. Ricerca Sistema Energetico - RSE, 2022.

[28] Daniel Fernández-Muñoz and Juan I Pérez-Díaz. “Optimisation models for the day-ahead energy and reserve self-scheduling of a hybrid wind–battery virtual power plant”. In: *Journal of Energy Storage* 57 (2023), p. 106296.

[29] Michel Fortin and Roland Glowinski. *Augmented Lagrangian methods: applications to the numerical solution of boundary-value problems.* Vol. 15. Elsevier, 2000.

[30] Anqi Fu, Junzi Zhang, and Stephen Boyd. “Anderson Accelerated Douglas–Rachford Splitting”. In: *SIAM Journal on Scientific Computing* 42.6 (2020), A3560–A3583.

[31] Erick Andrés Dorado Galatoire, Ángel Arcos-Vargas, and José Luis Martínez Ramos. "Additional revenues estimation in a market-based redispatch: An opportunity for flexibility". In: *Energy Conversion and Management: X* 24 (2024), p. 100745.

[32] Gestore Mercati Energetici. *Vademecum to the Italian Power Exchange.* URL: `https://www.mercatoelettrico.org/Portals/0/Documents/en-US/20260131VademecumBorsaElettrica_En.pdf`.

[33] Gestore Mercati Energetici (GME). *TESTO INTEGRATO DELLA DISCIPLINA DEL MERCATO ELETTRICO.* 2024.

[34] Euhanna Ghadimi et al. "Optimal parameter selection for the alternating direction method of multipliers (ADMM): Quadratic problems". In: *IEEE Transactions on Automatic Control* 60.3 (2014), pp. 644–658.

[35] Tom Goldstein et al. "Fast alternating direction optimization methods". In: *SIAM Journal on Imaging Sciences* 7.3 (2014), pp. 1588–1623.

[36] Veronika Grimm et al. "Transmission and generation investment in electricity markets: The effects of market splitting and network fee regimes". In: *European Journal of Operational Research* 254.2 (2016), pp. 493–509.

[37] Veronika Grimm et al. "Market-based redispatch may result in inefficient dispatch". In: *The energy journal* 43.5 (2022), pp. 205–230.

[38] Luigi Grippo and Marco Sciandrone. *Introduction to methods for nonlinear optimization.* Vol. 152. Springer Nature, 2023.

[39] Julia Grübel et al. "Nonconvex equilibrium models for energy markets: exploiting price information to determine the existence of an equilibrium". In: *Optimization Methods and Software* 38.1 (2023), pp. 153–183.

[40] De-Ren Han. "A survey on some recent developments of alternating direction method of multipliers". In: *Journal of the Operations Research Society of China* 10.1 (2022), pp. 1–52.

[41] Martin Hanke. "Accelerated Landweber iterations for the solution of ill-posed equations". In: *Numerische mathematik* 60.1 (1991), pp. 341–373.

[42] Tobias Harks and Julian Schwarz. "A unified framework for pricing in nonconvex resource allocation games". In: *SIAM Journal on Optimization* 33.2 (2023), pp. 1223–1249.

[43] Bing-Sheng He, Hai Yang, and SL Wang. "Alternating direction method with self-adaptive penalty parameters for monotone variational inequalities". In: *Journal of Optimization Theory and applications* 106.2 (2000), pp. 337–356.

[44] Bingsheng He, Feng Ma, and Xiaoming Yuan. "Convergence study on the symmetric version of ADMM with larger step sizes". In: *SIAM journal on imaging sciences* 9.3 (2016), pp. 1467–1501.

[45] Bingsheng He et al. "A strictly contractive peaceman–rachford splitting method for convex programming". In: *SIAM Journal on Optimization* 24.3 (2014), pp. 1011–1040.

[46] Kory W Hedman, Shmuel S Oren, and Richard P O'Neill. "A review of transmission switching and network topology optimization". In: *2011 IEEE power and energy society general meeting.* IEEE. 2011, pp. 1–7.

[47] Mingyi Hong, Zhi-Quan Luo, and Meisam Razaviyayn. "Convergence analysis of alternating direction method of multipliers for a family of nonconvex problems". In: *SIAM Journal on Optimization* 26.1 (2016), pp. 337–364.

[48] Rabih A Jabr. "Radial distribution load flow using conic programming". In: *IEEE transactions on power systems* 21.3 (2006), pp. 1458–1459.

[49] Thomas Kleinert et al. "A survey on mixed-integer programming techniques in bilevel optimization". In: *EURO Journal on Computational Optimization* 9 (2021), p. 100007.

[50] Nikolaos E Koltsaklis and Jaroslav Knápek. "Assessing flexibility options in electricity market clearing". In: *Renewable and Sustainable Energy Reviews* 173 (2023), p. 113084.

[51] Karsten Lehmann, Alban Grastien, and Pascal Van Hentenryck. "AC-feasibility on tree networks is NP-hard". In: *IEEE Transactions on Power Systems* 31.1 (2015), pp. 798–801.

[52] Can Li et al. "Mixed-integer linear programming models and algorithms for generation and transmission expansion planning of power systems". In: *European Journal of Operational Research* 297.3 (2022), pp. 1071–1082.

[53] Fangxing Li and Rui Bo. "Small test systems for power system economic studies". In: *IEEE PES general meeting*. IEEE. 2010, pp. 1–4.

[54] Steven H Low. "Convex relaxation of optimal power flow—Part I: Formulations and equivalence". In: *IEEE Transactions on Control of Network Systems* 1.1 (2014), pp. 15–27.

[55] Steven H Low. "Convex relaxation of optimal power flow—Part II: Exactness". In: *IEEE Transactions on Control of Network Systems* 1.2 (2014), pp. 177–189.

[56] Gang Luo and Qingzhi Yang. "A fast symmetric alternating direction method of multipliers". In: *Numerical Mathematics: Theory, Methods and Applications* 13.1 (2020), pp. 200–219.

[57] Vien Mai and Mikael Johansson. "Anderson acceleration of proximal gradient methods". In: *International Conference on Machine Learning*. PMLR. 2020, pp. 6620–6629.

[58] Palovic Martin et al. "Strategic behavior in market-based redispatch: International experience". In: *The Electricity Journal* 35.3 (2022), p. 107095.

[59] Sleiman Mhanna, Gregor Verbič, and Archie C Chapman. "Adaptive ADMM for distributed AC optimal power flow". In: *IEEE Transactions on Power Systems* 34.3 (2018), pp. 2025–2035.

[60] Daniel K Molzahn et al. "A survey of distributed optimization and control algorithms for electric power systems". In: *IEEE Transactions on Smart Grid* 8.6 (2017), pp. 2941–2962.

[61] Robert Nishihara et al. "A general analysis of the convergence of ADMM". In: *International conference on machine learning*. PMLR. 2015, pp. 343–352.

[62] Wenqing Ouyang et al. "Anderson acceleration for nonconvex ADMM based on Douglas-Rachford splitting". In: *Computer Graphics Forum*. Vol. 39. 5. Wiley Online Library. 2020, pp. 221–239.

[63] Narayana Prasad Padhy. "Unit commitment-a bibliographical survey". In: *IEEE Transactions on power systems* 19.2 (2004), pp. 1196–1205.

[64] G Rancilio et al. "Ancillary services markets in europe: Evolution and regulatory trade-offs". In: *Renewable and Sustainable Energy Reviews* 154 (2022), p. 111850.

[65] Line A Roald et al. "Power systems optimization under uncertainty: A review of methods and applications". In: *Electric Power Systems Research* 214 (2023), p. 108725.

[66] Mahir Sarfati, Mohammad Reza Hesamzadeh, and Pär Holmberg. “Production efficiency of nodal and zonal pricing in imperfectly competitive electricity markets”. In: *Energy Strategy Reviews* 24 (2019), pp. 193–206.

[67] David Schönheit et al. “Toward a fundamental understanding of flow-based market coupling for cross-border electricity trading”. In: *Advances in Applied Energy* 2 (2021), p. 100027.

[68] J Kyle Skolfield and Adolfo R Escobedo. “Operations research in optimal power flow: A guide to recent and emerging methodologies and applications”. In: *European Journal of Operational Research* 300.2 (2022), pp. 387–404.

[69] Terna S.p.A. *Dispatching Regulations - Italian Grid Code.* URL: `https://download.terna.it/terna/Chapter_4_8de0a956b9bc23f.pdf`.

[70] Terna S.p.A. *Procedura per la selezione delle risorse per MB e per la conversione delle offerte ai fini della partecipazione del gestore della rete alle piattaforme di bilanciamento - Italian Grid Code.* [in Italian]. URL: `https://download.terna.it/terna/Allegato_A.23_8dd298003bd41d6.pdf`.

[71] Wenyi Tian and Xiaoming Yuan. “An alternating direction method of multipliers with a worst-case $O(1/k^2)$ convergence rate”. In: *Mathematics of Computation* 88.318 (2019), pp. 1685–1713.

[72] Alex Toth and Carl T Kelley. “Convergence analysis for Anderson acceleration”. In: *SIAM Journal on Numerical Analysis* 53.2 (2015), pp. 805–819.

[73] Wim Van Ackooij et al. “Large-scale unit commitment under uncertainty: an updated literature survey”. In: *Annals of Operations Research* 271.1 (2018), pp. 11–85.

[74] Kenneth Van den Bergh et al. “Redispatching in an interconnected electricity system with high renewables penetration”. In: *Electric Power Systems Research* 127 (2015), pp. 64–72.

[75] Dawei Wang, Yunhui He, and Hans De Sterck. “On the asymptotic linear convergence speed of Anderson acceleration applied to ADMM”. In: *Journal of Scientific Computing* 88.2 (2021), p. 38.

[76] SL Wang and LZ Liao. “Decomposition method with a variable parameter for a class of monotone variational inequality problems”. In: *Journal of optimization theory and applications* 109.2 (2001), pp. 415–429.

[77] Yamin Wang, Lei Wu, and Shouxiang Wang. “A fully-decentralized consensus-based ADMM approach for DC-OPF with demand response”. In: *IEEE Transactions on Smart Grid* 8.6 (2016), pp. 2637–2647.

[78] Yu Wang, Wotao Yin, and Jinshan Zeng. “Global convergence of ADMM in nonconvex nonsmooth optimization”. In: *Journal of Scientific Computing* 78.1 (2019), pp. 29–63.

[79] Tao Yang et al. “A survey of distributed optimization”. In: *Annual Reviews in Control* 47 (2019), pp. 278–305.

[80] Yu Yang et al. “A survey of ADMM variants for distributed optimization: Problems, algorithms and features”. In: *arXiv preprint arXiv:2208.03700* (2022).

[81] Juyong Zhang et al. “Accelerating ADMM for efficient simulation and optimization”. In: *ACM Transactions on Graphics (TOG)* 38.6 (2019), pp. 1–21.

[82] Ray Daniel Zimmerman, Carlos Edmundo Murillo-Sánchez, and Robert John Thomas. “MATPOWER: Steady-state operations, planning, and analysis tools for power systems research and education”. In: *IEEE Transactions on power systems* 26.1 (2010), pp. 12–19.

This research work has been funded by the European Union - NextGenerationEU, Mission 4, Component I.4.1, CUP B83C22003220006.